UNIVERSITY OF
BRADFORD

CIVIL AND ENVIRONMENTAL ENGINEERING

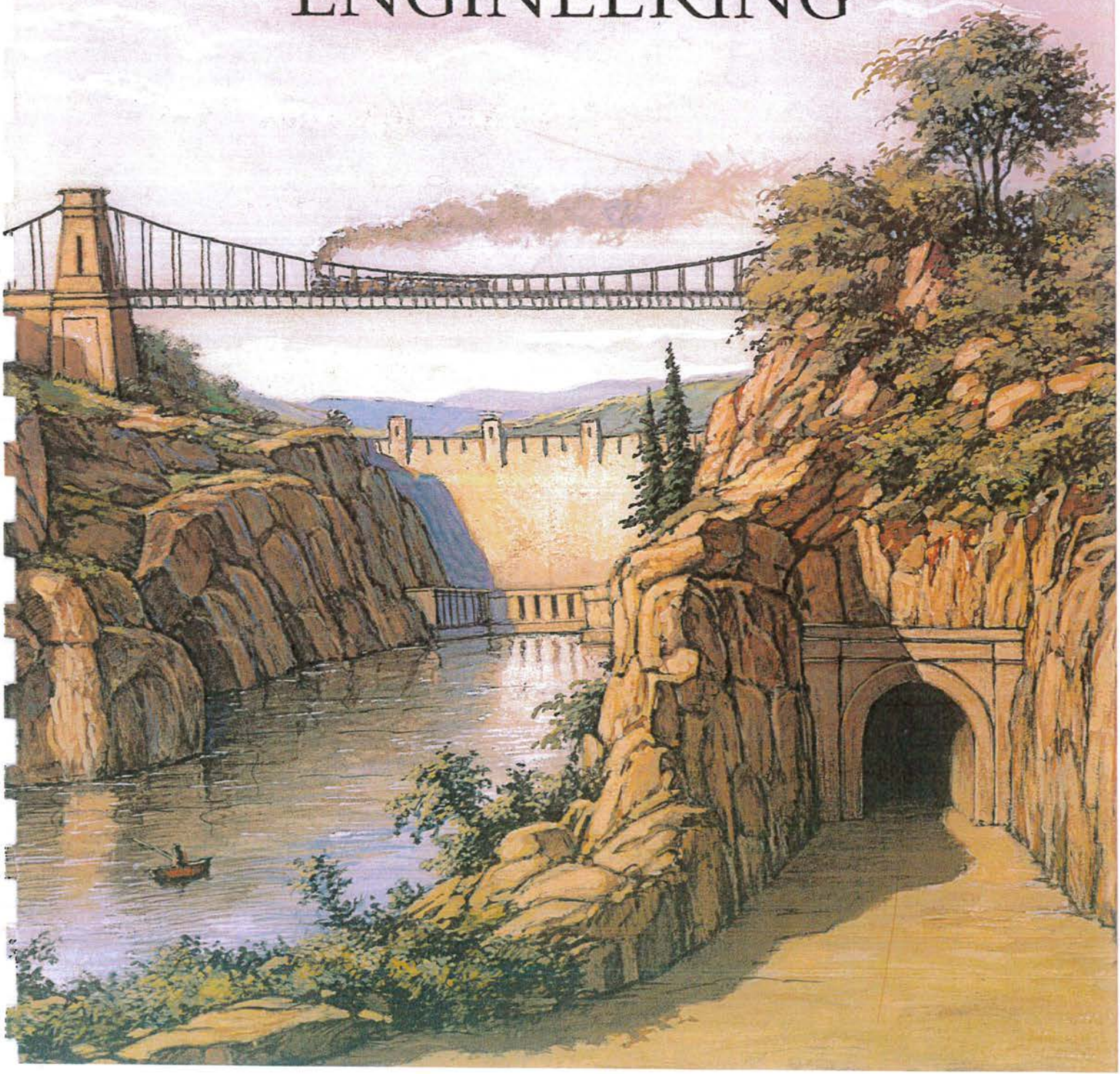

DEPARTMENT OF CIVIL AND ENVIRONMENTAL ENGINEERING
University of Bradford
Bradford
West Yorkshire
BD7 1DP
UK

Tel: +44 (0)1274 383876/77
Fax: +44 (0)1274 383888

MATHEMATICAL MODEL STUDY OF TIDAL CURRENTS, FLUSHING AND WATER QUALITY INDICATORS AROUND ST. AUBIN'S BAY, JERSEY

by

Professor Roger A Falconer

DSc(Eng), FEng, FICE, FCIWEM, FASCE

and

Morteza Kolahaldoozan

MSc

Department of Civil and Environmental Engineering
University of Bradford
BRADFORD
West Yorkshire
BD7 1DP

Tel: 01274 383871
Fax: 01274 383888

April 1998

EXECUTIVE SUMMARY

A mathematical model study has been undertaken to predict the hydrodynamic conditions around the coast of Jersey at a coarse grid scale and, in particular, around St. Aubin's Bay at a fine grid scale (i.e. 100 m). In addition, the concentration distributions of bacterial and nutrient level indicators have been predicted in St. Aubin's Bay and the surrounding waters, including: total and faecal coliforms, faecal streptococci, dissolved available inorganic nitrogen (DAIN) and phosphorus (DAIP).

The main findings from this study can be summarised as follows:-

- The coarse and fine grid models have used approximate open boundary data, based on information provided on the Admiralty Chart (2669). Ideally, comprehensive and expensive field data should be acquired to drive these models for accurate predictions. Nonetheless, the model predictions have shown good agreement with Admiralty Chart data at eight sites in the coarse grid model and two sites in the fine grid model.

- The tidal exchange predictions for St. Aubin's Bay showed that the tidal currents in the region were relatively low and the exchange coefficient after five tides varied between 0.5 and 0.6 for spring and neap tides. This range indicated that the Bay was reasonably well flushed for both tidal extremes with no major zones being apparent. Tracer from the Bay was advected along the eastern shoreline by the alongshore current, particularly during neap tides.

- The coliform predictions for the bounded conditions studied (i.e. consecutive spring and neap tides) suggested that worst conditions occurred in the Bay for spring tides and storm (or winter) events. The total coliform levels for much of the Bay were between 50 and 100 counts per 100 ml, although peak concentrations of over 2,000 counts per 100 ml were predicted during neap tides, and along the south east

shoreline of the Bay. The main cause of these relatively high values was predicted to be the Weighbridge Catchment discharge and it is recommended that consideration be given to reducing the effluent discharge levels from this outfall. However, the construction of the Fort Regent Cavern, and the consequential routing of storm overflows from the Weighbridge Outfall through the Bellozanne STW, will significantly reduce the input of coliforms to the Bay when it becomes operational.

- The bounded nutrient level predictions confirmed that the Bellozanne STW was the main source of DAIN and DAIP concentration levels in St. Aubin's Bay. Peak typical concentrations across the Bay, and away from the nearfield outfall site, were 0.05 mg/l for DAIN and less than 0.01 mg/l for DAIP. Reducing the Bellozanne STW nutrient inputs to 10 mg/l for DAIN and 1 mg/l for DAIP would reduce the predicted values across St. Aubin's Bay by between 40 to 50 % and 80 to 90 % for DAIN and DAIP respectively. These reductions are appreciable and it is recommended that consideration therefore be given to nitrogen reduction, particularly since nitrogen is the limiting factor in algal growth in marine waters (Stapleton and Kay, 1997).

- The DAIN and DAIP concentration levels were predicted to be relatively high along the south east shoreline of the Bay. These relatively high levels were predicted to arise from inputs through the Weighbridge Catchment outfall. It is therefore recommended that consideration be given, either to routing the Weighbridge Catchment through the Bellozanne STW and reducing the DAIN inputs accordingly, or discharging into deeper waters where rapid dilution may again be encountered.

CONTENTS

LIST OF TABLES

LIST OF FIGURES

LIST OF APPENDICES

1. INTRODUCTION

The main aims of this study were to set up a two-dimensional hydrodynamic and water quality model of the coastal waters along the south coast of Jersey, and to predict the tidal currents, the flushing characteristics of St. Aubin's Bay and the concentration distributions of various water quality indicators, including coliform levels and dissolved available inorganic nitrogen (DAIN) and phosphorous (DAIP) concentration distributions. The States of Jersey Public Services Department (PSD) is considering options for the upgrading of waste water treatment at the Bellozanne plant (see Stapleton and Kay, 1997) and the model has been used to predict the impact on various water quality indicator levels as a result of the proposed upgrading.

The main cause for concern is the potential for St. Aubin's Bay and the surrounding waters (see Figure 1) to become eutrophic and the need for the coastal zone to meet the requirements of current and proposed European Union legislation, and in particular the Urban Waste Water Treatment Directive (91/97/EEC) (UWWTD). A summary of the requirements of the Urban Waste Water Treatment Directive are given in Stapleton and Kay (1997), with this report providing a summary and analysis of the predicted tidal currents and water quality indicator levels in the coastal waters, both with and without nitrogen and phosphorus removal from the Bellozanne STW.

The latest version of the DIVAST (Depth Integrated Velocities And Solute Transport) model was set up for the coastal region based on existing Admiralty Chart bathymetric data and recorded tidal elevations. A course grid model was first set up to cover a coastal region of approximately 100 km x 80 km, with boundaries being taken from the Island of Guernsey, due south and east, to the French coast of Normandy and Brittany respectively (see Figure 2). This model then provided the hydrodynamic and water quality boundary conditions for a fine grid model of the region around the southern coast of Jersey, from Portelet Bay in the south west to the northern part of Royal Bay of Grouville along the east coast (see Figure 3).

The model was refined mathematically to include the ULTIMATE QUICKEST finite difference representation (Lin and Falconer, 1997a) for the advection terms in the water quality constituent transport equations, with this scheme being highly accurate and superior to widely used schemes, such as the QUICK scheme and third order upwinding, as included in previous versions of the widely used DIVAST model. This refined scheme produces negligible numerical (or artificial) diffusion, and does not give rise to undershoot or overshoot in regions of high concentration gradients, such as outfall sites or contaminant spill sites etc. (Leonard 1991, and Cahyono 1993). The latter property of this scheme is particularly important in modelling the distribution of water quality indicators from the discharge sites along the shoreline of St. Aubin's Bay, and the transport of these indicators eastwards around Greve D'Azette and St. Clement's Bay.

Following stability and convergence tests for both the hydrodynamic and water quality modules, the coarse grid model was compared with Admiralty Chart tidal velocities and elevations at 8 diamond sites located within the domain, as indicated in Figure 2. The fine grid model was then refined against 2 diamond sites within the domain, before being run for spring and neap tide conditions, and for summer (base flow) and winter (storm flow) conditions, to predict the flushing characteristics of St. Aubin's Bay and a range of water quality indicator distributions, both with and without input from the Bellozanne STW.

2. MODEL DETAILS

2.1 History

The original DIVAST (Depth Integrated Velocities And Solute Transport) model is based on a finite difference solution for predicting time varying water elevations and depth averaged velocity components and solute concentration distributions in the horizontal plane. It was first developed as part of a PhD programme by Falconer [1976]. The model has subsequently been extensively developed and refined, with particular emphasis being focused on the treatment of the advective accelerations, wind effects, bed friction, turbulence, high concentration gradients, dispersion and diffusion, water quality

constituents, sediment transport processes and flooding and drying. The model has also been calibrated and verified extensively against laboratory and field measured data, with details of the model refinements and verification tests being reported in over 100 publications by the original model developer, namely Professor Falconer. The model has been successfully applied to over 80 site specific studies by 35 consulting engineering firms and water industry related companies, and is now widely used within the UK and overseas. Also, the original TRIVAST (Layer Integrated Velocities And Solute Transport) model is again based on a finite difference solution for predicting time varying water elevations and layer averaged velocity components and solute concentration distributions in the horizontal plane, and vertical velocity components and solute fluxes in the vertical plane. This model was first developed by Hall [1987], and Falconer et al [1991], and recently refined by Lin and Falconer [1997b].

2.2 Overview

DIVAST and TRIVAST are comprehensive and versatile models for predicting the water elevation and velocity components in the horizontal and vertical planes, sediment transport fluxes and up to ten user specified water quality constituents. The models have been widely applied to model well mixed coastal, estuarine and inland water bodies. The 2-D model includes an improved wind stress representation, through the use of an assumed second order parabolic velocity profile, to give a quasi-three-dimensional effect [Falconer and Chen, 1991].

The hydrodynamic modules are based upon the solution of the depth and layer integrated Navier-Stokes equations and include the effects of:- local and advective accelerations, the earth's rotation, free surface pressure gradients, wind action, bed resistance and a simple mixing length turbulence model. The differential equations are written in their pure differential form, thereby allowing momentum conservation in the finite difference sense. Particular emphasis has been focused in the model development on the treatment of the advective accelerations, the surface wind stress and the complex hydrodynamic phenomenon of flooding and drying, with the corresponding hydrodynamic equations being given in Appendix A.

For the water quality and sediment transport module, the advective-diffusion equation is solved for a range of water quality constituents as specified previously. The general depth and layer integrated equations include:- local and advective transport, turbulent dispersion and diffusion (including wind effects where appropriate), source and sink inputs, decay rates and kinetic transformation processes. For the sediment transport module, the equilibrium suspended flux is included in the model using the van Rijn formulation [see van Rijn, 1984a, b]. However, other formulations are also available, including formulae proposed by Engelund and Hansen [1967]. As for the hydrodynamic module, the water quality constituents and sediment transport equations are also given in Appendix A.

For the 2-D model, the governing differential equations are solved using the finite difference technique and using a scheme based on the alternating direction implicit formulation. The advective accelerations are written in a time centred form for stability, with these terms and the turbulent diffusion terms being centred by iteration. Whilst the model has no stability constraints, there is a Courant number restriction for accuracy in the hydrodynamic module, with the Courant number indicating the speed of the physical to the numerical wave, and with this restriction being given by:-

$$\frac{\Delta t}{\Delta x}\sqrt{gH} < 8 \qquad \text{---(1)}$$

where Δt = time step, Δx = grid size, g = gravity and H = maximum depth.

The finite difference equations are formulated on a space staggered grid scheme, with the water surface elevations and x-direction velocity components being initially solved for during the first half time step by using the method of Gauss elimination and back substitution. The water quality indicators and sediment flux distributions are then evaluated, before proceeding to the second half time step and repeating the process for the implicit description of the y-direction derivatives and velocity components. In the water quality and sediment transport modules, the advection terms are treated using the higher order accurate ULTIMATE QUICKEST formulation, with this scheme reducing considerably the introduction of artificial diffusion and eliminating undershoot and overshoot in regions of high concentration gradients. Full details of the finite difference equations are given in Appendix B.

3. MODEL APPLICATION

3.1 General

The Island of Jersey is the largest of the Channel Islands and is located in the English Channel. The coastal region of particular interest is St. Aubin's Bay and the adjacent coastal waters along the southern shores of the Island. Surface water and treated sewage outfalls enter this bay from eight sites including, from west to east along the Bay foreshore:- the catchments of (i) St. Aubin's, (ii) La Haule A, (iii) La Haule B, (iv) St. Peter's Valley, (v) Waterworks Valley, (vi) Bellozanne Valley, (vii) the sewage treatment works (STW) and (viii) St Helier at Weighbridge. Discharges and water quality indicators entering the Bay were considered from five sites, incorporating combinations of the above eight, and including:- (i) St. Aubin's Catchment, (ii) St Peter's Valley, (iii) Waterworks Valley, (iv) Bellozanne Valley and the STW, and (v) Weighbridge Catchment. The Sewage Treatment Works and Bellozanne Valley were discharged from the same site in the model, but were treated as separate inputs in the analysis.

For each site two discharge inputs were considered, i.e. termed herein a base flow (BF) and a storm flow (SF), with full details of the model input discharges and water quality indicator levels for total coliforms, faecal coliforms, faecal streptococci, dissolved available inorganic nitrogen (DAIN) and dissolved available inorganic phosphorous (DAIP) being given in Table 1. In addition to modelling the various inputs given in Table 1, for the base flows and storm flows, the current and water quality indicator fields were also predicted for spring and neap tides, corresponding to ranges of approximately 9.27 m and 3.95 m respectively.

3.2 Model Specification

The course grid computational domain was set-up with dimensions of 100 km x 81 km between 1.5° longitude west from Greenwich. For this coarse grid model a mesh of 111 x 90 grid squares was used, with a uniform grid spacing of 900 m. At the centre of the sides of each grid square a representative depth of the bed elevation below datum was required. For this purpose bathymetric data given on the Admiralty Chart No. 2669 were

Catchment	St. Aubin's Valley (with La Haule A)		St. Peter's Valley (with La Haule B)		Waterworks Valley		Bellozanne Valley		Weighbridge Catchment		STW	
Solute Type	B.F.[1]	S.F.[2]	B.F.	S.F.	B.F.	S.F.	B.F.	S.F.	B.F.	S.F.	B.F.	S.F.
Flow (m3/s)	0.033	0.127	0.058	0.204	0.034	0.134	0.020	0.077	0.095	0.367	0.232	0.268
Total Coliform (counts/100 ml)	1.41E+5	1.5E+5	2.6E+5	6.3E+5	2.1E+5	6.3E+5	8.4E+3	7.8E+5	1.4E+5	2.1E+7	2.2E+3	5.5E+4
Faecal Coliform (counts/100 ml)	1.98E+4	1.5E+4	3.3E+3	1.6E+5	9.0E+3	1.4E+5	2.6E+3	3.8E+5	1.8E+4	5.7E+6	4.0E+2	3.1E+4
Faecal Streptococci (counts/100 ml)	1.07E+4	6.6E+3	2.5E+3	5.2E+4	2.1E+3	6.1E+4	7.0E+2	9.1E+4	2.4E+3	2.4E+5	50	1.7E+3
Dissolved Available Inorganic Nitrogen (mg/l)	12.68	13.32	15.00	11.44	12.79	13.27	12.91	13.24	11.63	12.56	28.82	26.12
Dissolved Available Inorganic Phosphorus (mg/l)	0.087	0.135	0.204	0.132	0.087	0.132	0.084	0.131	0.033	0.046	10.84	7.075

[1] Base Flow
[2] Storm Flow

Table 1: Discharge Inputs for Different Catchments in St. Aubin's Bay

used, together with additional data acquired from other maps. The data were digitised using a digitised ground modelling package (i.e. DGM) to generate interpreted depths at the required grid locations. The digitising software package DGM uses linear interpolation.

For the bed roughness characteristics, no data were available and a typical value of 20 mm was assumed for the Nikuradse roughness parameter k_s. The Coriolis accelerations representing the effect of the earth's rotation was included in the model, with the angle of latitude being set to 49.4°.

The open seaward boundaries along the western and northern limits were driven by velocity components obtained by interpolation from the Admiralty Chart diamond data in close proximity to these boundaries. Clearly, these estimated data provide only a crude approximation to the true spring and neap tide conditions at any time along these boundaries, and ideally an extensive and comprehensive field data acquisition programme would be desirable to obtain more reliable boundary data. In addition to these velocity boundary conditions, water elevations were specified at St. Malo (see Figure 2).

For the fine grid model, the computational domain was set up with dimensions of 18.6 km x 10.8 km, covering St. Aubin's Bay and the coastal waters to the east of the Island. The domain was covered using a mesh of 186 x 108 grid squares, with a uniform grid spacing of 100 m. The depths between datum and the bed were again specified at the centre of the sides of each grid square, in the same manner as for the coarse grid model. The boundary conditions for the fine grid model consisted of water elevations being specified along the western boundary, and with velocity components being specified along the eastern and northern boundaries (see Figure 3). The corresponding water elevations and velocity components specified at each boundary grid square were obtained by interpolation from the closest adjacent coarse grid square cells. For the southern open boundary the normal velocity gradient was assumed to be zero, with the open boundary therefore effectively acting as a free streamline.

4. MATHEMATICAL MODEL RESULTS

4.1 Hydrodynamic Coarse Grid Model Calibration

The purpose of the coarse grid model was to simulate the flow patterns around the island of Jersey and to provide appropriate boundary conditions for a more accurate fine grid model. As outlined in the model specification given in the previous section, the coarse grid model was set up to predict only the velocity and water elevation fields at this stage of the study. To predict the velocity field in any region accurately, the first step is for the model to be calibrated. For this purpose the model was run for several different bed and open boundary approximations to obtain the closest fit between the measured and predicted data.

The hydrodynamic model was calibrated by comparing the predicted velocities at sites G, J, K, L, M, N, Q, and S, with the corresponding magnitude and direction components being specified on the Admiralty Chart (No. 2669). Likewise, the spring and neap tide predicted and specified water elevations were compared at St. Helier and St. Malo. Comparisons of the predicted and Admiralty Chart velocities are given for the respective sites in Figures 4 to 11 and with the water elevation comparisons being given in Figures 12 and 13 respectively, with all comparisons being undertaken for the third tidal cycle.

As can be seen from the velocity magnitude and direction comparisons, the computer predicted and measured values were in close agreement, particularly since the model was driven by relatively imprecise open boundary data. Likewise, the water elevation comparisons between the measured and predicted data agree particularly closely for St. Helier, which is in the main region of interest for this study. The water elevation comparisons do not agree quite so well at St. Malo, but this site is well away from the Jersey coastline.

Following calibration the model was then applied to the region, with water elevations and velocity field predictions being produced at mid-flood, high, mid-ebb and low spring and neap tides respectively, with the corresponding velocity field predictions being

illustrated in Figures 14 to 21 respectively. In comparing these velocity field predictions with the Admiralty Tidal Stream Atlas NP264, the flow patterns were similar to those observed in the field and illustrated in the Atlas. The results show a strong alongshore current around the southern coast of Jersey at mid-flood and mid-ebb tide, both for spring and neap conditions, with the corresponding current field being much weaker near high slack water. It is also worth noting that the general net mass fluid flux was from west to east when integrated over the total cycle indicating that the effluent discharges in St. Aubin's Bay would generally be advected eastwards.

With the predicted velocities at the data sites generally exhibiting good agreement with the Admiralty Chart data, and the tidal currents agreeing well with the Tidal Stream Atlas, the coarse grid model was then used with a degree of confidence to drive the fine grid model. With the coarse grid model providing the relevant boundary conditions, the fine grid model was then set up to simulate the hydrodynamic and water quality indicators in St Aubin's Bay and the adjacent coastal waters. Firstly, the fine grid model was verified against field data available within the area of interest at diamond sites G and J. The results of these comparisons, for both spring and neap tides, are shown in Figures 22 to 24 respectively. As can be seen from the figures, the water elevations and the computed and Admiralty Chart specified velocity magnitudes and directions were again in good agreement with one another. Hence, it was assumed that the model was predicting the hydrodynamic conditions reasonably accurately across the domain and therefore the model was used to predict the water quality indicators with some degree of confidence. The detailed flow patterns for the fine grid model have been used to drive the water quality model and are shown and discussed in the next sections.

4.2 Tidal flushing of St. Aubin's Bay

Following checking and application of the hydrodynamic model, and before studying the water quality indicator distributions from the effluent sites around St. Aubin's Bay, a tidal flushing study was first undertaken to establish the tidal exchange characteristics of the Bay. Initially the Bay was assumed to be uniformly polluted with a conservative tracer of concentration of 35 mg/l (see Figure 25). Beyond the entrance to the Bay the concentration was set to zero. This approach is similar to that which would commonly be used in a

physical hydraulic model study, where a temporary barrier would be sited across the Bay entrance and dye first mixed uniformly within the Bay. At time t = 0, and after initial disturbances had died down, the barrier would be removed and the tidal generator simultaneously switched on (Nece and Falconer, 1989). The same approach was adopted in this numerical model study. Hence at t = 0 the hydrodynamic boundary conditions were introduced and the dye flushed out of the Bay as the hydrodynamic flow field developed. The resulting dye distributions are shown at low and high tide, for spring and neap tide conditions, in Figures 26 to 29 respectively.

From these results it can be seen that the dye remains much closer to the shoreline for spring tide conditions, although more dye is flushed out of St. Aubin's Bay. In contrast, for neap tide conditions the dye plume spreads over a much larger area, but the shoreline concentrations are relatively high. Also, less dye is flushed out of the domain.

To quantify the graphical results, the tidal exchange coefficient was evaluated for both spring and neap tide conditions. This coefficient gives a measure of the exchange from within the Bay with the offshore adjacent waters. The average per-cycle exchange coefficient, which indicates that fraction of water within a basin or segment of a basin which is removed (flushed out) and replaced with ambient water during each tidal cycle, is represented by the equations (Nece and Falconer, 1989):-

$$E = 1 - R \qquad (2)$$

$$R = (C_n/C_o)^{1/n} \qquad (3)$$

where E = average per-cycle exchange coefficient, R = average per-cycle retention coefficient, C_o = initial spatial average tracer concentration, and C_n = spatial average tracer concentration for the same volume after n tidal cycles, where n is an integer. The resulting exchange coefficients are shown at the end of tides 1 to 5 and for spring and neap tide conditions in Figure 30.

The exchange coefficient for both spring and neap conditions after 5 tides is over 0.5, which indicates that approximately 97% of the enclosed fluid volume is exchanged every 5 tides. This value is comparable with well flushed marinas and small boat harbours studied in

the USA and higher than similar studies carried out for semi-enclosed embayments in the UK (Nece and Falconer, 1989). This suggests that the basin exchanges well with the adjacent offshore waters and the enclosed fluid is extensively flushed out by the tide and the alongshore current during each tide. However, on being flushed out of the Bay, much of the efflux fluid mass is advected eastwards on leaving the Bay.

4.3 Coliform Predictions

Following the tidal exchange investigations, the model was then set up to predict the total and faecal coliform and faecal streptococci distributions, with inputs for the existing conditions from five inputs, including:- St. Aubin's Catchment, St. Peter's Valley, Waterwork Valley, Bellozanne Valley (including the Sewage Treatment Works), and Weighbridge Catchment. For each simulation considered the model was run for two flow scenarios, defined as base flow (BF) and storm flow (SF). For the catchments base flow refers to summer conditions, i.e. typical flow and pathogenic inputs for April to September, and storm flow refers to winter conditions, i.e. typical flow and pathogenic inputs for October to March. The decay rates for coliforms (i.e. both total and faecal) were specified in terms of T_{90} values of 10 hours and 30 hours for day and night periods respectively. These T_{90} values correspond to first order decay rates of 5.52 day^{-1} and 1.842 day^{-1} respectively.

The resulting low tide (worst case) total coliform predictions for base and storm flow inputs and for spring and neap tides are given in Figures 31 to 34 respectively. The results show that for the base flow inputs the concentration in the Bay is highest for spring tide conditions, with a fairly large region of the Bay having a concentration of between 10 and 50 counts per 100 ml and between 50 and 1000 in the close proximity of the outfall (see Figure 31). For storm flow conditions the mean concentration in the Bay was higher, typically 1000 counts per 100 ml, but in particular high concentrations were predicted off the south east headland. Also, along the eastern shore of the Bay the coliform levels exceeded 2000 counts per 100 ml. For neap tide conditions the lower currents along the shore and just eastwards of St. Aubin's Bay tended to confine the plumes and tended to give rise to slightly higher shoreline concentrations of typically 50 to 100 counts per 100 ml for the base flow and about 2,000 counts per 100 ml for the storm flow conditions in the

vicinity of the outfalls. These predicted values were conservative (i.e. worst case), based on relatively low decay rates, and were primarily dominated by the inputs from the Weighbridge Catchment. The input from the Sewage Treatment Works had a much less significant effect on the receiving waters. Also, it is worth noting that the mean Bay concentrations for total and faecal coliforms under storm flow conditions were also unduly pessimistic, due to the very high total loads at the outfall sites.

For the corresponding faecal coliform predictions shown in Figures 35 to 38, the concentrations were typically up to an order of magnitude less. The base flow conditions were predicted to lead to average concentrations of between 1 and 10 counts per 100 ml in the Bay for spring conditions and lower for neap. The shoreline concentrations to the east of the Bay were again extended along the coast for neap tide conditions. Likewise, for storm flow conditions the Weighbridge Catchment was predicted to yield peak concentrations of over 2,000 counts per 100 ml in parts of the Bay and with this contour extending along some shoreline reaches to the east of the Bay. As before, these predictions were based on conservative decay rates, but the results indicate that treatment measures should be considered to reduce the high effluent inputs from the Weighbridge Catchment outfall, particularly since shoreline concentrations in excess of 2,000 counts per 100 ml do not comply with the EU Bathing Water Directive.

4.4 Nutrient Level Distribution Predictions

For the nutrient inputs into the fine grid model, both dissolved available inorganic nitrogen DAIN (= nitrate N + nitrite N + ammoniacal N) and dissolved available inorganic phosphorus DAIP (= orthophosphate phosphorus) were considered. The various base and storm flow inputs for both nutrient components were as given in Table 1. The corresponding results for baseflow and stormflow, for spring and neap tides, and for the existing and the proposed inputs (i.e. with DAIN input at the STW at Bellozanne reduced to 10 mg/l), are shown in Figures 39 to 46 respectively.

The resulting spring tide predictions show that, although the DAIN input from the STW was higher than that from the Weighbridge Catchment input (i.e. typically double), the latter was on the edge of the alongshore current and was advected onto the south-east

shoreline of the Island. The STW was the main source of DAIN input into St. Aubin's Bay and lead to local concentrations across most of the Bay of between 0.01 to 0.05 mg/l, and near the STW outfall the concentration peaks were about 0.1 to 0.5 mg/l. When the proposed DAIN input from the Bellozanne STW was reduced to 10 mg/l, then the concentration of DAIN over most of the Bay was less than 0.05 mg/l and the outfall plume was much reduced in size, with local shoreline concentrations being in the range 0.05 to 0.1 mg/l.

For neap tide conditions the stronger alongshore current exacerbated the Weighbridge Catchment effects along the south eastern shoreline, with the 0.01 to 0.05 mg/l contour stretching well towards the most south-easterly tip of the Island (see Figure 44), and with the shoreline concentrations around the eastern headland of St. Aubin's Bay being about 0.5 mg/l. The concentration in the Bay was generally lower for neap tide conditions, primarily due to the lower in-Bay current not advecting the DAIN effluent from the outfall site. As before, reducing the STW DAIN input to 10 mg/l reduced the local concentration in the vicinity of the outfall by nearly 50 %. However, the far-field concentration was only reduced marginally.

Finally, comparisons were made of the predicted DAIN concentration distributions in St. Aubin's Bay, at low and high spring tide, for the existing and proposed storm flow outputs from the Bellozanne STW (i.e. the worst case scenario). The resulting predictions shown in Figures 47 to 50 respectively, show that reducing the DAIN input from 26.12 mg/l to 10 mg/l will reduce the corresponding concentration distributions around the Bay by typically nearly 50% (see Table 2), with a corresponding reduction in the extent of the DAIN plume. However, reducing the DAIN input levels from Bellozanne has little or no impact on the relatively high levels arising from the Weighbridge Catchment, on the south eastern side of St. Aubin's Bay.

In the final simulations, predictions were made of the DAIP concentration distributions, with the resulting low tide predictions being shown in Figures 51 to 58, for base and storm flows, with the existing inputs and the Bellozanne STW DAIP inputs reduced to 1 mg/l, and for spring and neap tides respectively. The predicted spring tide

	Existing Condition										Proposed Condition			
	Total Coliform (cts/100ml)		Faecal Coliform (cts/100ml)		Faecal Streptococci (cts/100ml)		DAIN (mg/l)		DAIP (mg/l)		DAIN (mg/l)		DAIP (mg/l)	
	B.F [1]	S.F [2]	B.F.	S.F.	B.F.	S.F.	B.F.	S.F.	B.F.	S.F.	B.F.	S.F.	B.F.	S.F.
Mid Ebb Tide	0.4266	70.22	0.29E-1	19.14	0.45E-2	0.5925	0.39E-3	0.68E-3	0.11E-3	0.85E-4	0.21E-3	0.49E-3	0.11E-4	0.15E-4
Low Tide	0.4688	85.63	0.33E-1	23.33	0.48E-2	0.6817	0.57E-3	0.98E-3	0.16E-3	0.12E-3	0.29E-3	0.71E-3	0.16E-4	0.21E-4
Mid Flood Tide	0.3446	64.97	0.25E-1	17.70	0.36E-2	0.5060	0.51E-3	0.89E-3	0.14E-3	0.11E-3	0.27E-3	0.65E-3	0.15E-4	0.21E-4
High Tide	0.2708	39.97	0.18E-1	10.90	0.33E-2	0.3777	0.35E-3	0.62E-3	0.98E-4	0.76E-4	0.19E-3	0.46E-3	0.11E-4	0.15E-4

[1] Base Flow
[2] Storm Flow

Table 2a Mean Concentration Levels for Spring Tide across the Whole Computational Domain

	Existing Condition										Proposed Condition			
	Total Coliform (cts/100ml)		Faecal Coliform (cts/100ml)		Faecal Streptococci (cts/100ml)		DAIN (mg/l)		DAIP (mg/l)		DAIN (mg/l)		DAIP (mg/l)	
	B.F.	S.F.	B.F.	S.F.	B.F.	S.F.	B.F.	S.F.	B.F.	S.F.	B.F.	S.F.	B.F.	S.F.
Mid Ebb Tide	41.03	0.62E+4	2.649	0.17E+4	0.4388	56.31	0.36E-1	0.61E-1	0.10E-1	0.78E-2	0.19E-1	0.44E-1	0.98E-3	0.13E-2
Low Tide	81.90	0.91E+4	4.847	0.25E+4	0.8951	99.03	0.96E-1	0.1560	0.27E-1	0.21E-1	0.48E-1	0.1094	0.26E-2	0.35E-2
Mid Flood Tide	30.62	0.49E+4	2.066	0.13E+4	0.3380	44.95	0.39E-1	0.68E-1	0.11E-1	0.84E-2	0.21E-1	0.49E-1	0.11E-2	0.15E-2
High Tide	13.02	0.18E+4	0.828	0.48E+3	0.1650	18.82	0.14E-1	0.25E-1	0.40E-2	0.31E-2	0.75E-2	0.18E-1	0.40E-3	0.54E-3

Table 2b Mean Concentration Levels for Spring Tide across St. Aubin's Bay

Table 2 Mean Concentration Levels for Spring Tides

results showed that the main source of input to St. Aubin's Bay was the Bellozanne STW, with the plume covering a region near to the outfall and with a concentration of between about 0.001 and 0.1 mg/l. There were few differences between the base and storm flow inputs. When the Bellozanne STW input was reduced to 1 mg/l, then the corresponding plumes within the Bay were reduced considerably and the concentration was less than 0.005 mg/l everywhere, except very close to the outfall site. The mean spring tide concentrations across St. Aubin's Bay were reduced by typically 80 % (see Table 2).

Likewise, the neap tide results were again very similar, indicating that the DAIP concentration levels only exceeded 0.005 mg/l in a region close to the outfall and this plume was considerably reduced in plan surface area when the Bellozanne inputs were reduced to 1 mg/l. Hence, the model predictions indicated that the phosphorus levels across St. Aubin's Bay were generally low at below 0.005 mg/l, except in the region of the outfall. Similarly, as for the DAIN concentration distribution, these levels were considerably reduced when the Bellozanne STW inputs (i.e. base and storm flows) were reduced to 1 mg/l (see Table 2).

5. CONCLUSIONS

The States of Jersey Public Services Department is considering options for upgrading the Bellozanne Sewage Treatment Works. The design criteria being considered are the current and proposed European Union Urban Waste Water Treatment Directive (91/971/EEC) (UWWTD) and comprehensive field surveys of St. Aubin's Bay and the surrounding coastal waters have been undertaken. In parallel with this study the report herein highlights the outcome of a mathematical model study to predict the hydrodynamic conditions around Jersey Island and, in particular, in and around St. Aubin's Bay. Following the hydrodynamic study a comprehensive water quality study has been undertaken to assess the tidal exchange characteristics of St. Aubin's Bay and the concentration distributions of bacterial indicator and nutrient levels including:- total and faecal coliforms, faecal streptococci, dissolved available inorganic nitrogen and dissolved available inorganic phosphorus respectively. In particular, conditions have been assessed

for the current inputs and proposed new inputs from the Sewage Treatment Works at Bellozanne.

The main findings from this study can be summarised as follows:-

- A course grid hydrodynamic model has been set up from Guernsey due east and south to the French coast and using a regular 900 m grid. The model was driven by boundary data obtained from the Admiralty Chart and with good agreement being obtained between predicted and specified tidal currents and directions at eight sites within the domain.

- A fine grid hydrodynamic and water quality model has been set up, covering much of the south and eastern coastal zones around Jersey Island. The model used a 100 m regular grid, with boundary conditions obtained from the coarse grid model. As before, good agreement was obtained between predicted and specified tidal currents and directions at two sites within the domain.

- The tidal exchange predictions for St. Aubin's Bay showed that the tidal currents in the region were relatively low and that the tidal exchange coefficient after five tides was between 0.5 and 0.6. Such values indicated that the Bay was generally well flushed, with neap tides exhibiting a more uniform flushing with no marked dead zones. In contrast, flushing was poorer near to the shoreline for spring tides.

- The coliform predictions for bounded conditions, i.e. consecutive neap and spring tides, suggested that worst conditions occurred in the Bay for total coliforms during spring tide and for storm flow conditions with values across much of the Bay being typically 50 to 1,000 counts per 100 ml. The worst conditions occurred along the shoreline to the east of St. Aubin's Bay where, for neap tides and storm flow conditions, the peak concentrations reached above 2,000 counts per 100 ml. This relatively high concentration came from the Weighbridge Catchment effluent discharge and it is recommended that consideration be given to reducing the coliform input levels from this outfall. However, the construction of the Fort Regent Cavern,

and the consequential routing of storm overflows from the Weighbridge Outfall through the Bellozanne STW, will significantly reduce the input of coliforms to the Bay when it becomes operational.

- The nutrient level predictions, again bounded by simulating consecutive neap and spring tide conditions, showed that the Bellozanne STW was the main source of DAIN and DAIP concentration levels in St. Aubin's Bay, but that the Weighbridge Catchment input primarily contributed to the plume advecting along the south-eastern shoreline of the Island. The peak local concentrations across the Bay for DAIN inputs was about 0.05 mg/l for spring and neap tides and with the peak values in the shoreline plume from the Weighbridge Catchment outfall being about 0.5 mg/l.

When the DAIN input from the Bellozanne STW was reduced to 10 mg/l, then the DAIN concentration levels over most of the Bay were less than 0.05 mg/l and with the peak outfall concentration being about 0.05 to 0.1 mg/l. Thus, reducing the DAIN inputs through the STW to 10 mg/l generally reduced the Bay concentrations by typically close to 50 % (i.e. about 46%).

For the DAIP inputs for the existing effluent discharge, then the concentration levels across the Bay were typically less than 0.01 mg/l and were between 0.001 and 0.1 mg/l in the proximity of the outfall. When the STW effluent was reduced to 1 mg/l, the concentration plume across the Bay were considerably reduced in plan surface area, with concentrations exceeding 0.005 mg/l only very close to the outfall. Comparisons of the mean concentrations across the Bay (Table 2) for both base and storm flows, showed that by reducing the DAIP effluent to 1 mg/l from the Bellozanne STW would reduce the mean concentrations by typically 80 to 90 %.

These results showed that nutrient removal from the Bellozanne STW works would reduce the DAIN concentrations by typically up to 50 % in St. Aubin's Bay and with the DAIP concentrations being reduced by typically 80 %. These reductions are appreciable and it is there fore recommended that consideration therefore be given to nitrogen reduction, particularly since nitrogen is the limiting factor in algal growth in marine waters

(Stapleton and Kay, 1997). Again the Weighbridge Catchment has a noticeable impact on raising the nutrient levels along the south-east coastal zone of the Island and steps to reduce the nutrient input via this outfall may also be worthy of consideration.

6. ACKNOWLEDGEMENTS

The authors would like to thank Dr Clive Swinnerton (Chief Executive, Public Services Department, States of Jersey) and his colleagues, particularly Mr. Boyd Bennie, for their support and encouragement throughout this project.

The authors are also grateful to Professor David Kay and Carl Stapleton (Centre for Research into Environment and Health, University of Leeds) for their assistance and provision of data etc. at all stages of the project.

7. REFERENCES

Bowie, G.L. et. al, (1985), "Rates, Constants and Kinetics Formulations in Water Quality Modelling", Environmental Research Laboratory, US EPA, Athens, GA, Report No. EPA/600/3-85/040, June, pp. 475

Brown, L.C. and Barnwell, T.O. Jr, (1987), "The Enhanced Stream Water Quality Models QUAL2E and QUAL2E-UNCAS: Documentation and User Manual", Environmental Research Laboratory, US EPA, Athens, GA, Report No. EPA/600/3-87/007, May, pp. 189

Cahyono, M., (1993), "Three-Dimensional Numerical Modelling of Sediment Transport Processes in Non-Stratified Estuarine and Coastal Waters", PhD thesis, University of Bradford, pp. 315

Elder, J.W., (1959), "The Dispersion of Marked Fluid in Turbulent Shear Flow", Journal of Fluid Mechanics, Vol. 5, Part 4, pp. 544-560

Engelund, F. and Hansen, E., (1967), "A Monograph on Sediment Transport in Alluvial Streams", Teknisk Forlag, Copenhagen

Falconer, R.A., (1976), "Mathematical Modelling of Jet-Forced Circulation in Reservoirs and Harbours", PhD Thesis, University of London, London, pp. 237

Falconer, R.A., (1986), "A Two-Dimensional Mathematical Model Study of the Nitrate Levels in an Inland Natural Basin", Proceeding of International Conference on Water Quality Modelling in the Inland Natural Environment, BHRA Fluid Engineering, Bournemouth, England, Paper J1, June, pp. 325-344

Falconer, R.A., (1993), "An Introduction to Nearly Horizontal Flows", in Coastal, Estuarial and Harbour Engineer's Reference Book, eds. Abbott and Price, E and F N Spon Ltd., London, pp. 27-36

Falconer, R.A. and Chen, Y., (1991), "An Improved Representation of Flooding and Drying and Wind Stress Effect in a 2-D Tidal Numerical Model", Proceedings of the Institution of Civil Engineers, Part 2, Research and Theory, Vol. 91, pp. 659-678

Falconer, R.A., George, D.G. and Hall, P., (1991), "Three-Dimensional Numerical Modelling of Wind-Driven Circulation in a Shallow Homogeneous Lake", Journal of Hydrology, Vol. 124, pp. 59-79

Fischer, H.B., (1973), "Longitudinal Dispersion and Turbulent Mixing in Open Channel Flow", Annual Review of Fluid Mechanics, Vol.5, pp. 59-78

Fischer, H.B., List, E.J., Koh, R.C.Y., Imberger, J. and Brooks, N.H., (1979), "Mixing in Inland and Coastal Waters", Academic Press, New York

French, R.H., (1986), "Open Channel Hydraulics", McGraw-Hill Co., Singapore, pp. 705

Hall, P., (1987), "Numerical Modelling of Wind Induced Lake Circulation", PhD Thesis, University of Birmingham, Birmingham

Henderson, F.M., (1966), "Open Channel Flow", Collier-Macmillan Co. Ltd., McGraw-Hill Co., New York

Kuipers, J. and Vreugdenhil, C.B., (1973), "Calculation of Two-Dimensional Horizontal Flow", Delft Hydraulics Laboratory Technical Rep. S163, Part 1, pp. 1-44

Leonard, B.P., (1991), "The ULTIMATE Conservative Difference Scheme Applied to Unsteady One-Dimensional Advection", Computer Methods and Applications in Mechanical Engineering, Vol. 88, pp. 17-79

Lin, B. and Falconer, R.A., (1997a), "Tidal Flow and Transport Modelling Using the ULTIMATE QUICKEST Scheme", Journal of Hydraulic Engineering, ASCE, Vol.123, No.4, pp.303-314.

Lin, B. and Falconer, R.A., (1997b), "Three-Dimensional Layer Integrated Modelling of Estuarine Flows with Flooding and Drying", Estuarine, Coastal and Shelf Science, Academic Press Ltd., (in press)

Nece, R.E. and Falconer, R.A., "Hydraulic Modelling of Tidal Circulation and Flushing in Coastal Basins", Proceeding of the Institution of Civil Engineers part 1, Design and Construction, October 1989, Vol. 86, pp. 913-936

O'Neill, J.G., "Field Techniques for Validation of Bacterial Decay and Dispersion Models", in Hydraulic and Environmental Modelling of Coastal, Estuarine and River Waters, Ed. R.A. Falconer et. al., Gower Technical, Aldershot, 1989, pp. 694

Rodi, W., (1984), "Turbulence Models and their Application in Hydraulics", IAHR, Second Edition, Delft, The Netherlands, pp. 1-104

van Rijn, L.C., (1984a), "Sediment Transport Part 1: Bed Load Transport", Journal of Hydraulic Engineering, ASCE, Vol. 110, pp. 1431-1456

van Rijn, L.C., (1984b), "Sediment Transport Part 11: Suspended Load Transport", Journal of Hydraulic Engineering, ASCE, Vol. 110, pp. 1613-1641

Stapleton, C. and Kay, D.S., "Tropic Status of St Aubin's Bay", Report to States of Jersey Public Services Department, November 1997, pp. 28.

Wu, J., (1969), "Wind Stress and Surface Roughness at Air-Sea Interface", Journal of Geophysical Research, Vol. 74, pp. 444-4

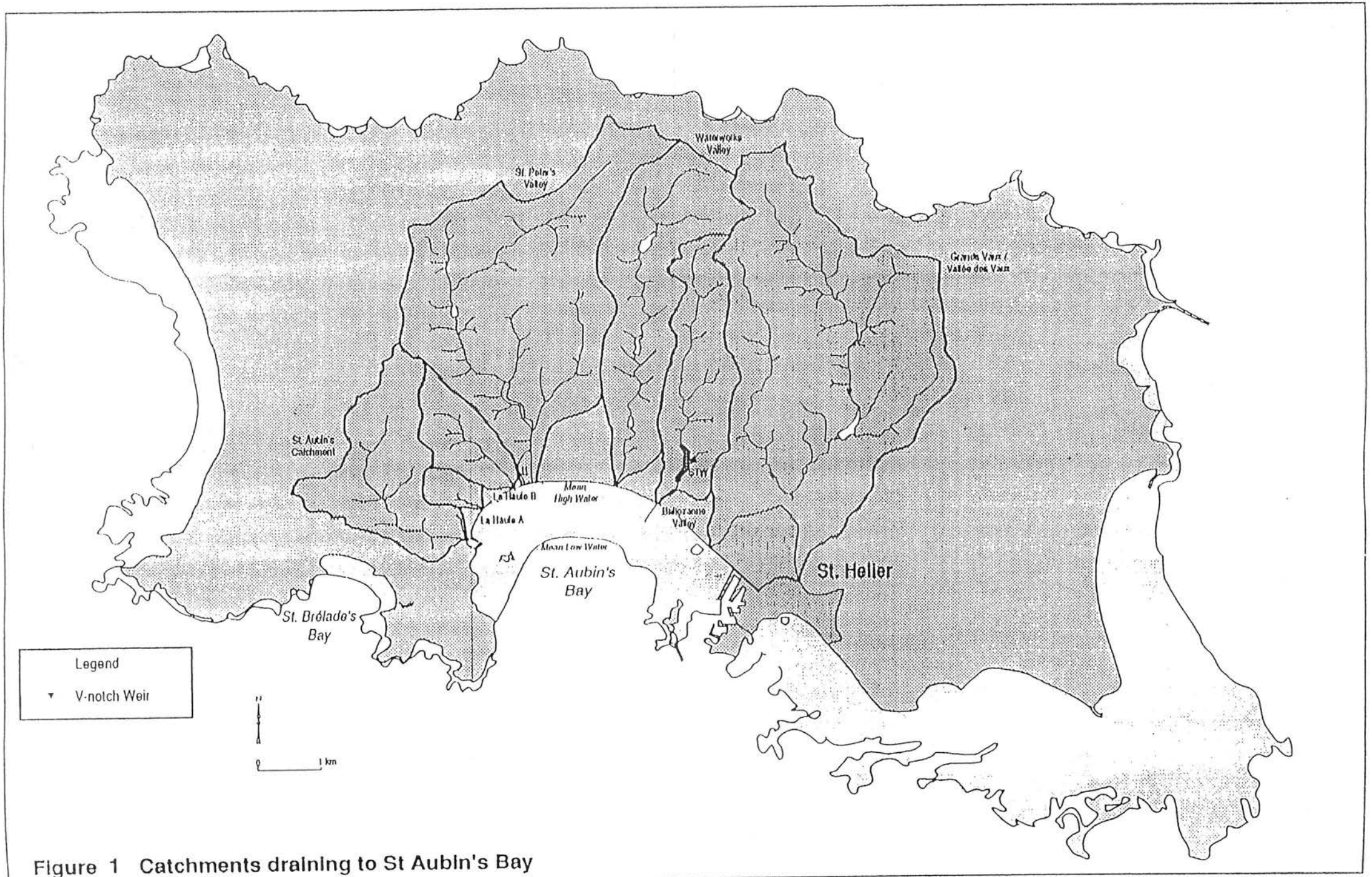

Figure 1 Catchments draining to St Aubin's Bay

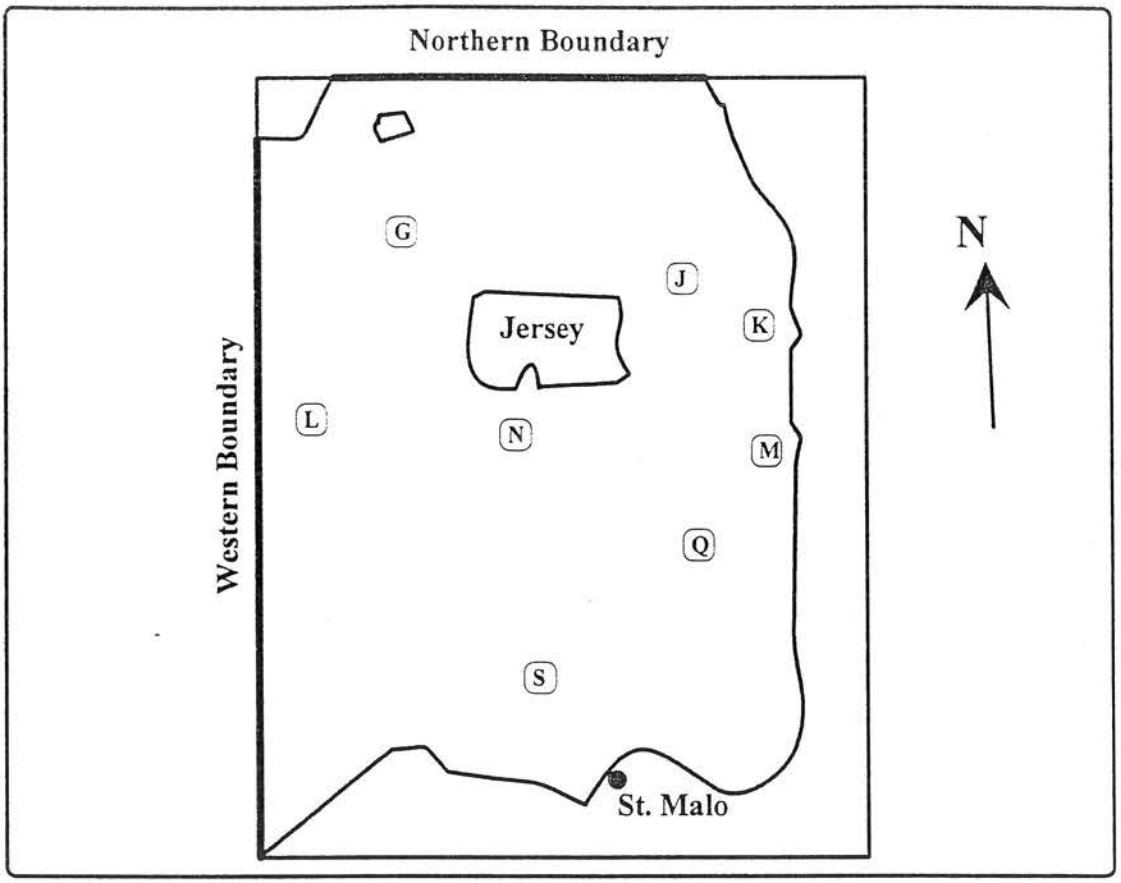

Figure 2 Sketch of the coarse grid domain

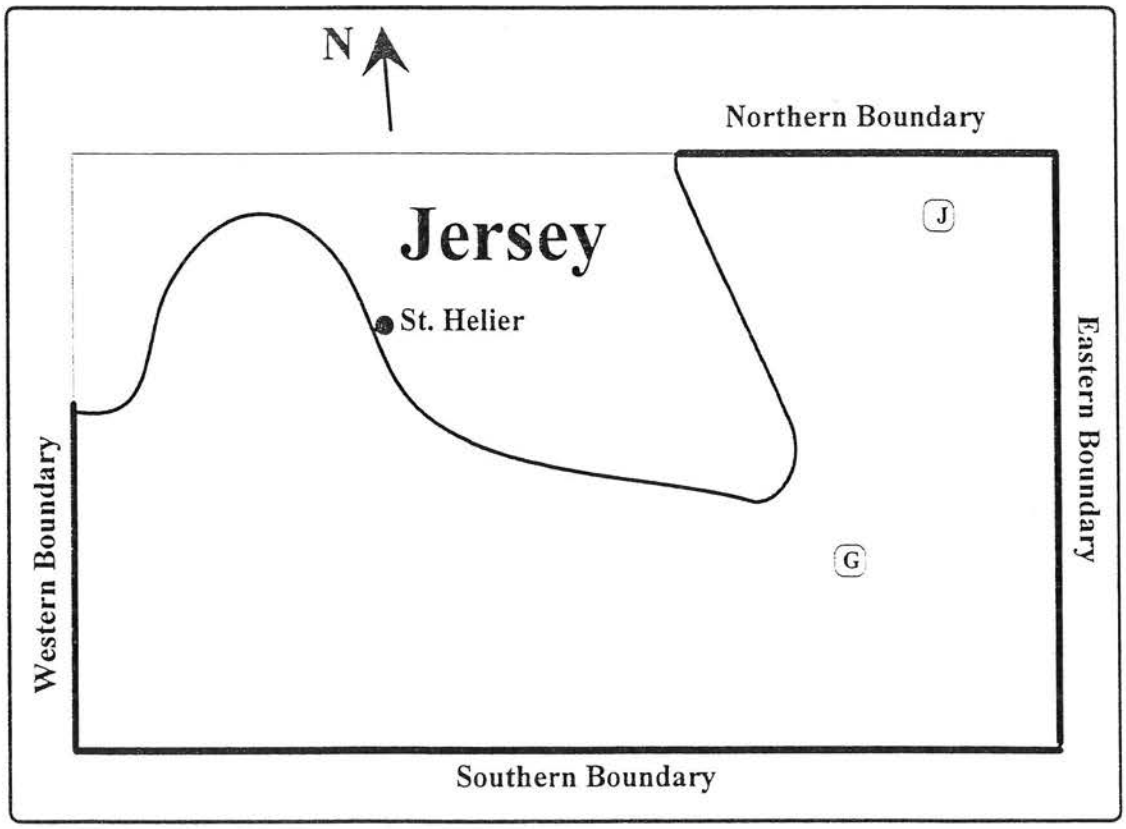

Figure 3 Sketch of the fine grid domain

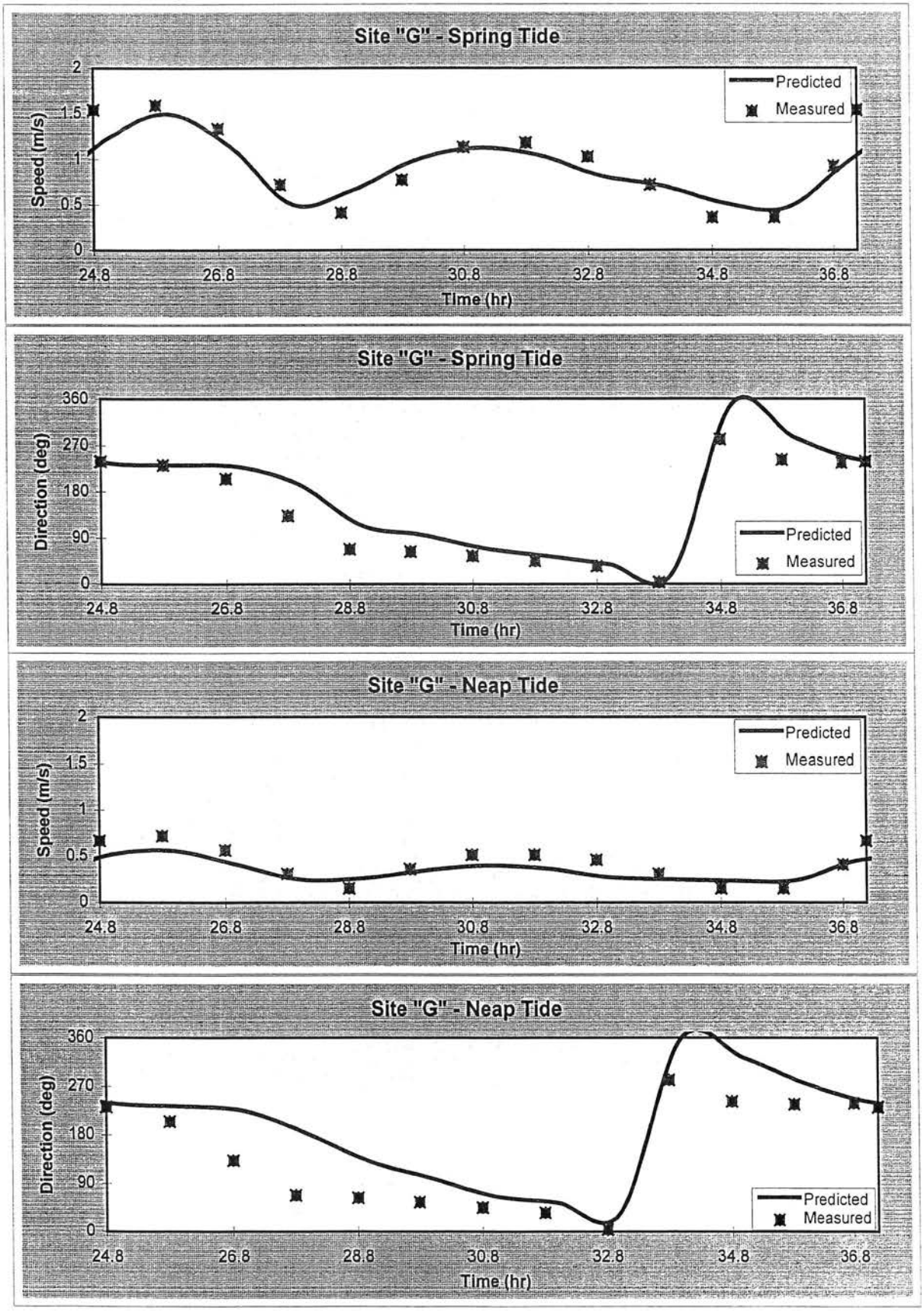

Figure 4 Comparison of predicted coarse grid and measured velocity components at site G

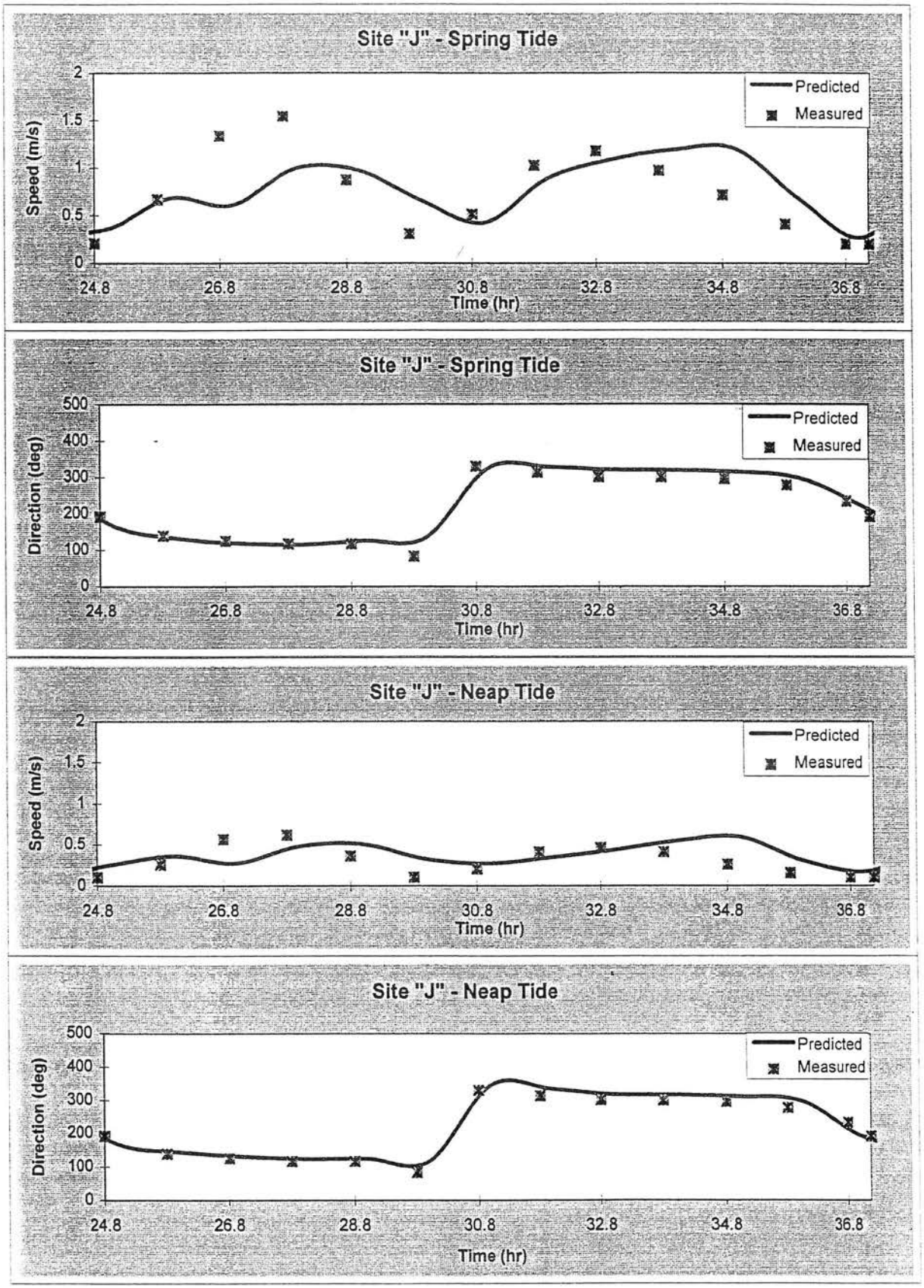

Figure 5 Comparison of predicted coarse grid and measured velocity components at site J

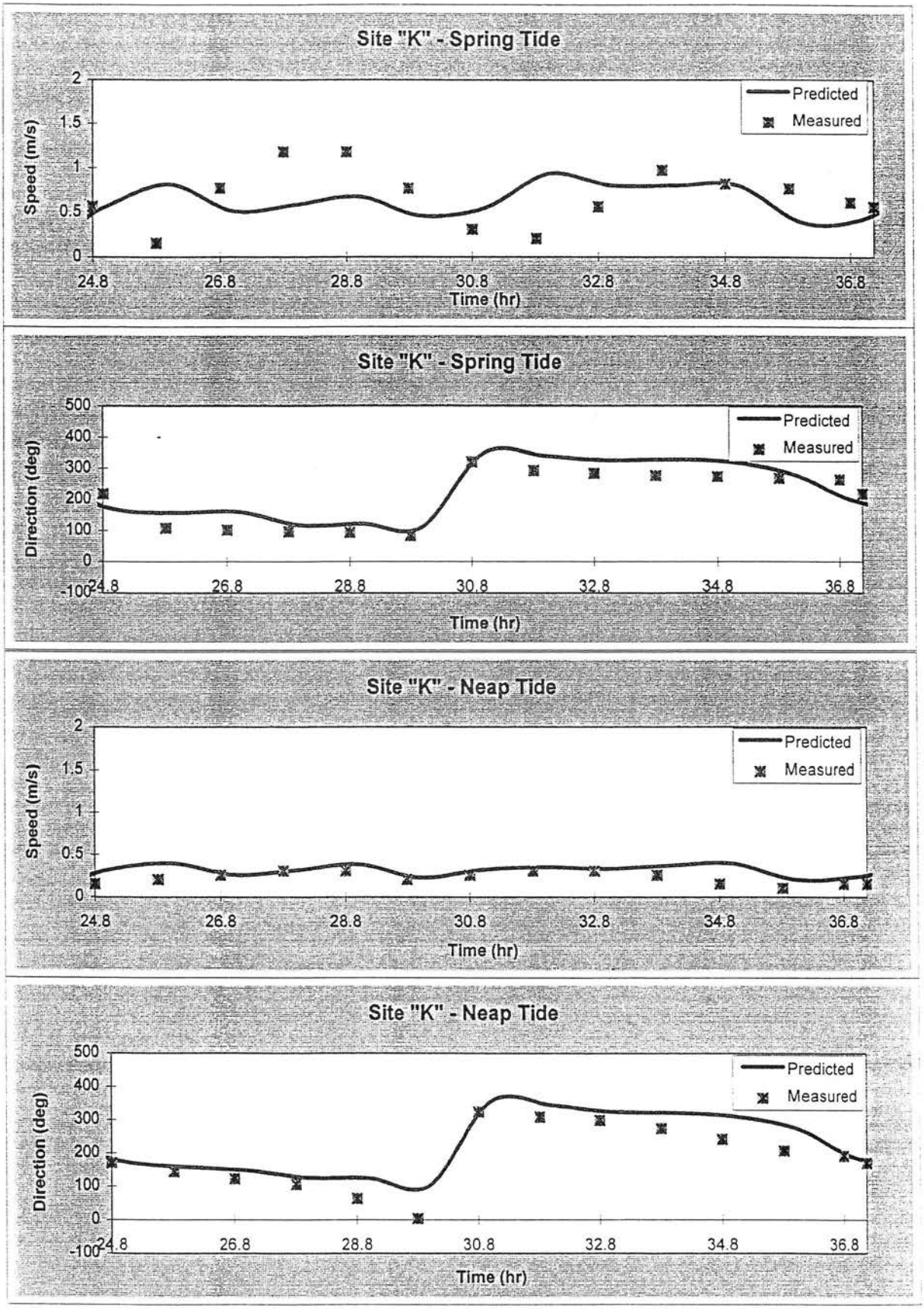

Figure 6 Comparison of predicted coarse grid and measured velocity components at site K

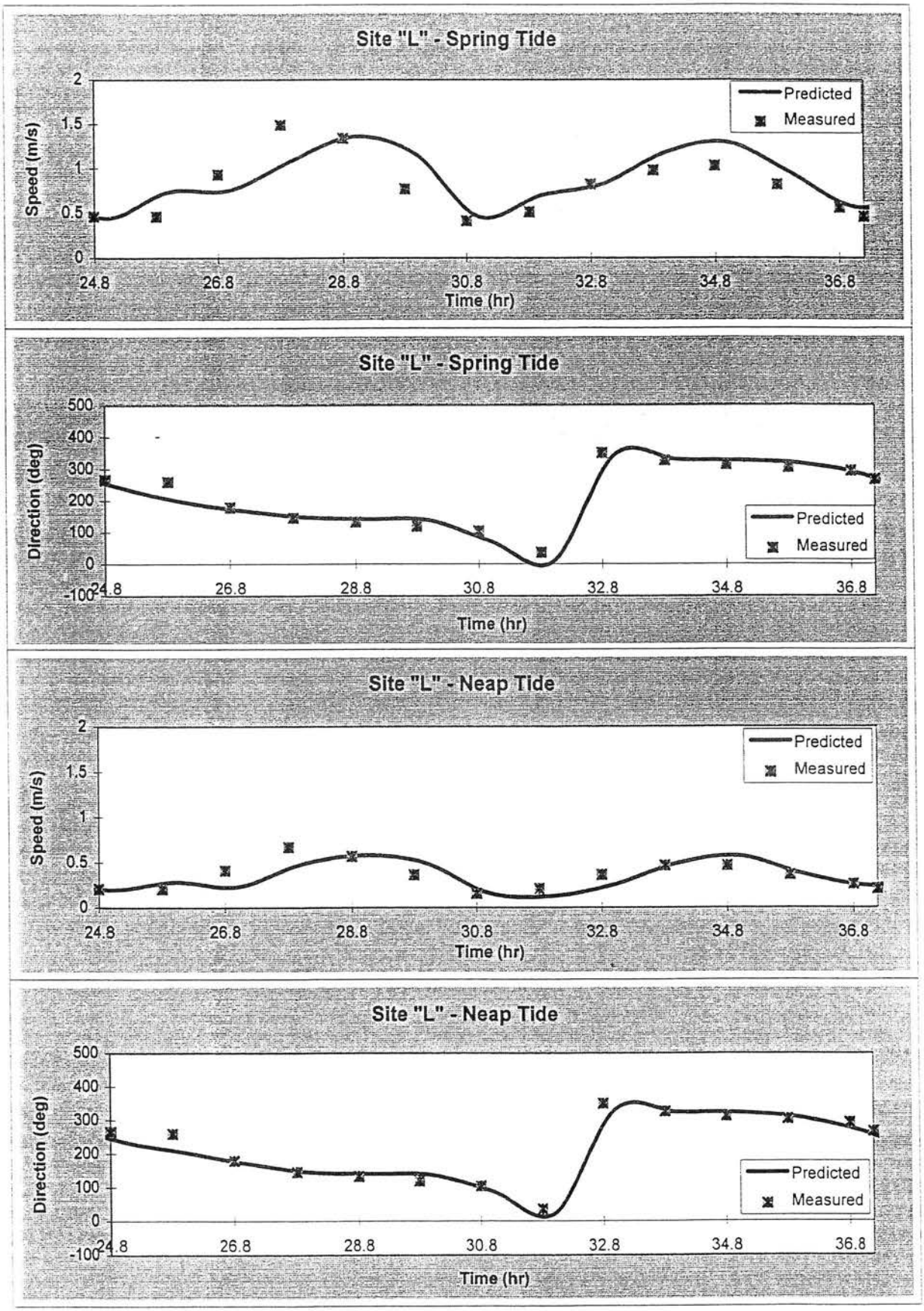

Figure 7 Comparison of predicted coarse grid and measured velocity components at site L

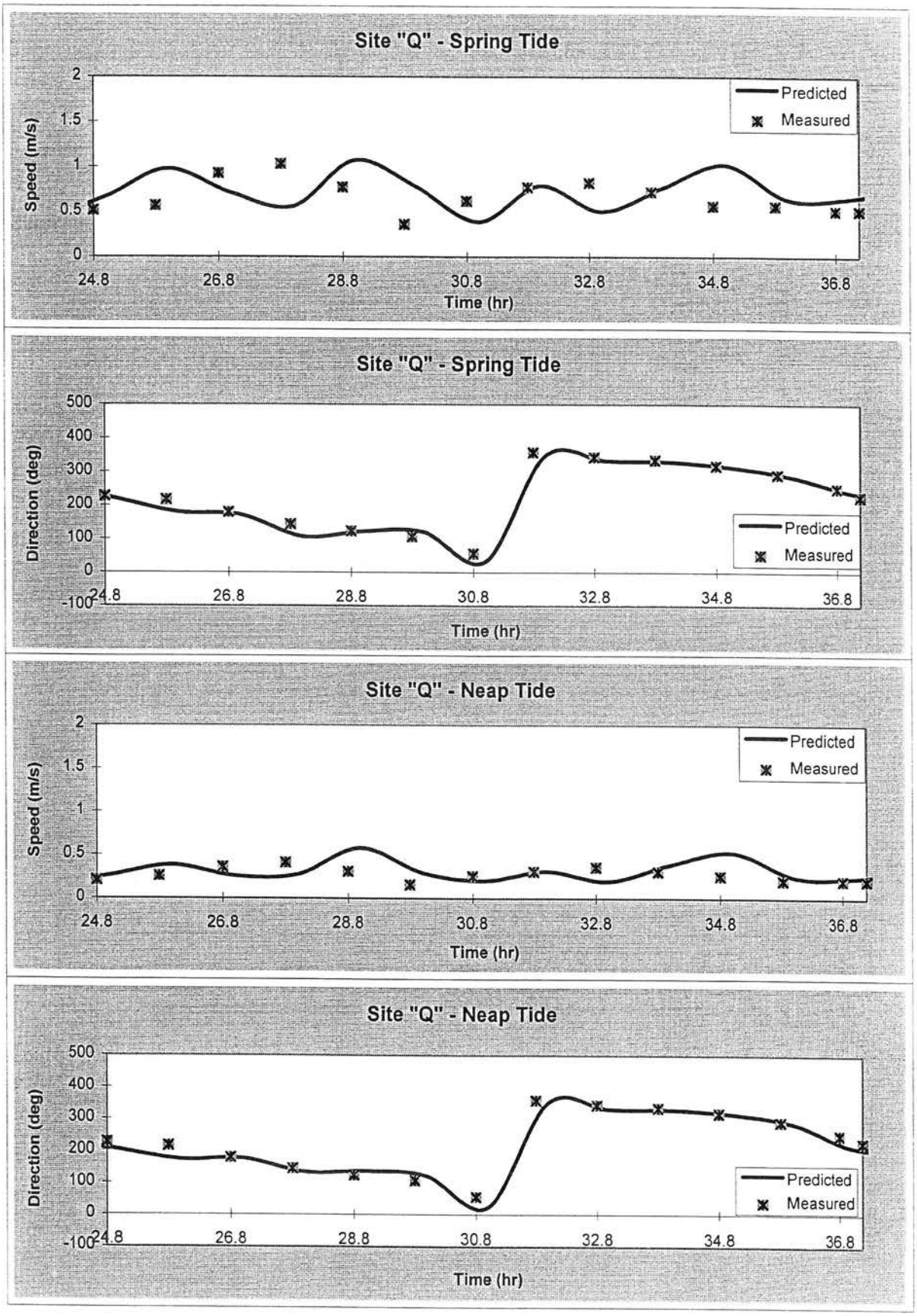

Figure 10 Comparison of predicted coarse grid and measured velocity components at site Q

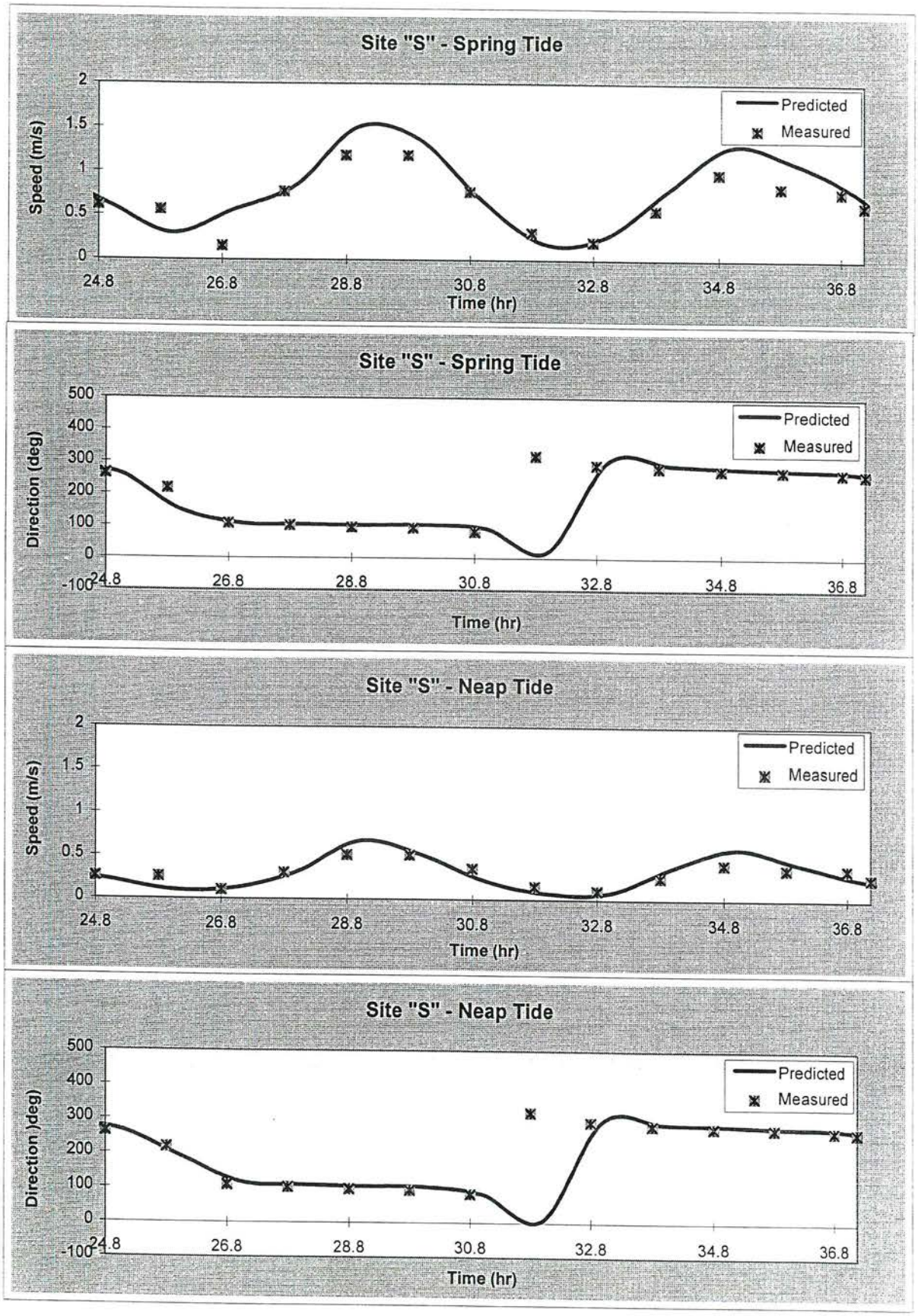

Figure 11 Comparison of predicted coarse grid and measured velocity components at site S

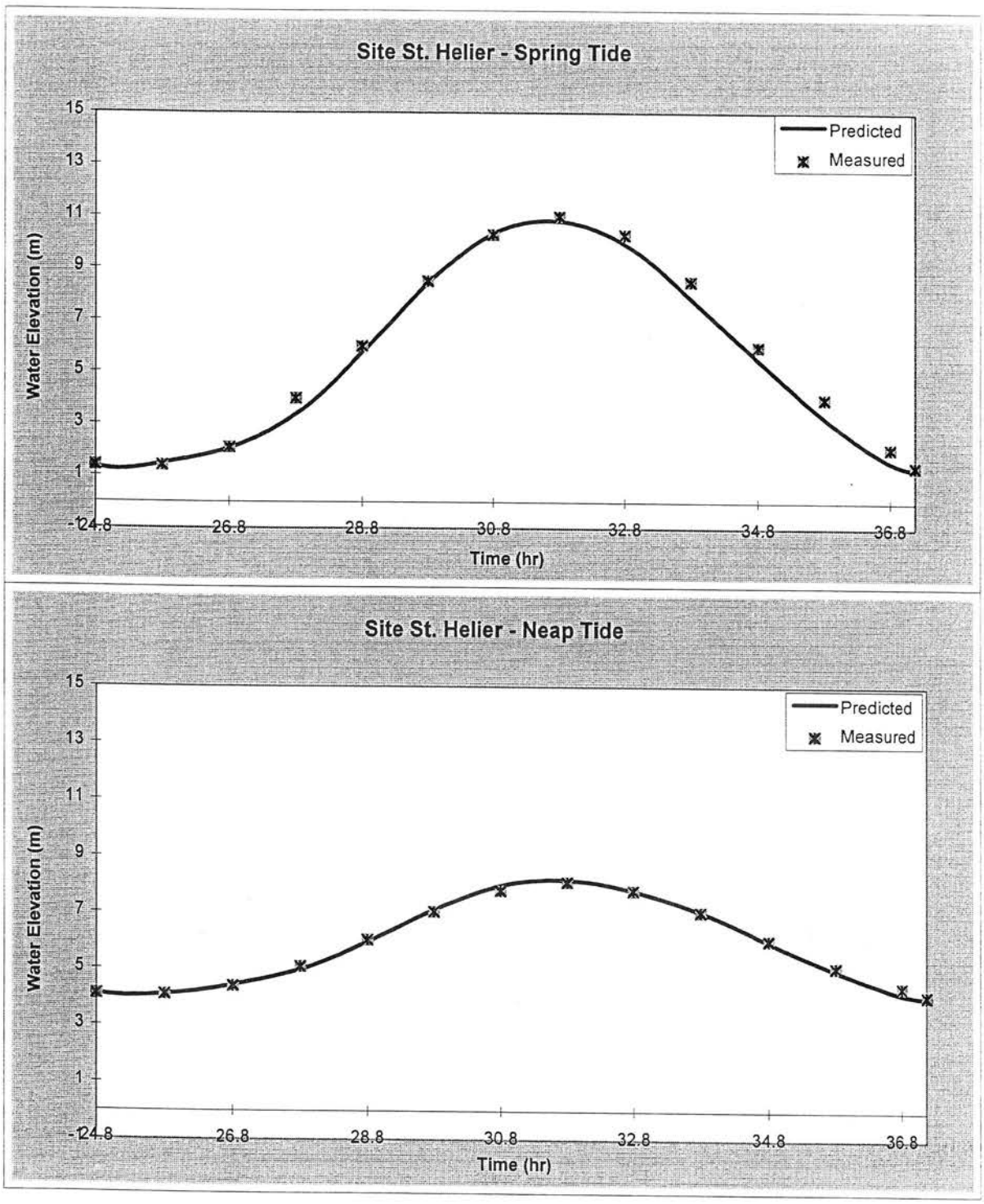

Figure 12 Comparison of predicted coarse grid and measured water elevations at St. Helier

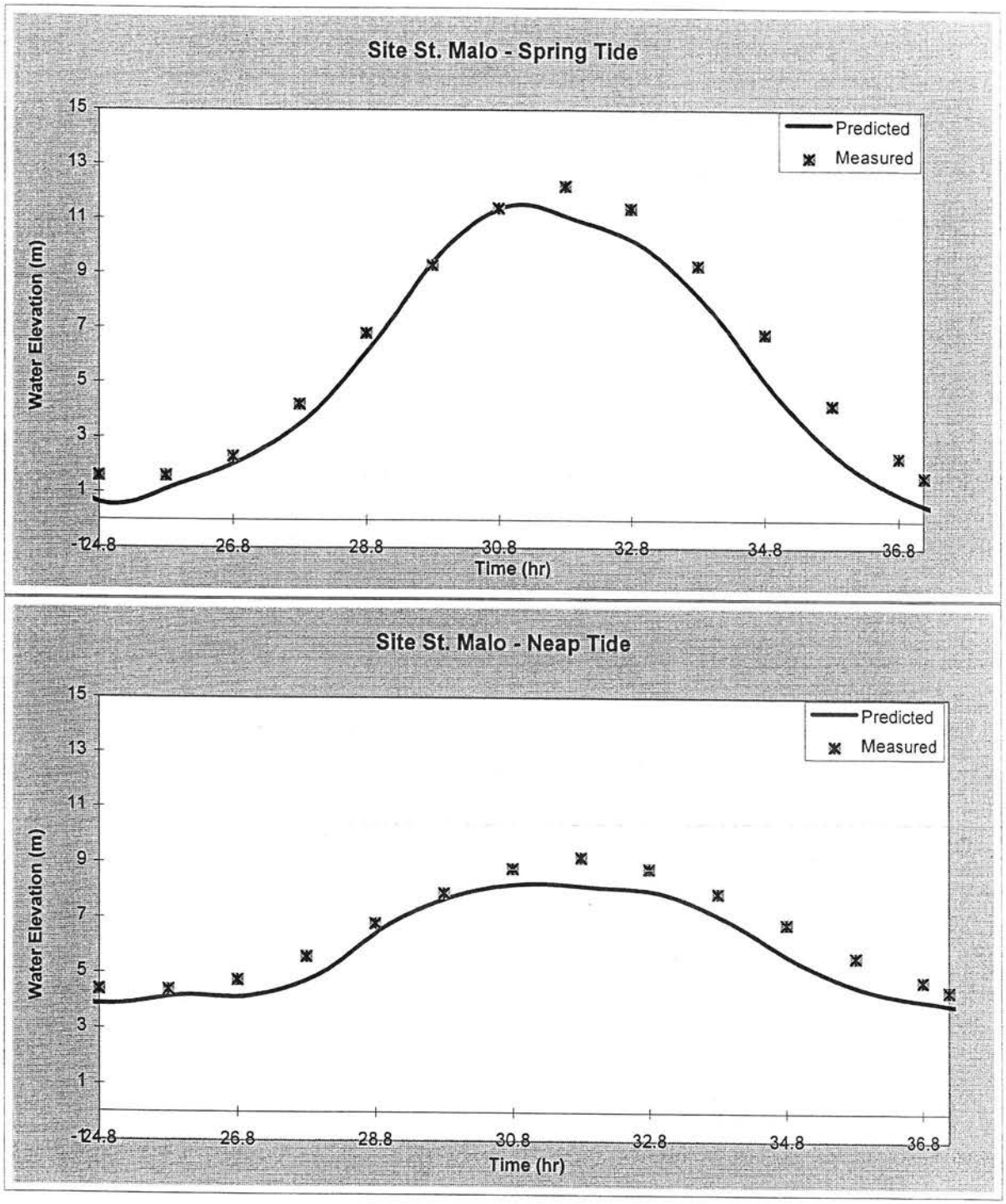

Figure 13 Comparison of predicted coarse grid and measured water elevations at St. Malo

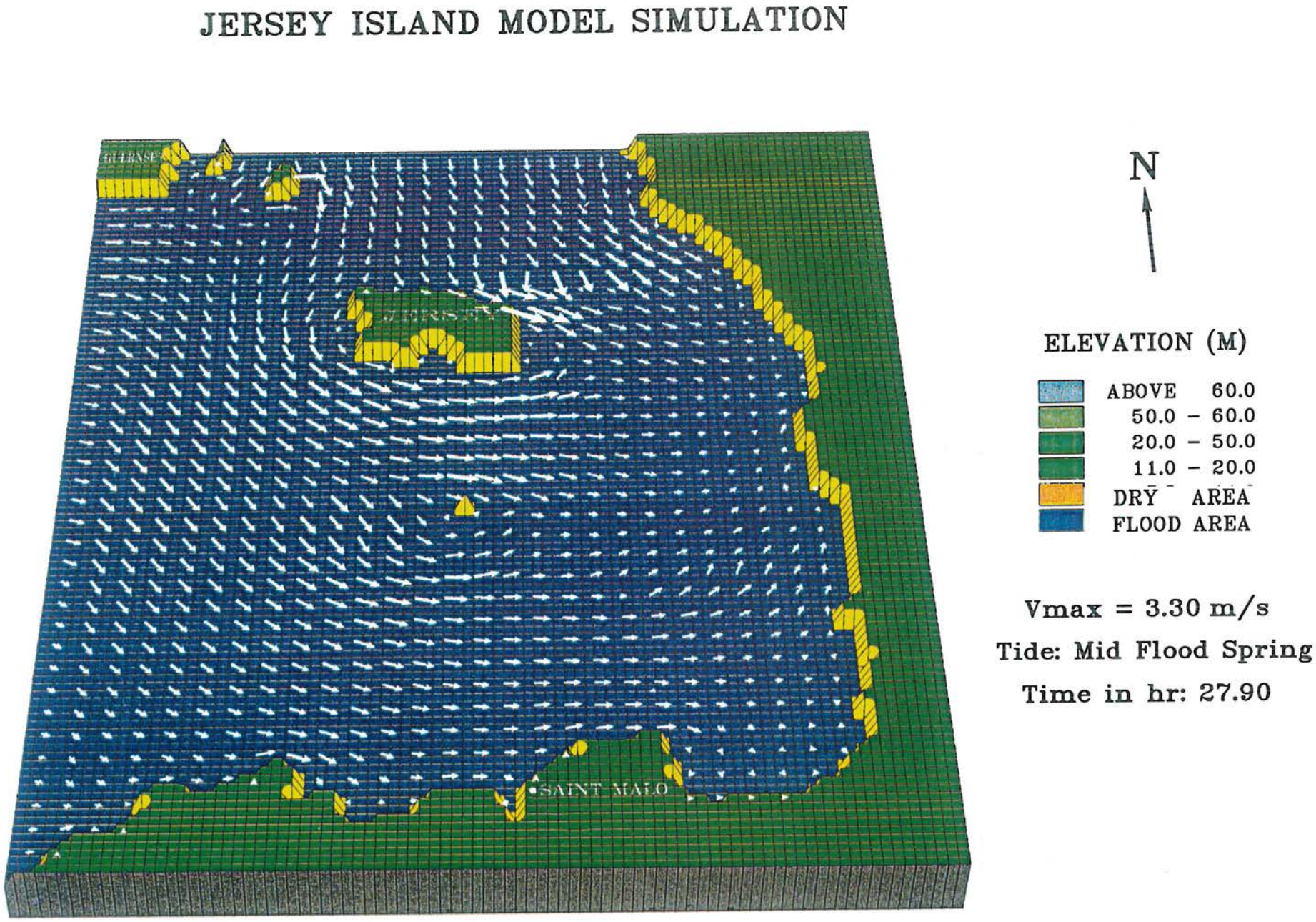

Figure 14 Tidal currents around Jersey Island at mid-flood spring tide (coarse grid)

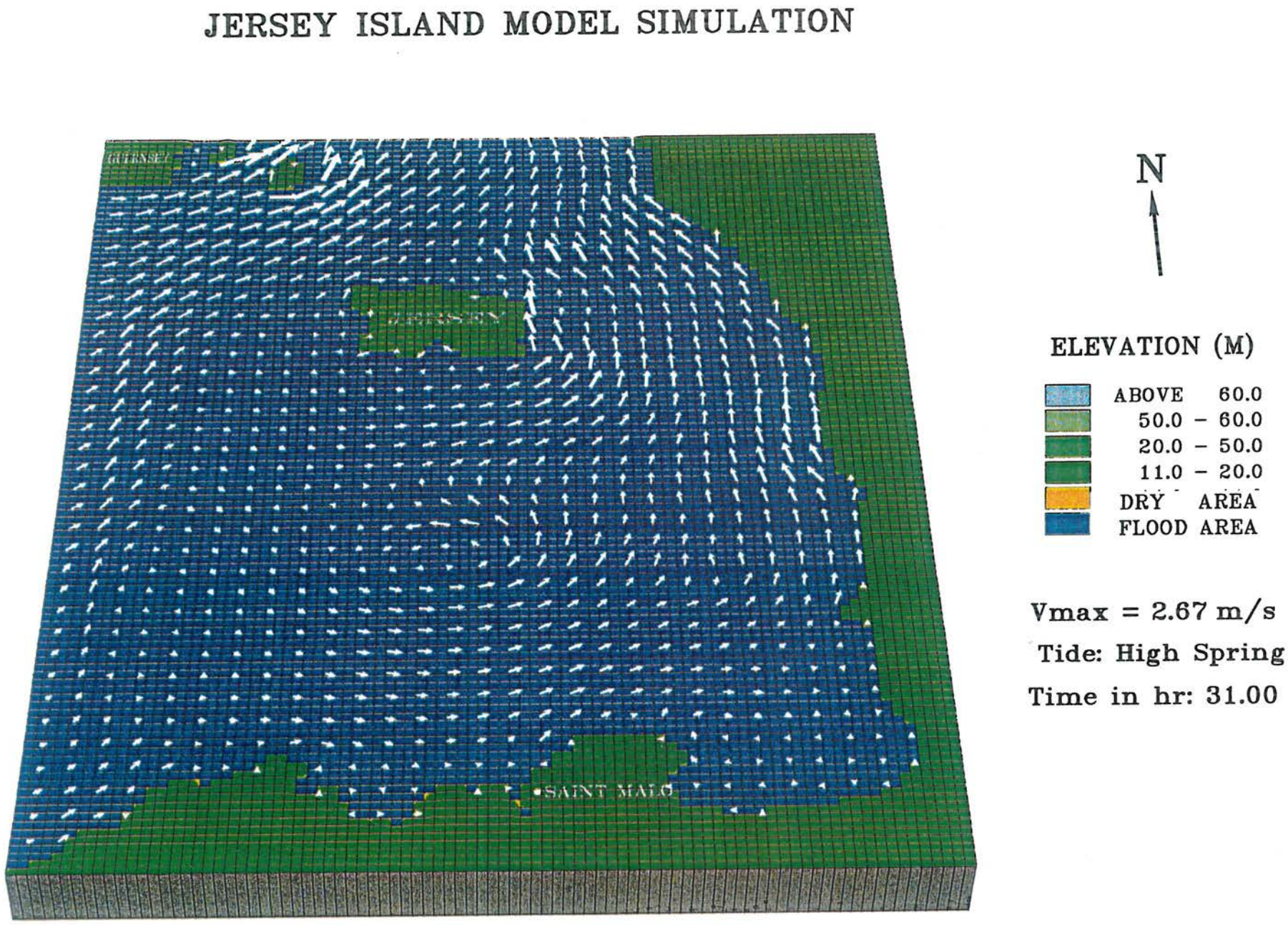

Figure 15 Tidal currents around Jersey Island at high spring tide (coarse grid)

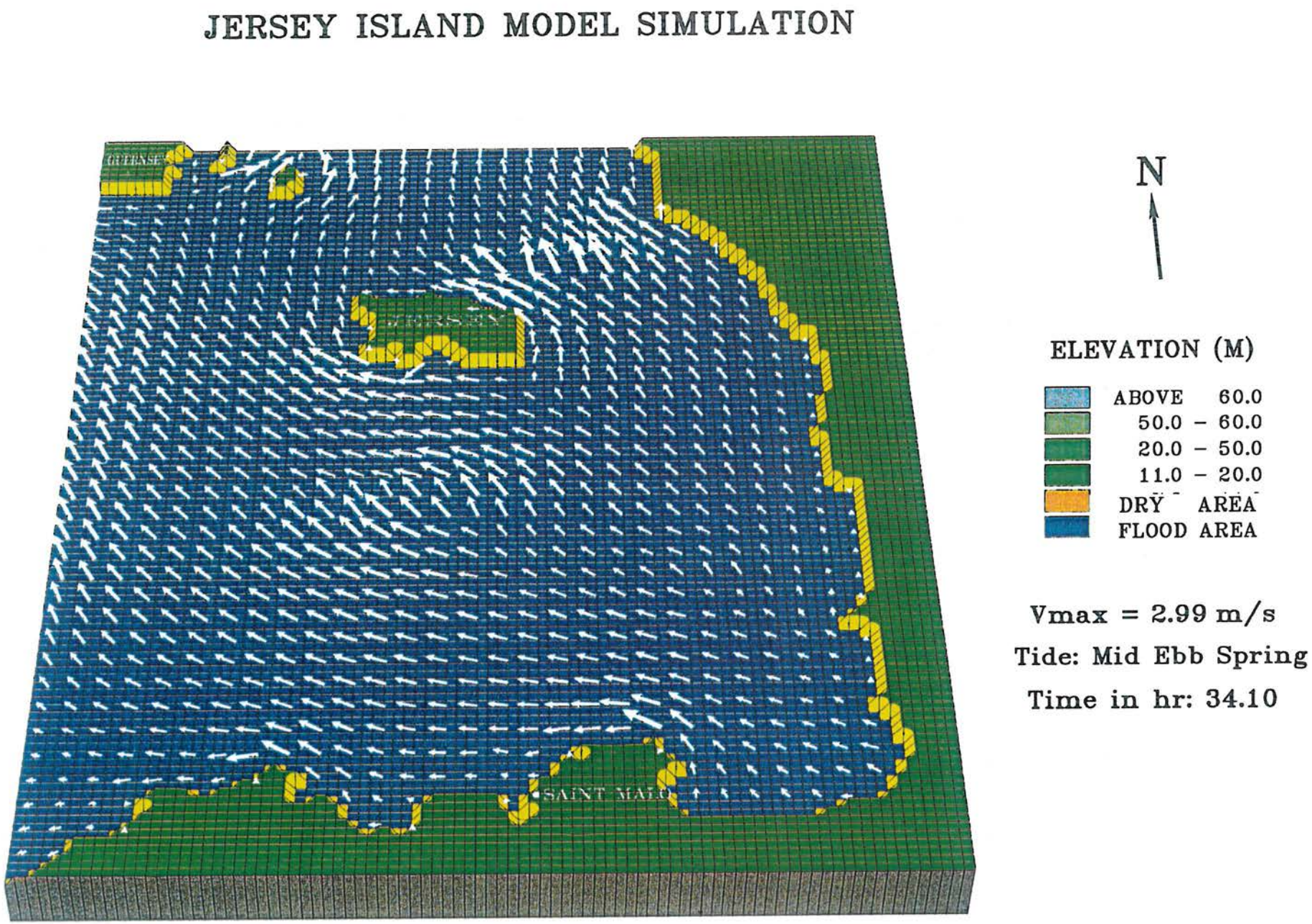

Figure 16 Tidal currents around Jersey Island at mid-ebb spring tide (coarse grid)

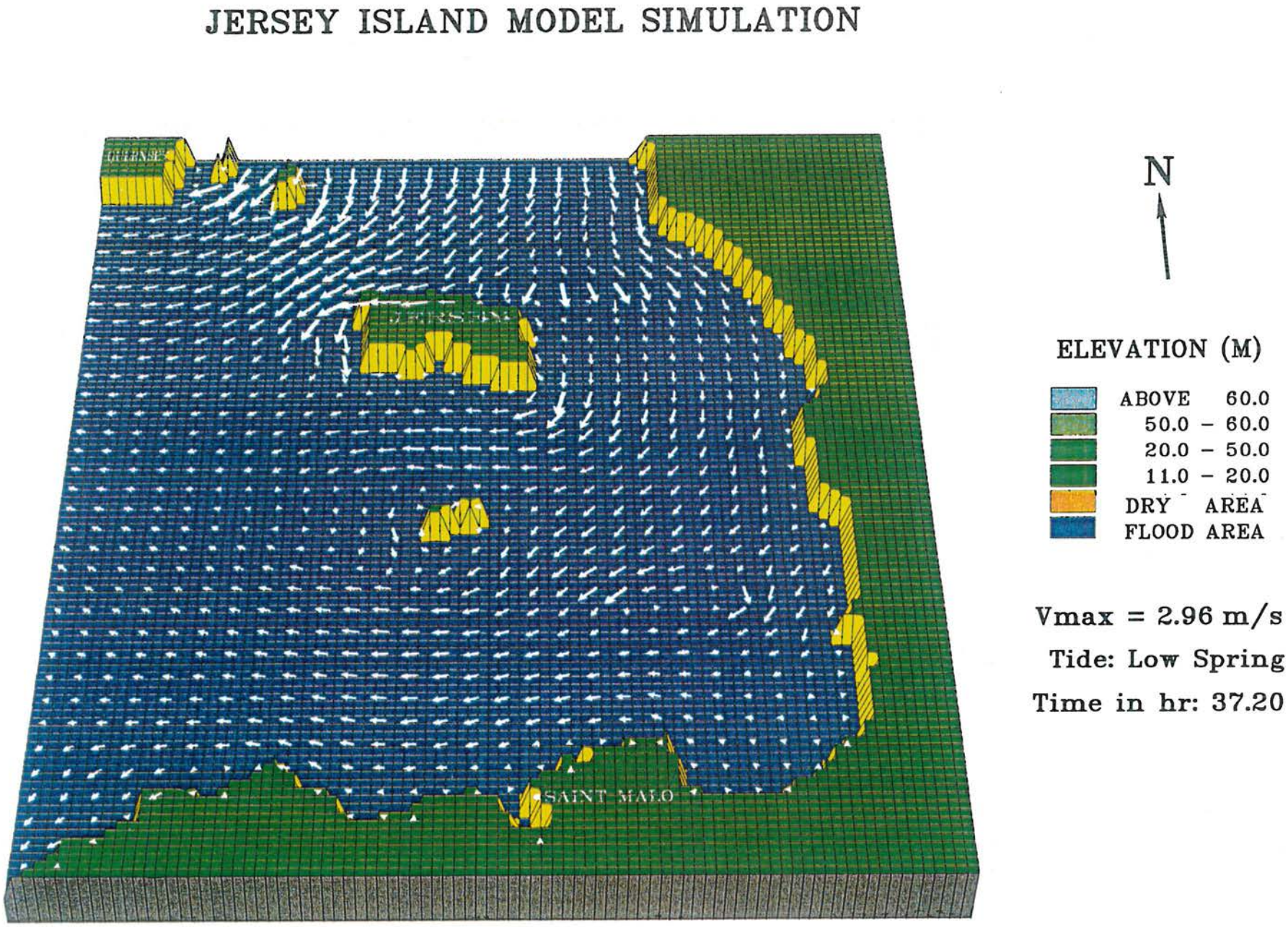

Figure 17 Tidal currents around Jersey Island at low spring tide (coarse grid)

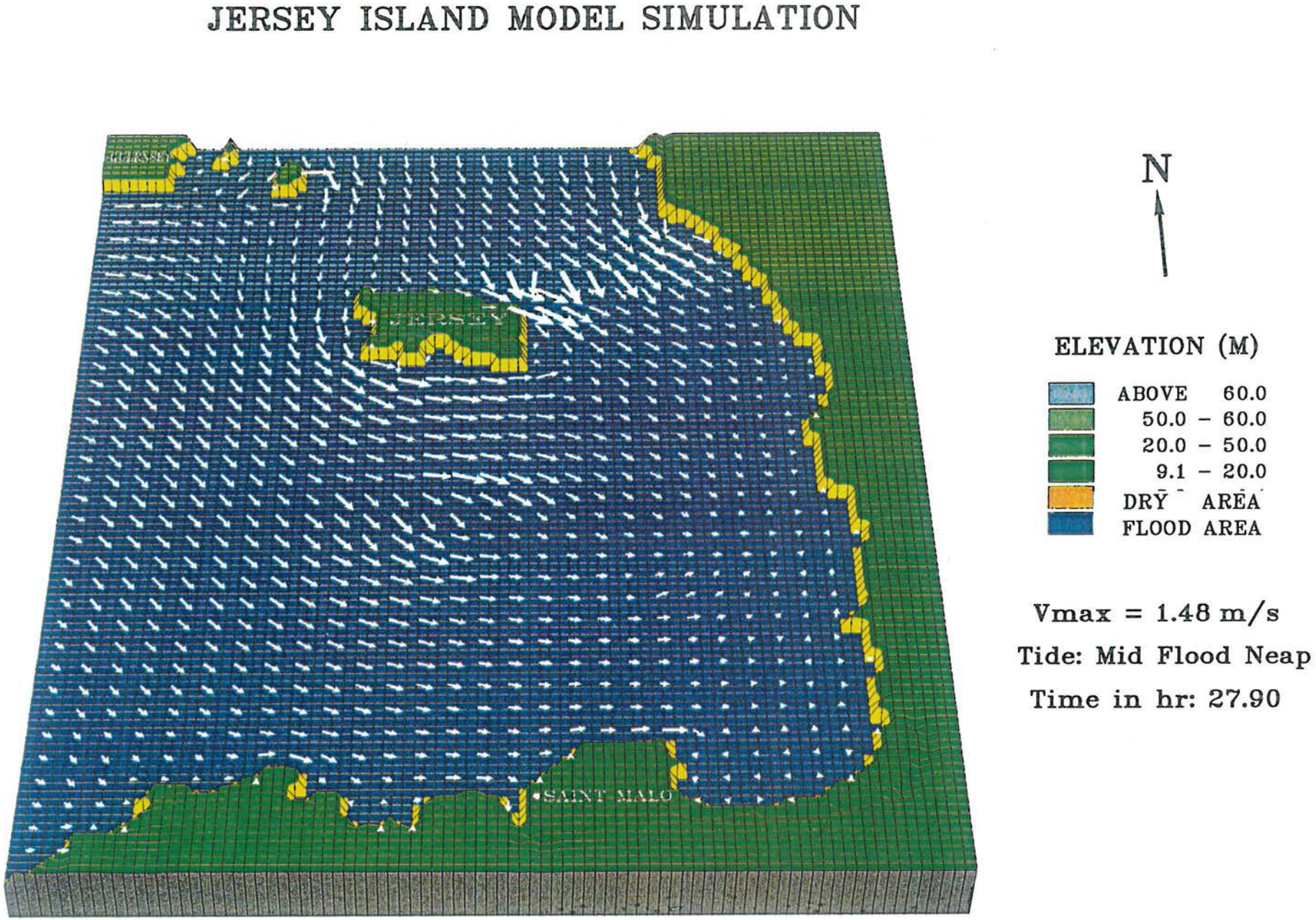

Figure 18 Tidal currents around Jersey Island at mid-flood neap tide (coarse grid)

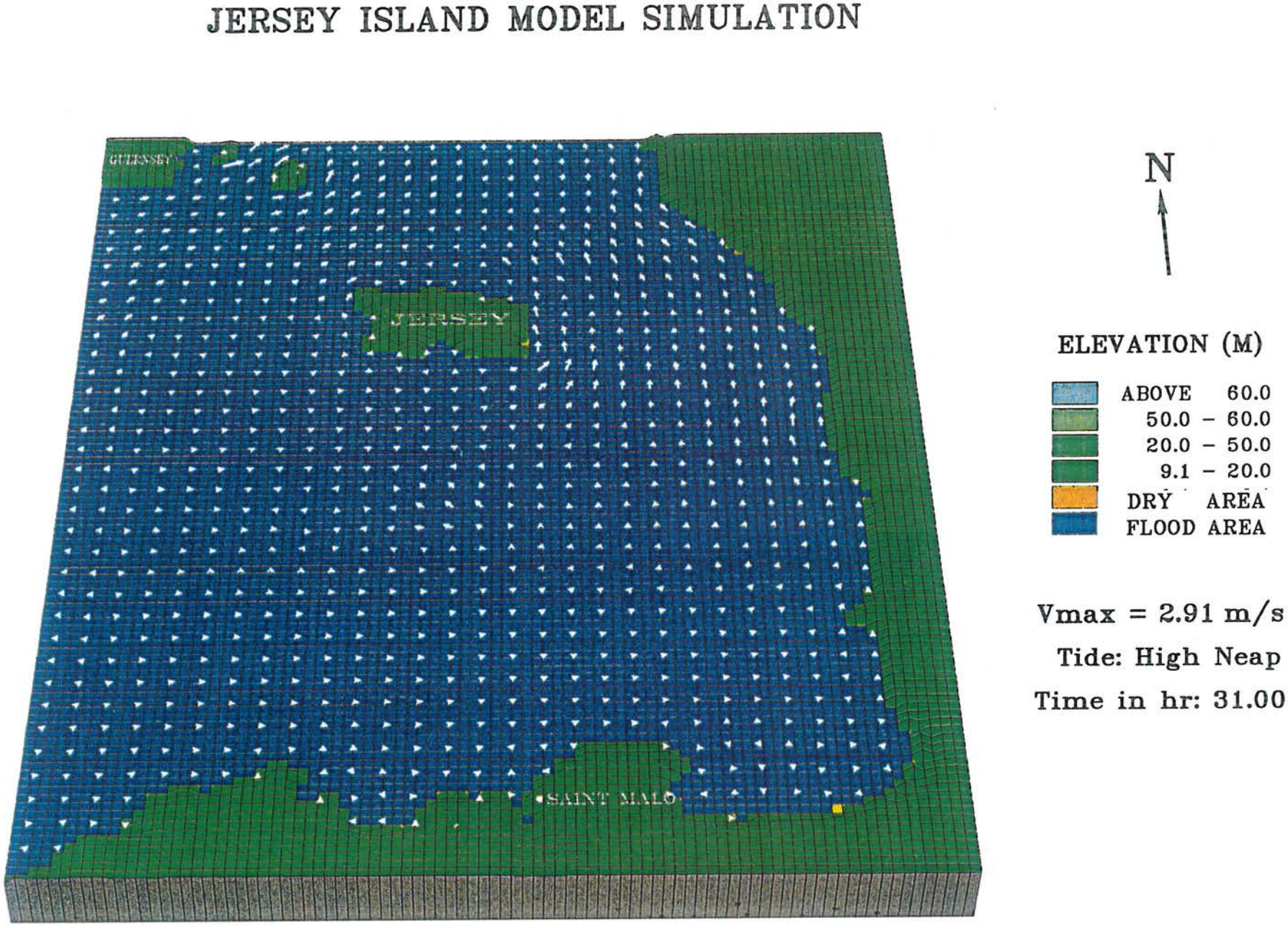

Figure 19 Tidal currents around Jersey Island at high neap tide (coarse grid)

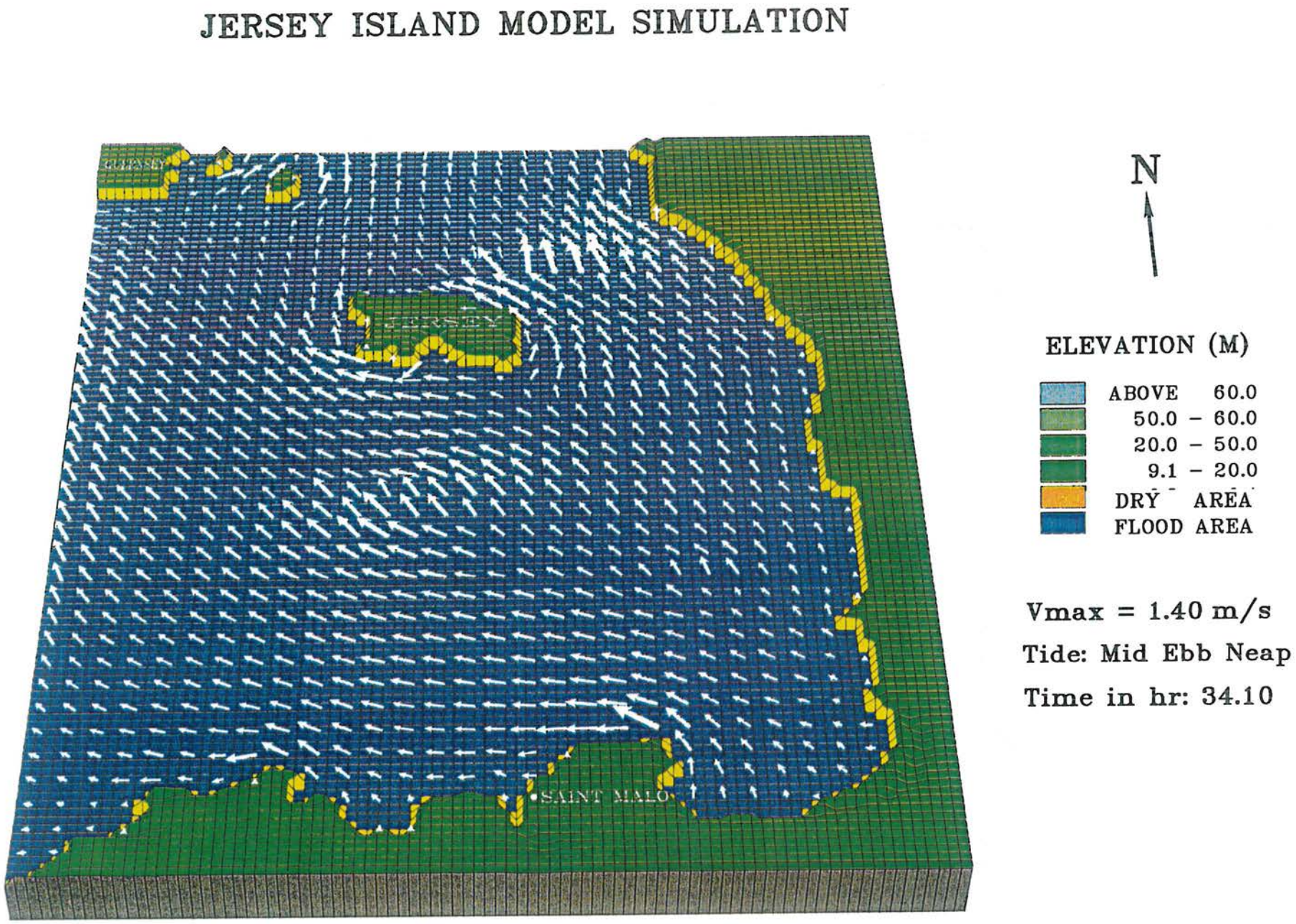

Figure 20 Tidal currents around Jersey Island at mid-ebb neap tide (coarse grid)

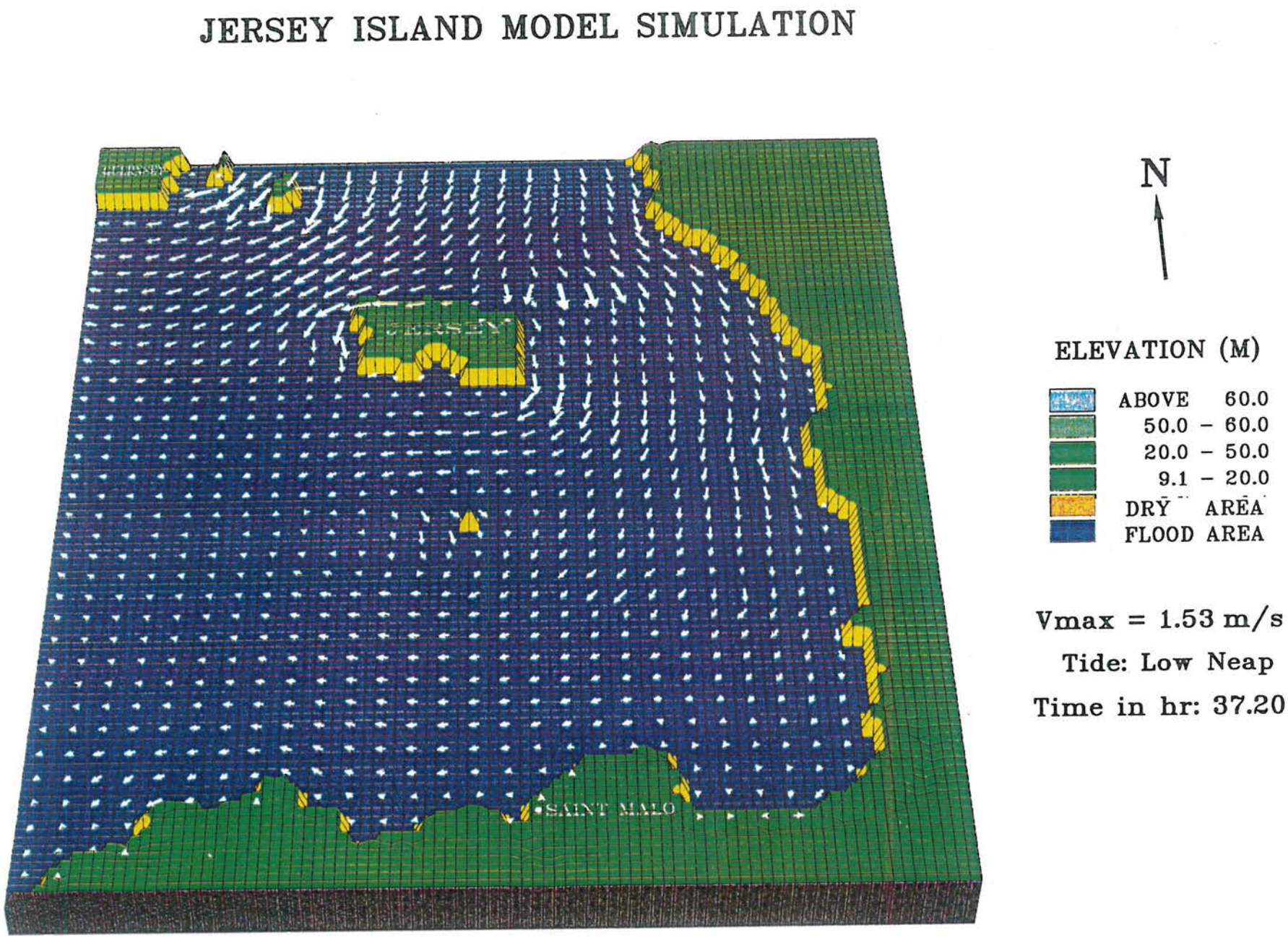

Figure 21 Tidal currents around Jersey Island at low neap tide (coarse grid)

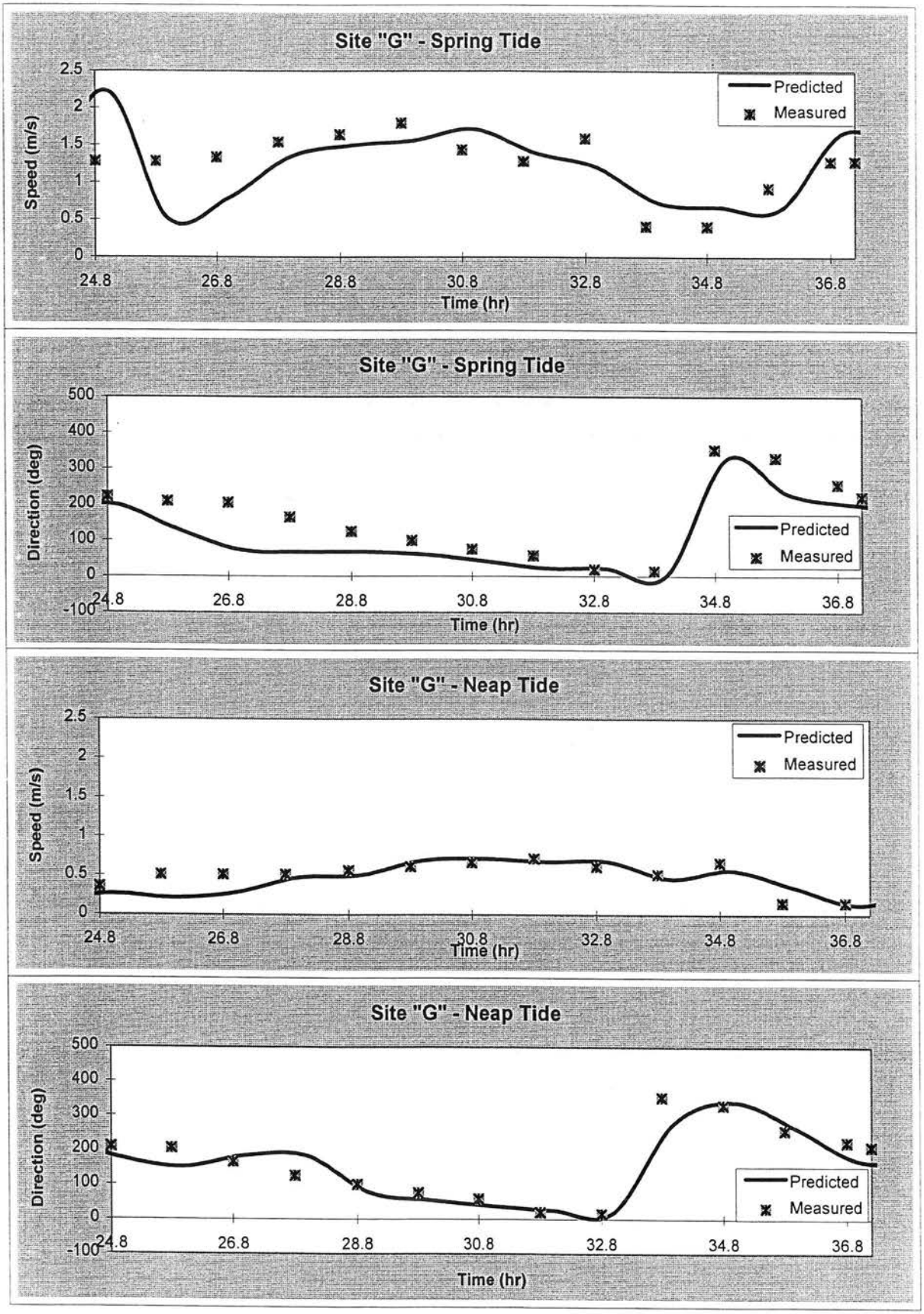

Figure 22 Comparison of predicted fine grid and measured velocity components at site G

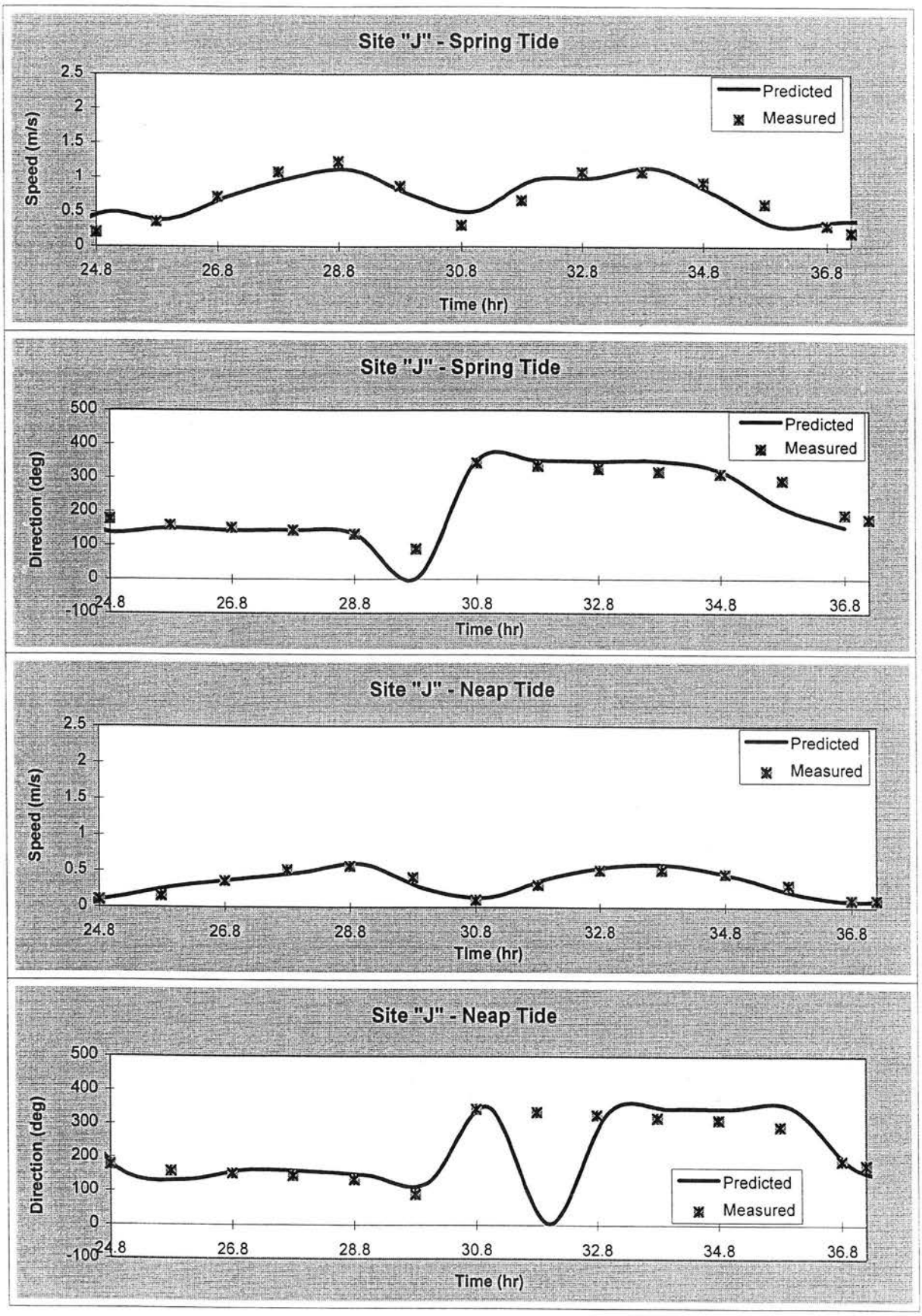

Figure 23 Comparison of predicted fine grid and measured velocity components at site J

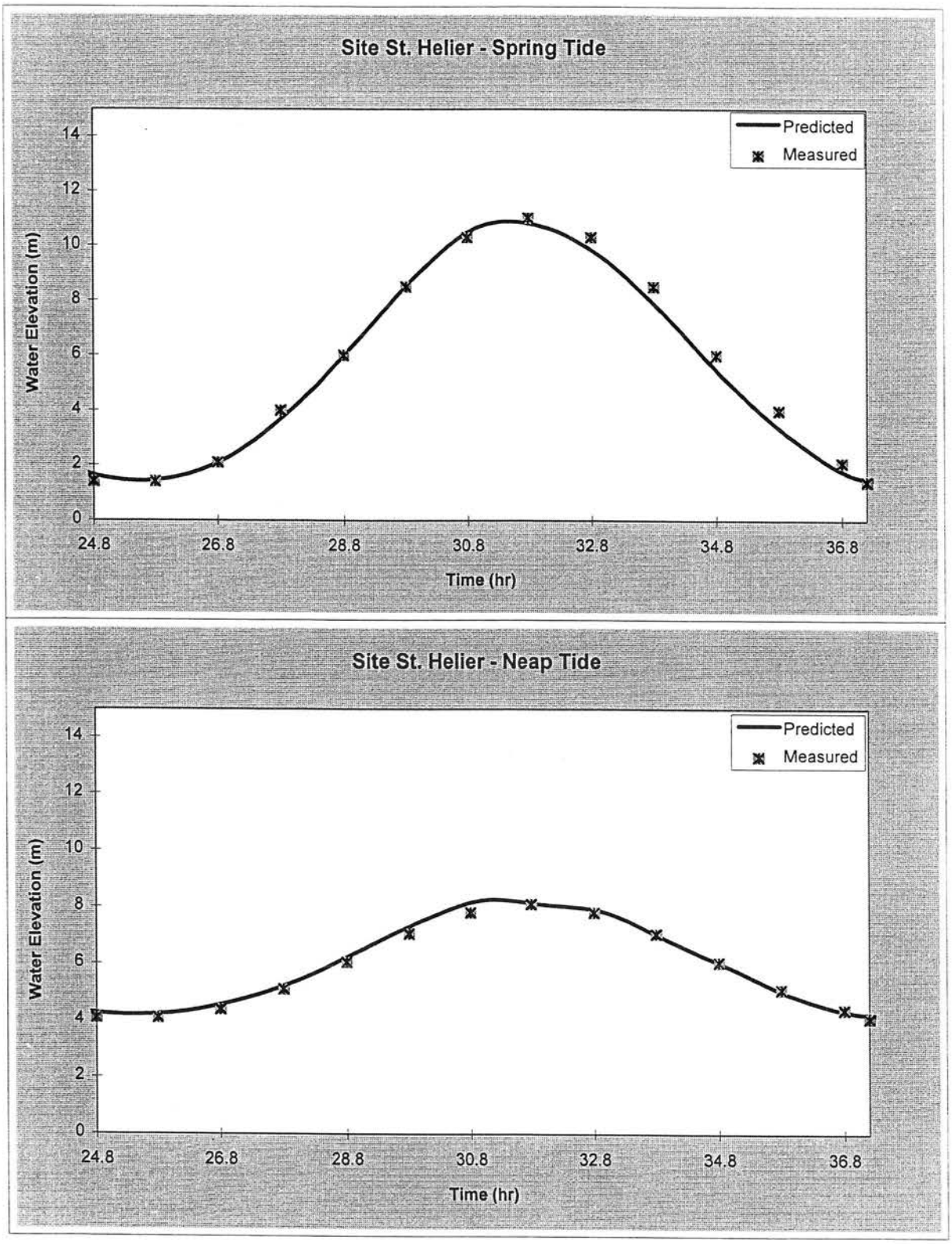

Figure 24 Comparison of predicted fine grid and measured water elevations at St. Helier

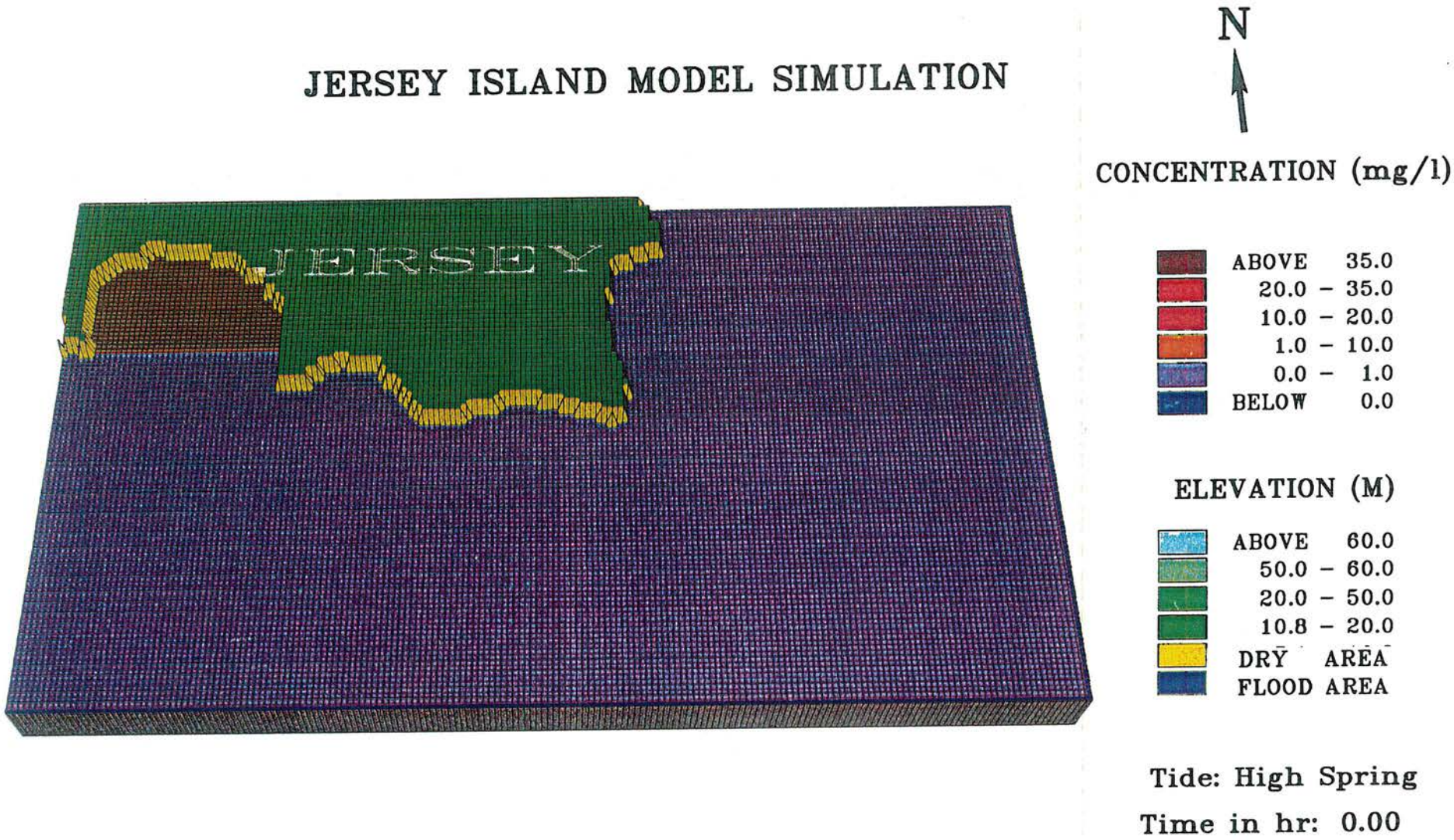

Figure 25 Initial concentration distribution in St. Aubin's Bay at start of simulation

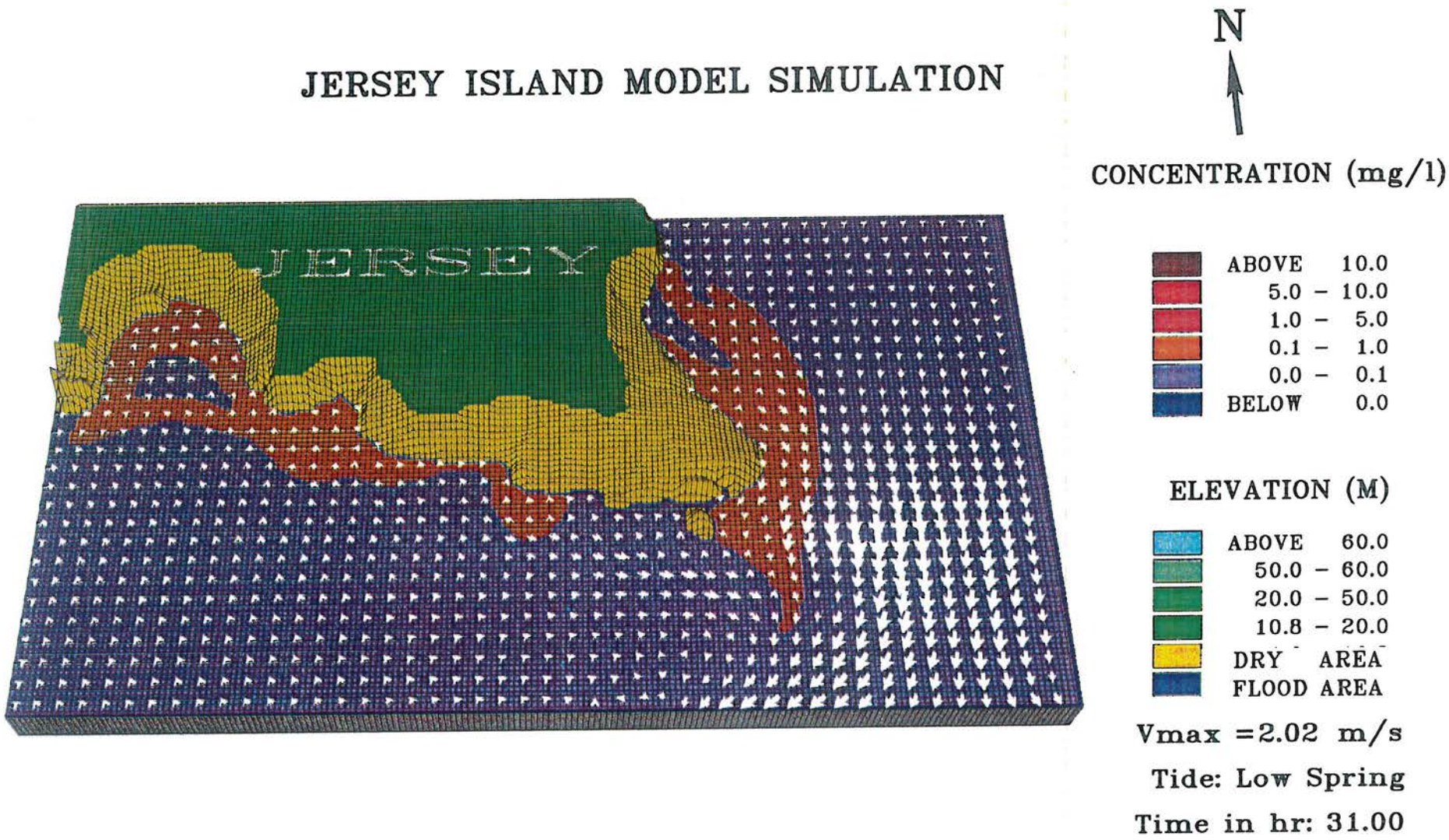

Figure 26 Tracer distribution around Jersey Coastline at low spring tide during third tide

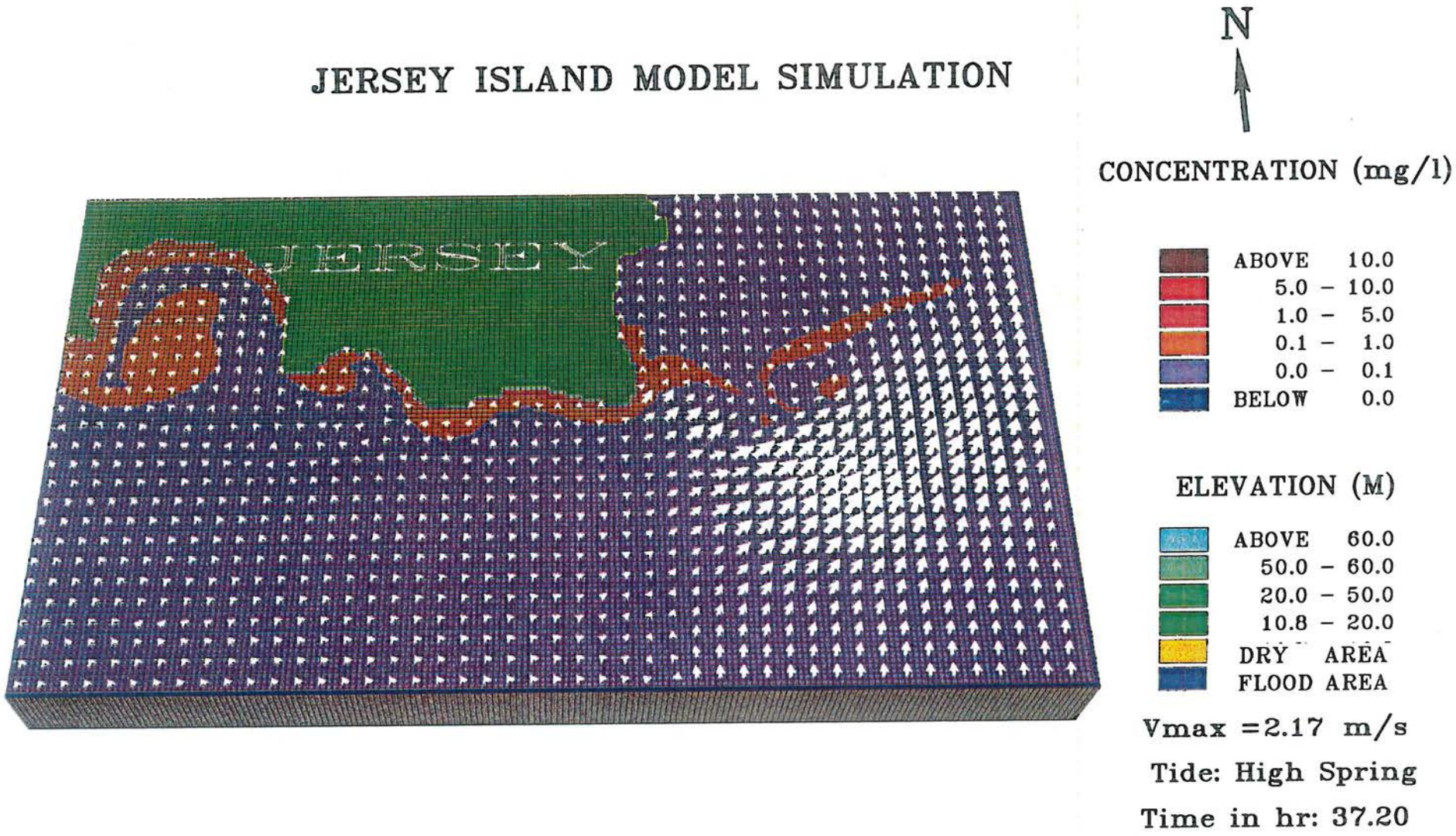

Figure 27 Tracer distribution around Jersey Coastline at high spring tide at end of third tide

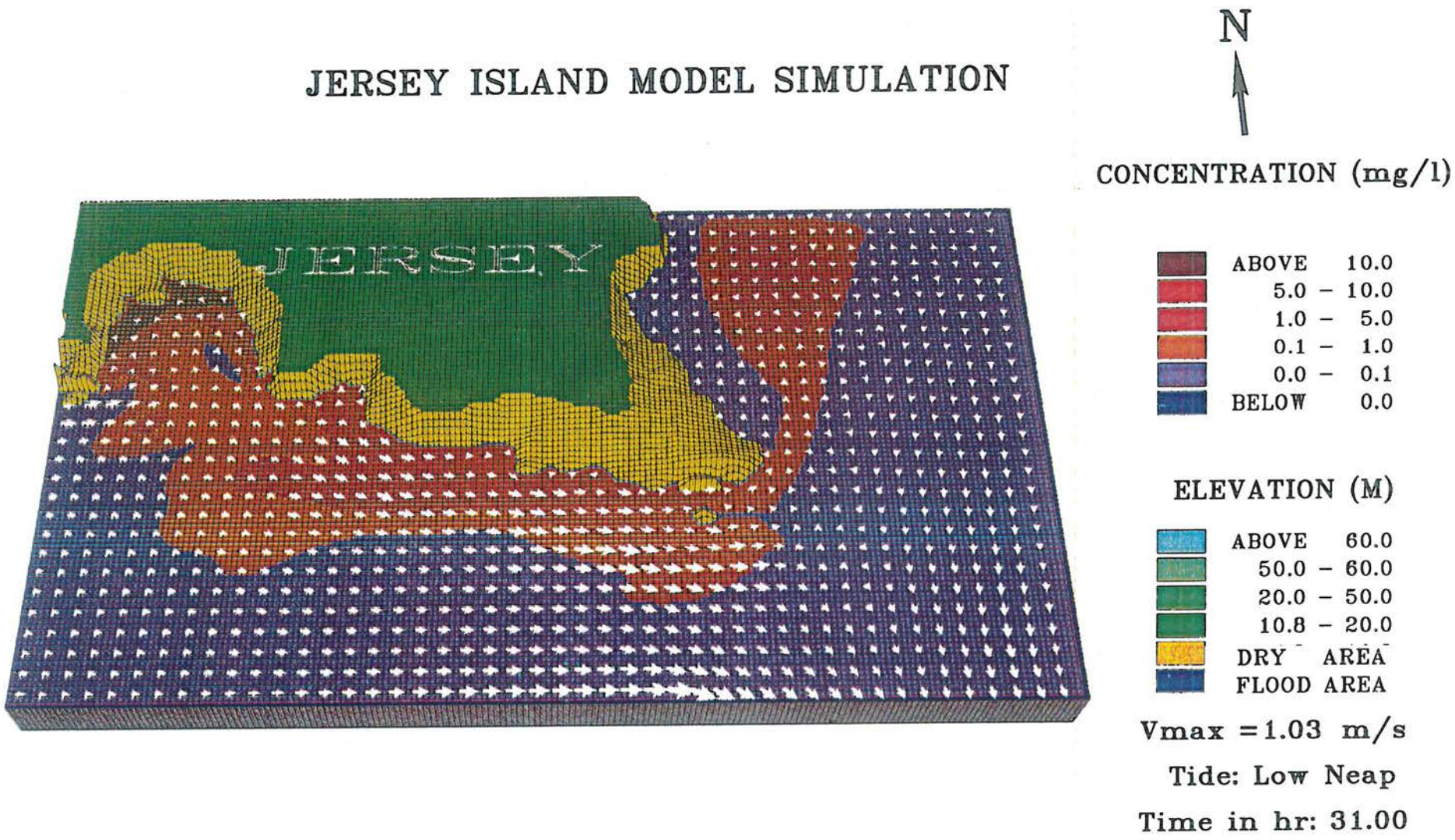

Figure 28 Tracer distribution around Jersey Coastline at low neap tide during third tide

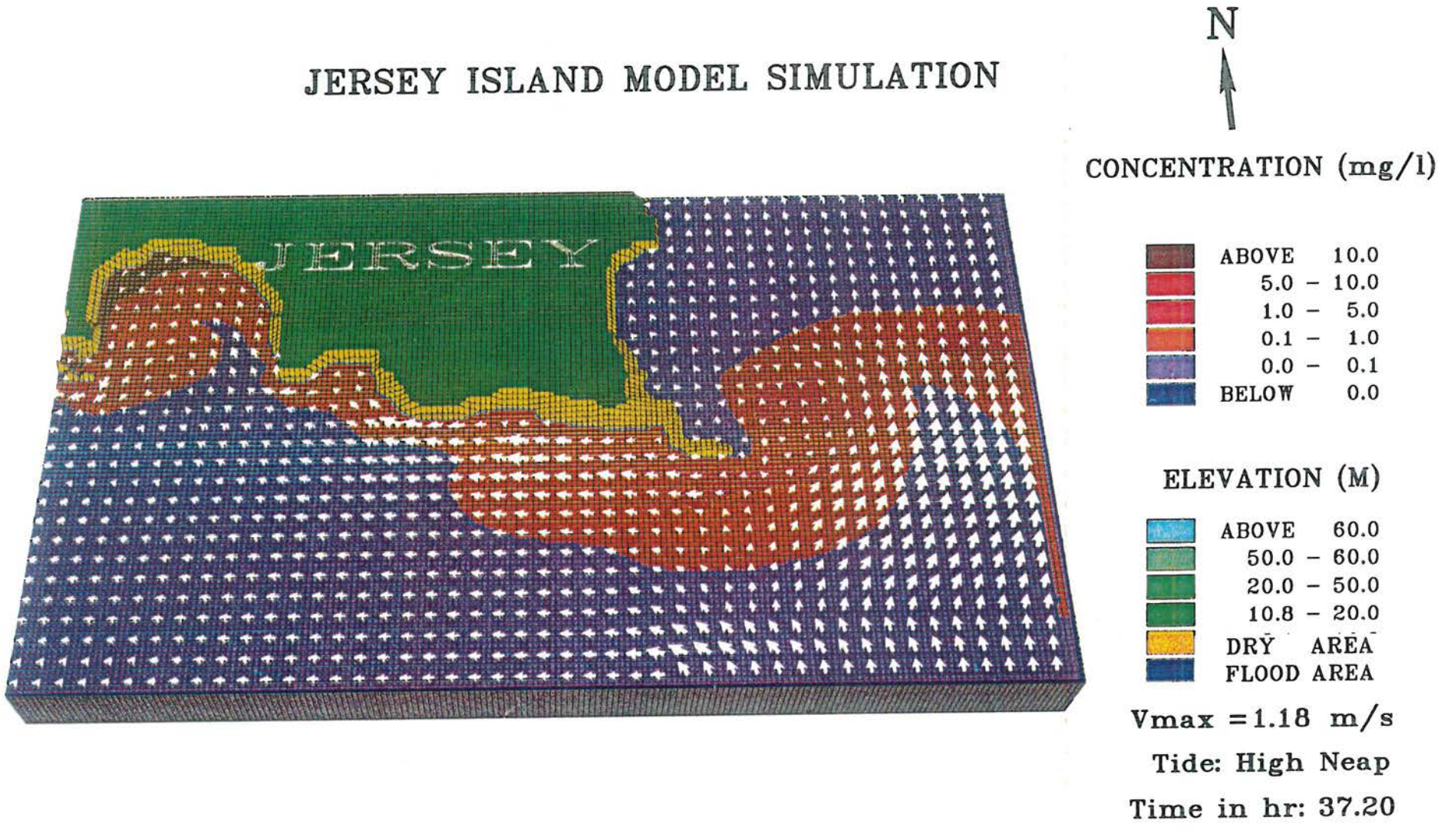

Figure 29 Tracer distribution around Jersey Coastline at high neap tide at end of third tide

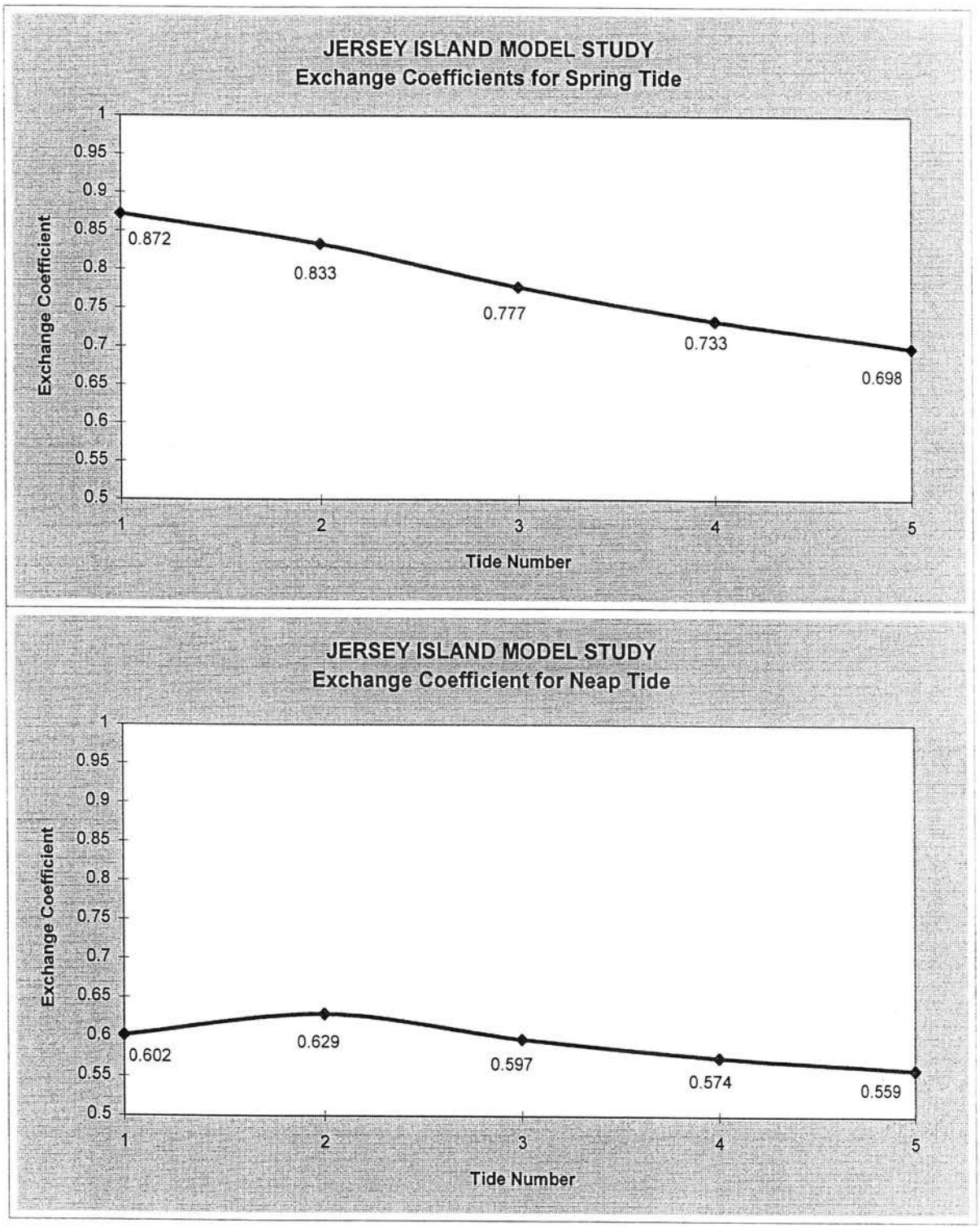

Figure 30 Tidal exchange coefficient for St. Aubin's Bay for spring and neap tides

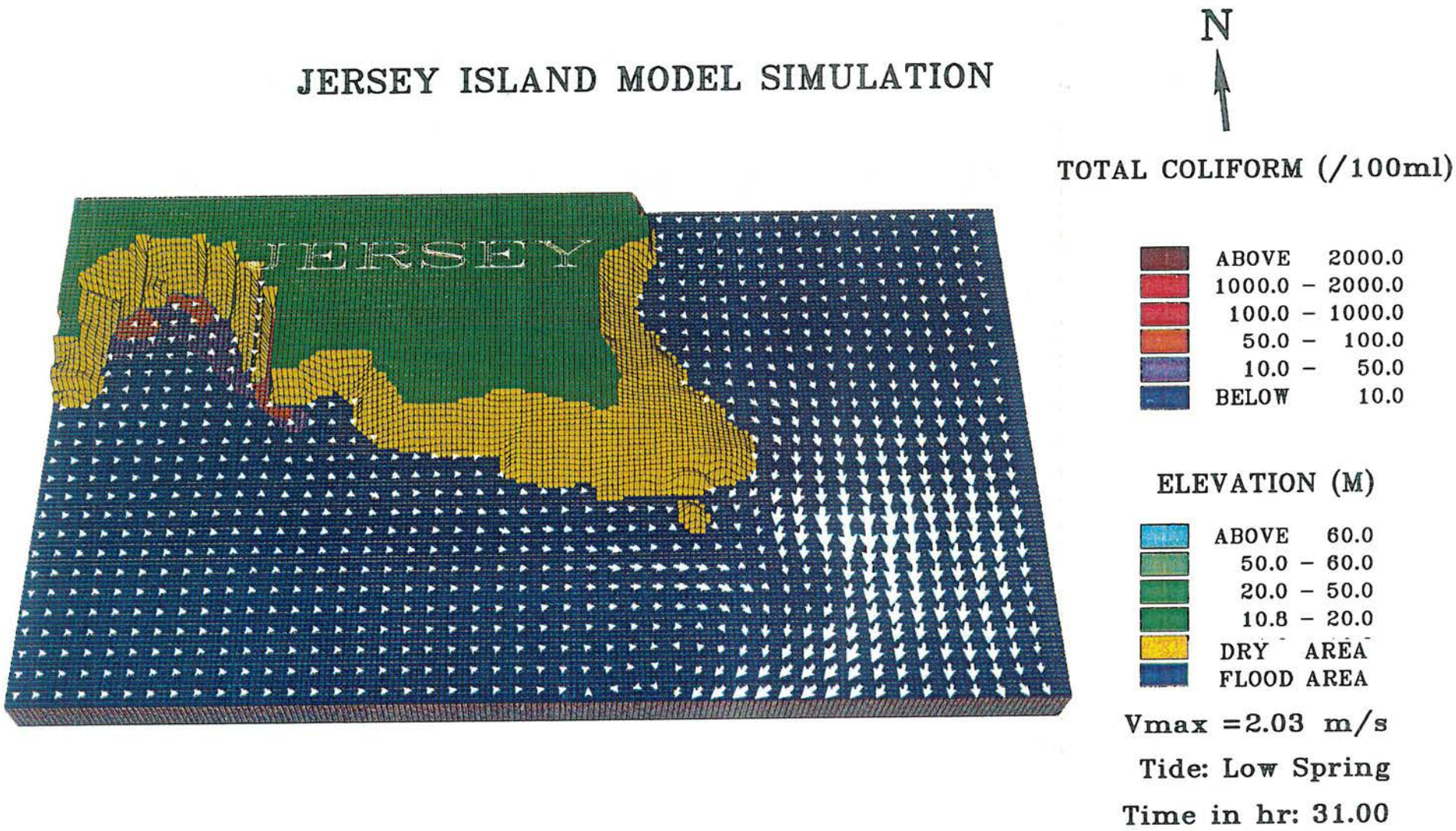

Figure 31 Predicted total coliform distribution for existing base flow inputs at low spring tide

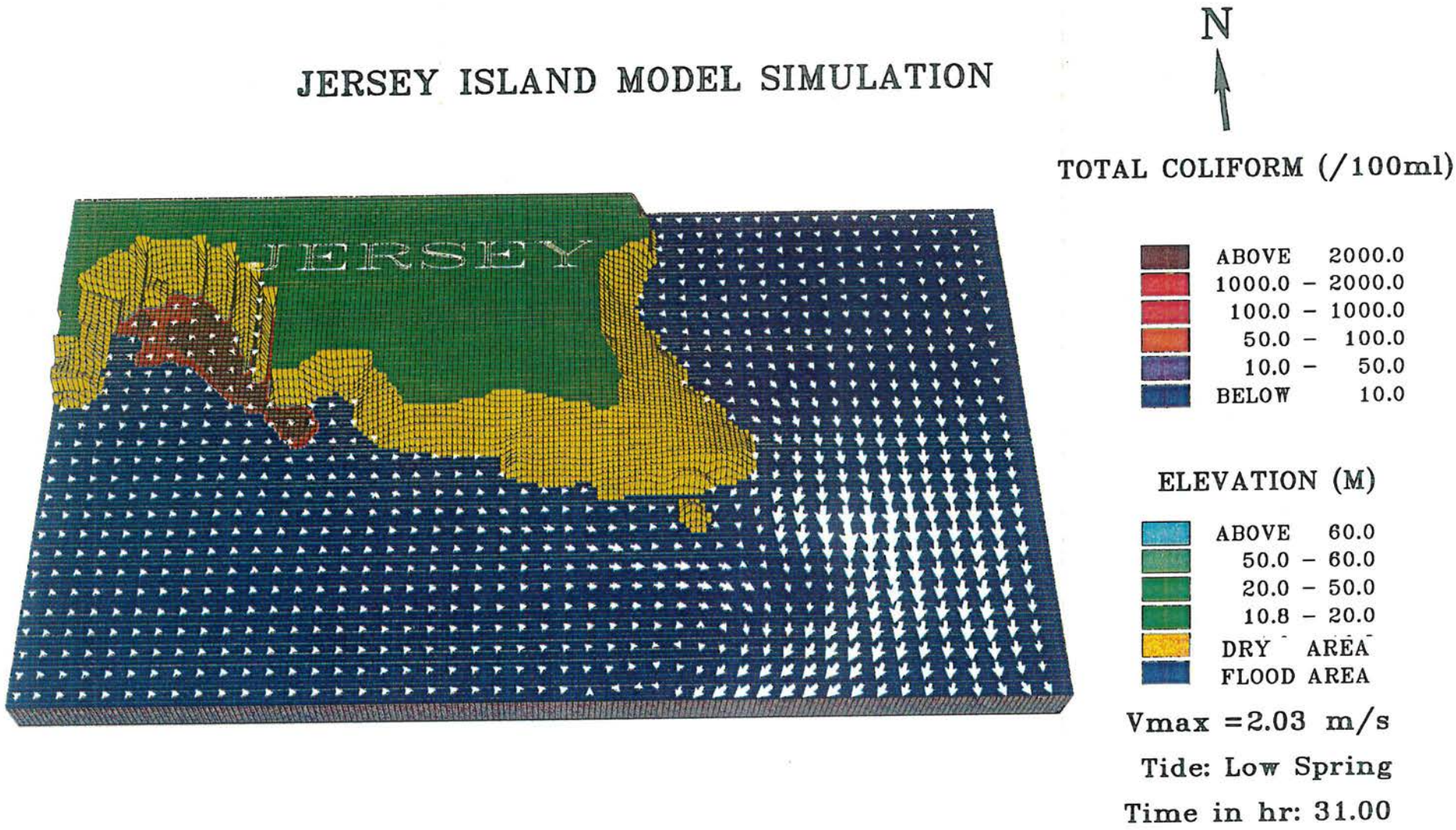

Figure 32 Predicted total coliform distribution for existing storm flow inputs at low spring tide

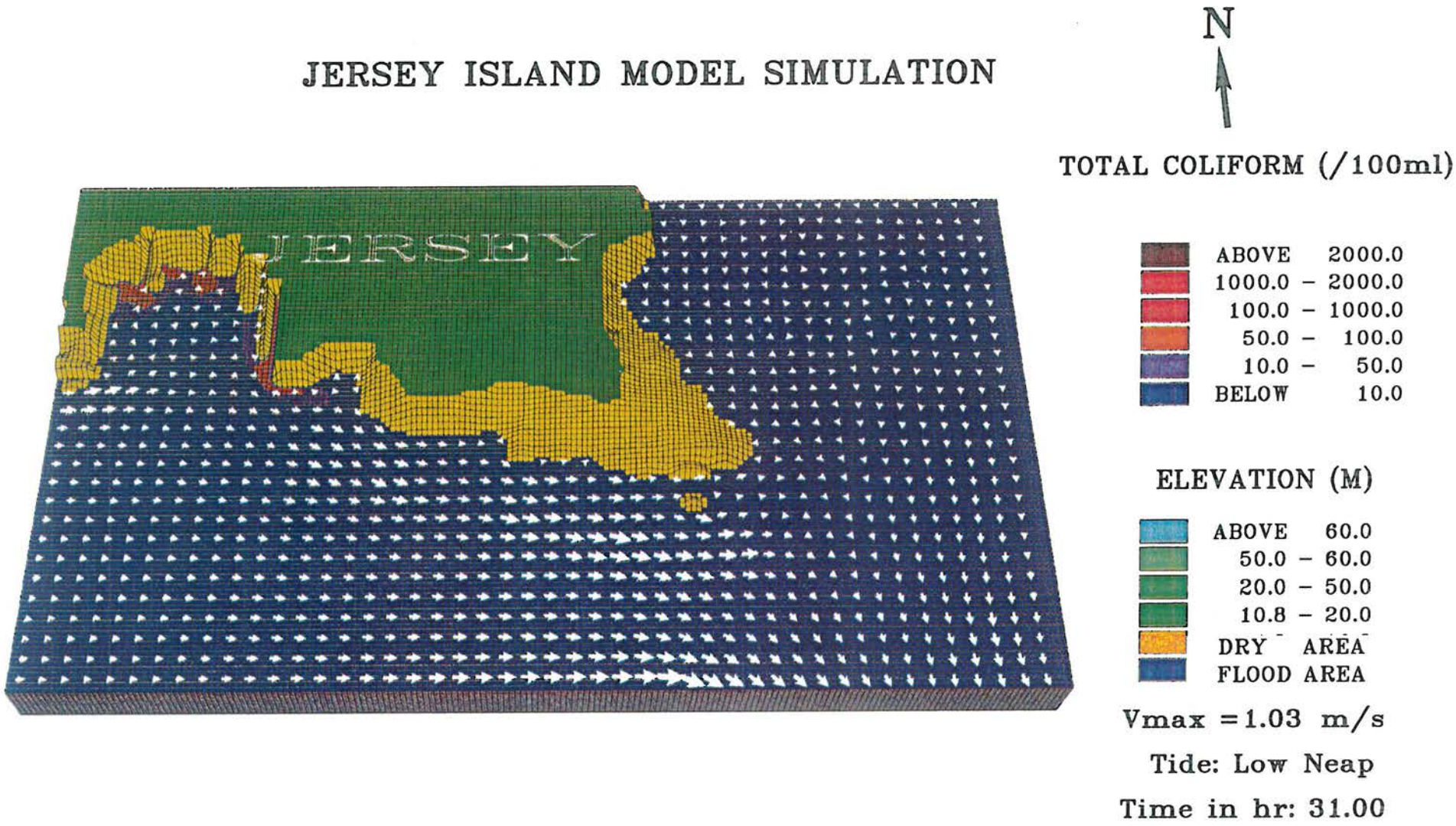

Figure 33 Predicted total coliform distribution for existing base flow inputs at low neap tide

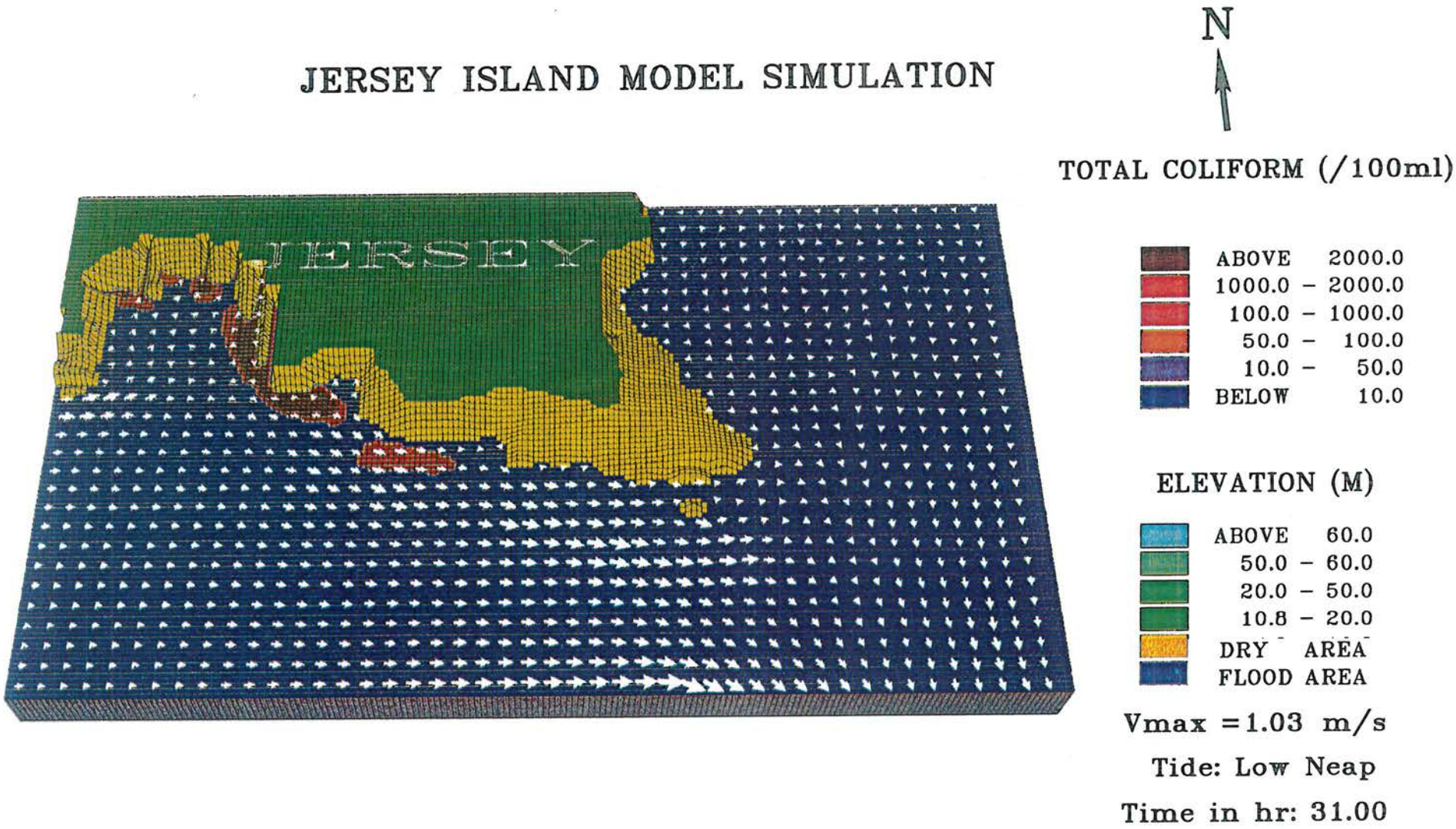

Figure 34 Predicted total coliform distribution for existing storm flow inputs at low neap tide

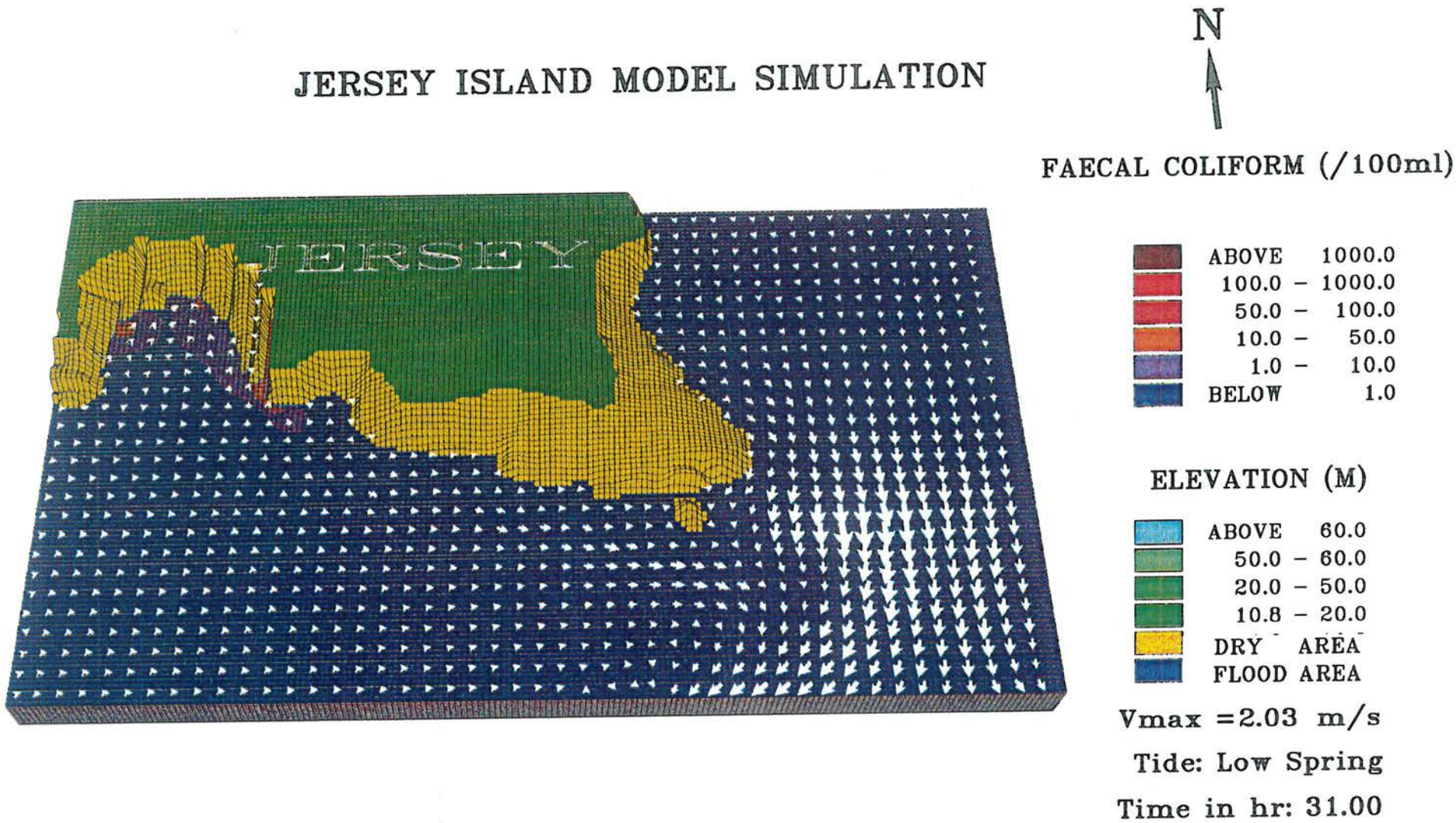

Figure 35 Predicted faecal coliform distribution for existing base flow inputs at low spring tide

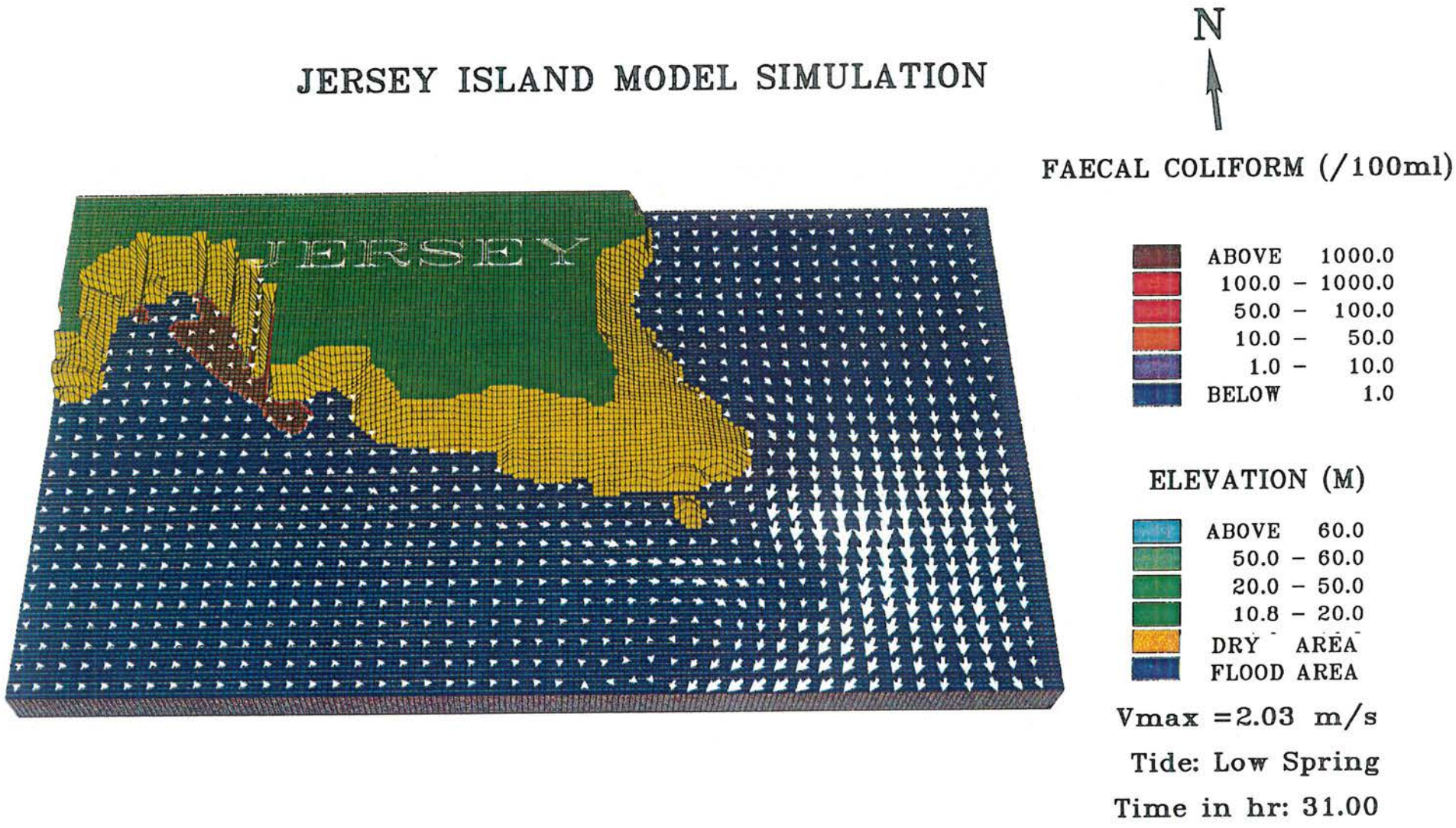

Figure 36 Predicted faecal coliform distribution for existing storm flow inputs at low spring tide

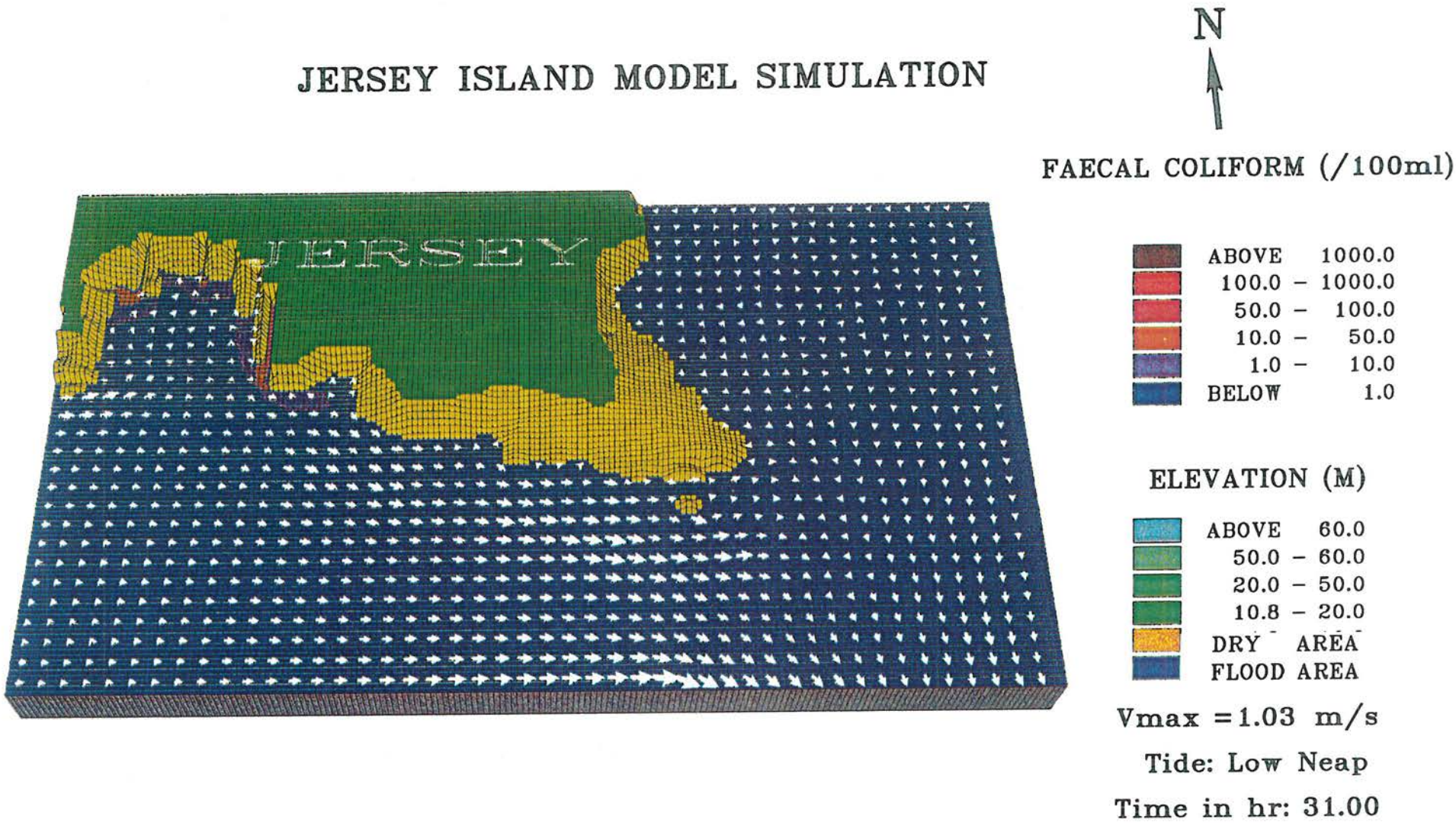

Figure 37 Predicted faecal coliform distribution for existing base flow inputs at low neap tide

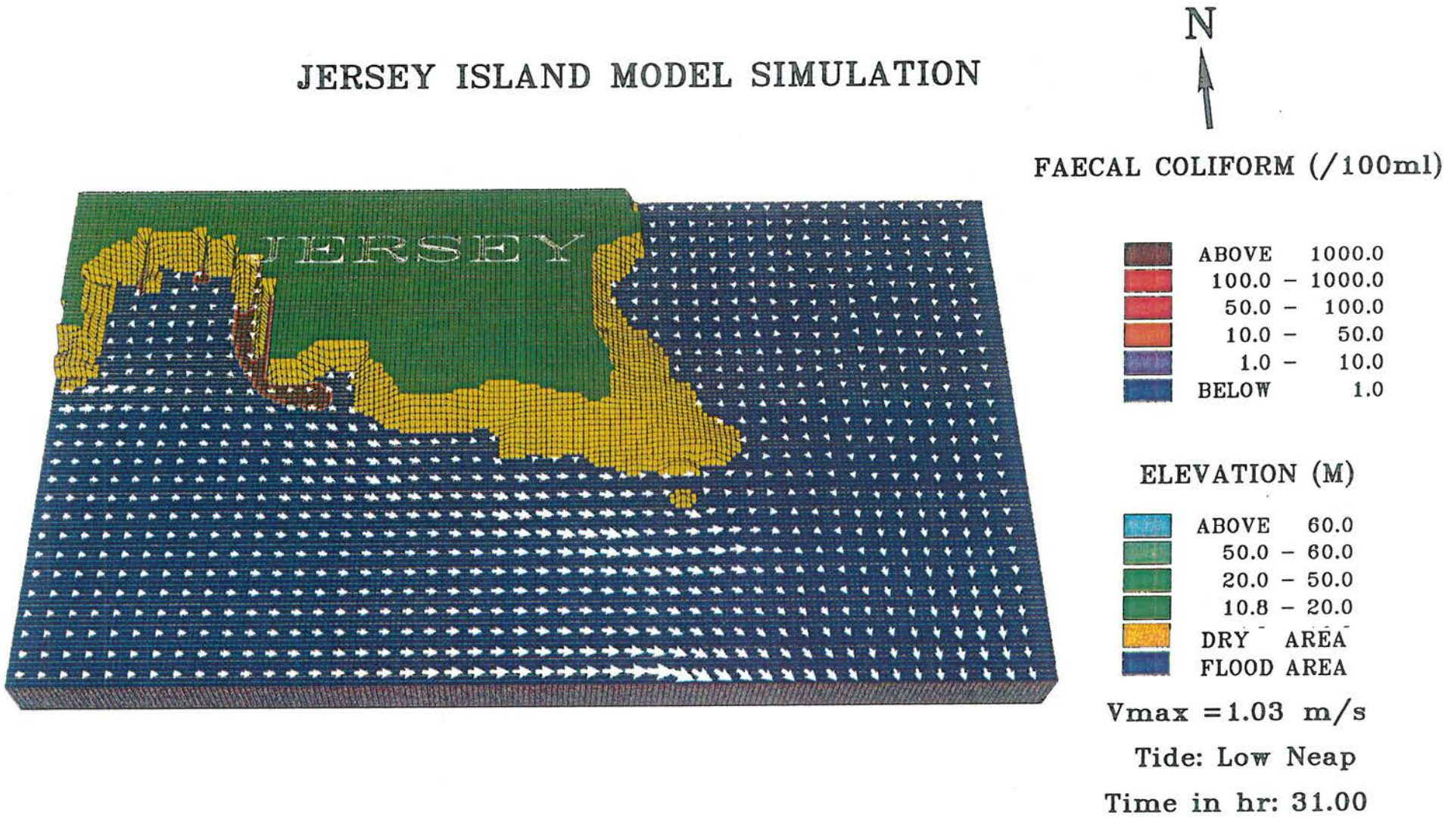

Figure 38 Predicted faecal coliform distribution for existing storm flow inputs at low neap tide

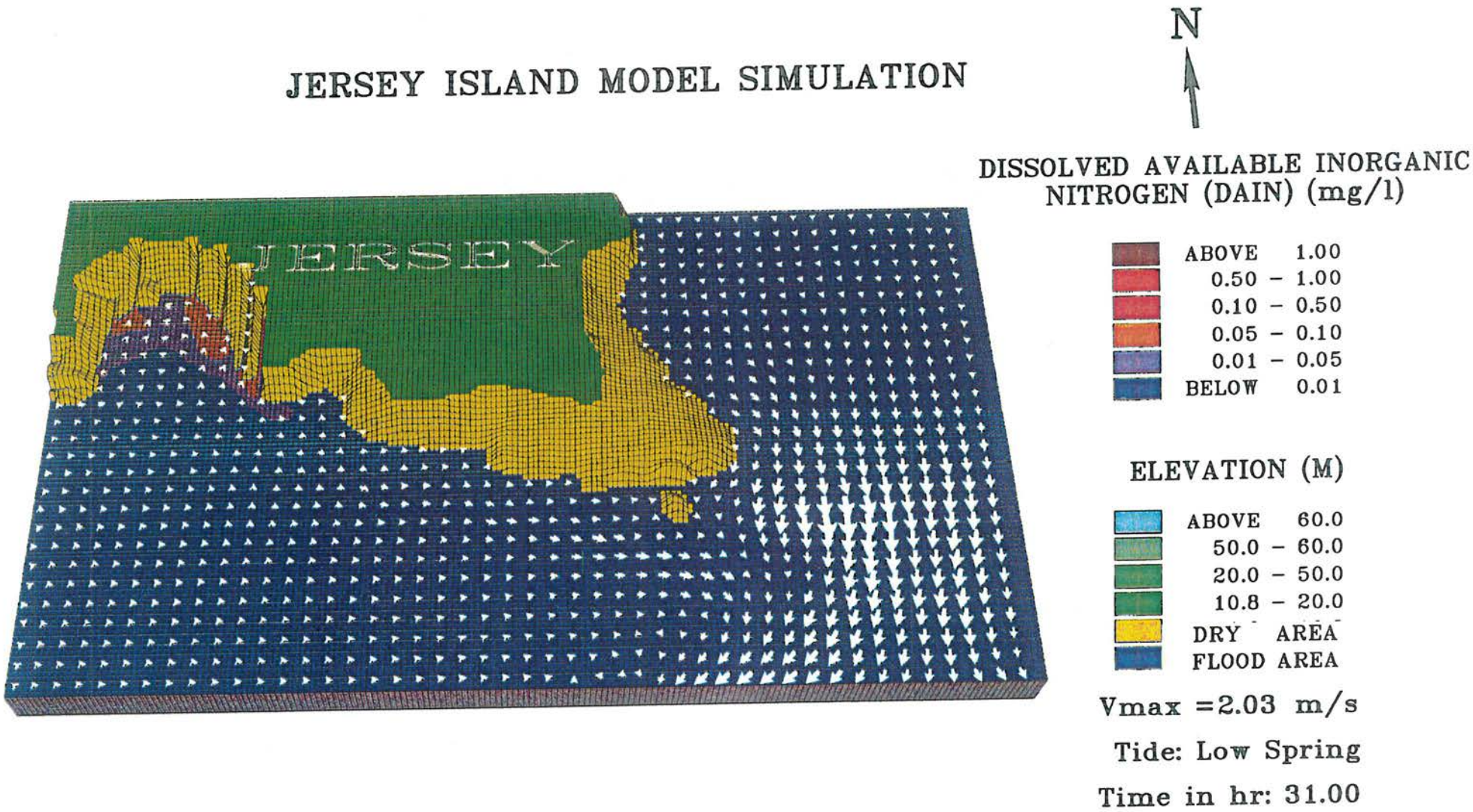

Figure 39 Predicted DAIN distribution for existing base flow inputs at low spring tide

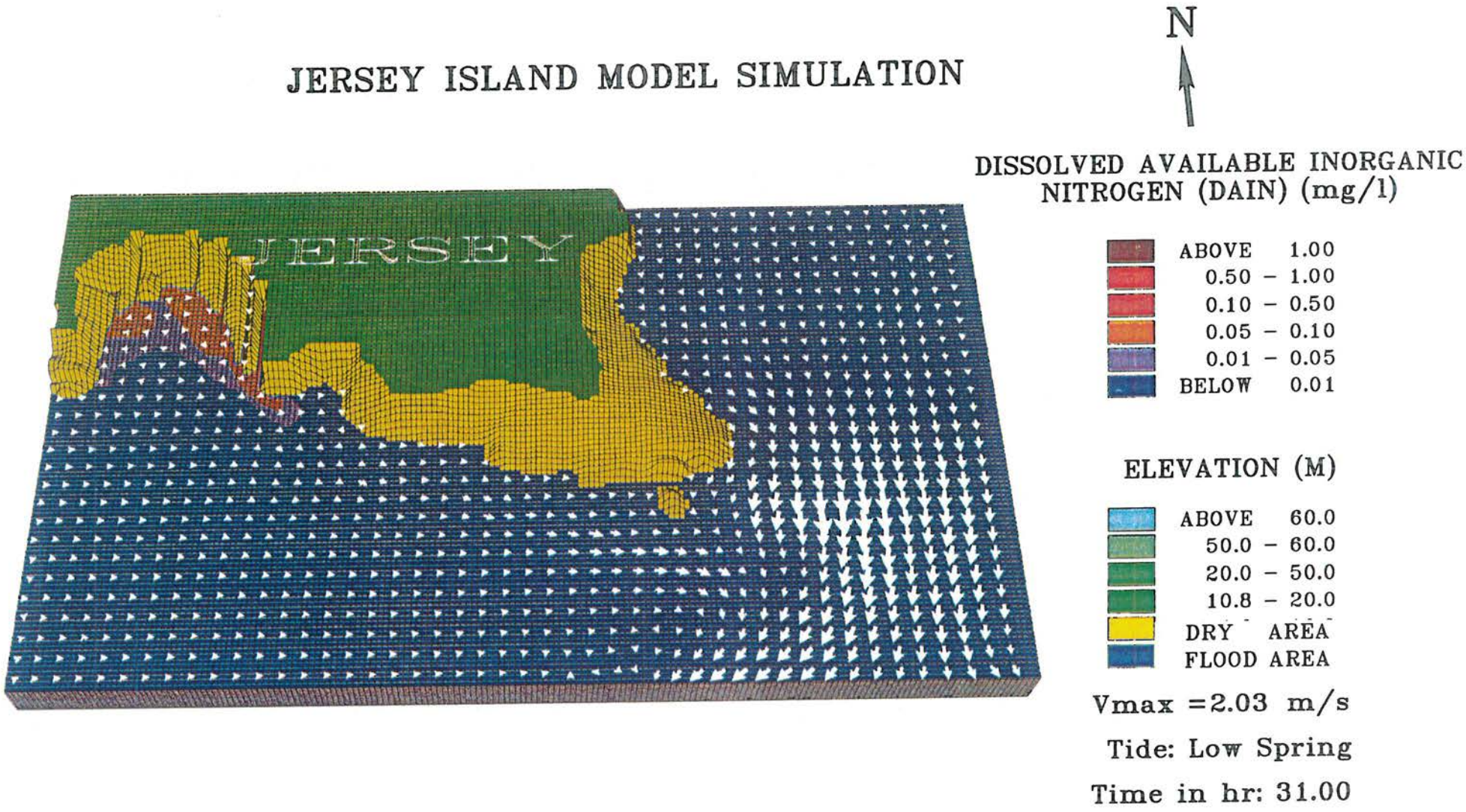

Figure 40 Predicted DAIN distribution for existing storm flow inputs at low spring tide

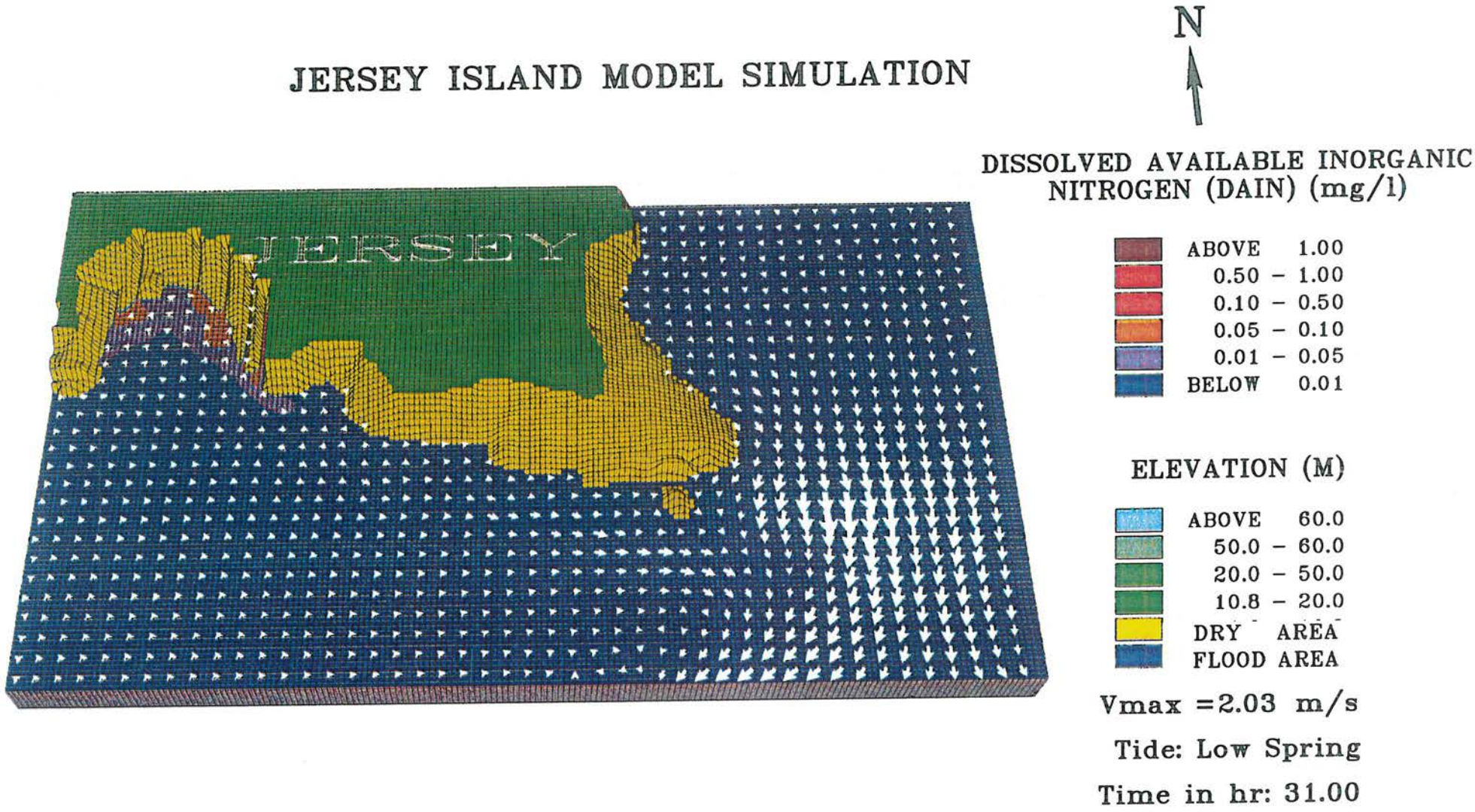

Figure 41 Predicted DAIN distribution for proposed Bellazone STW and other base flow inputs at low spring tide

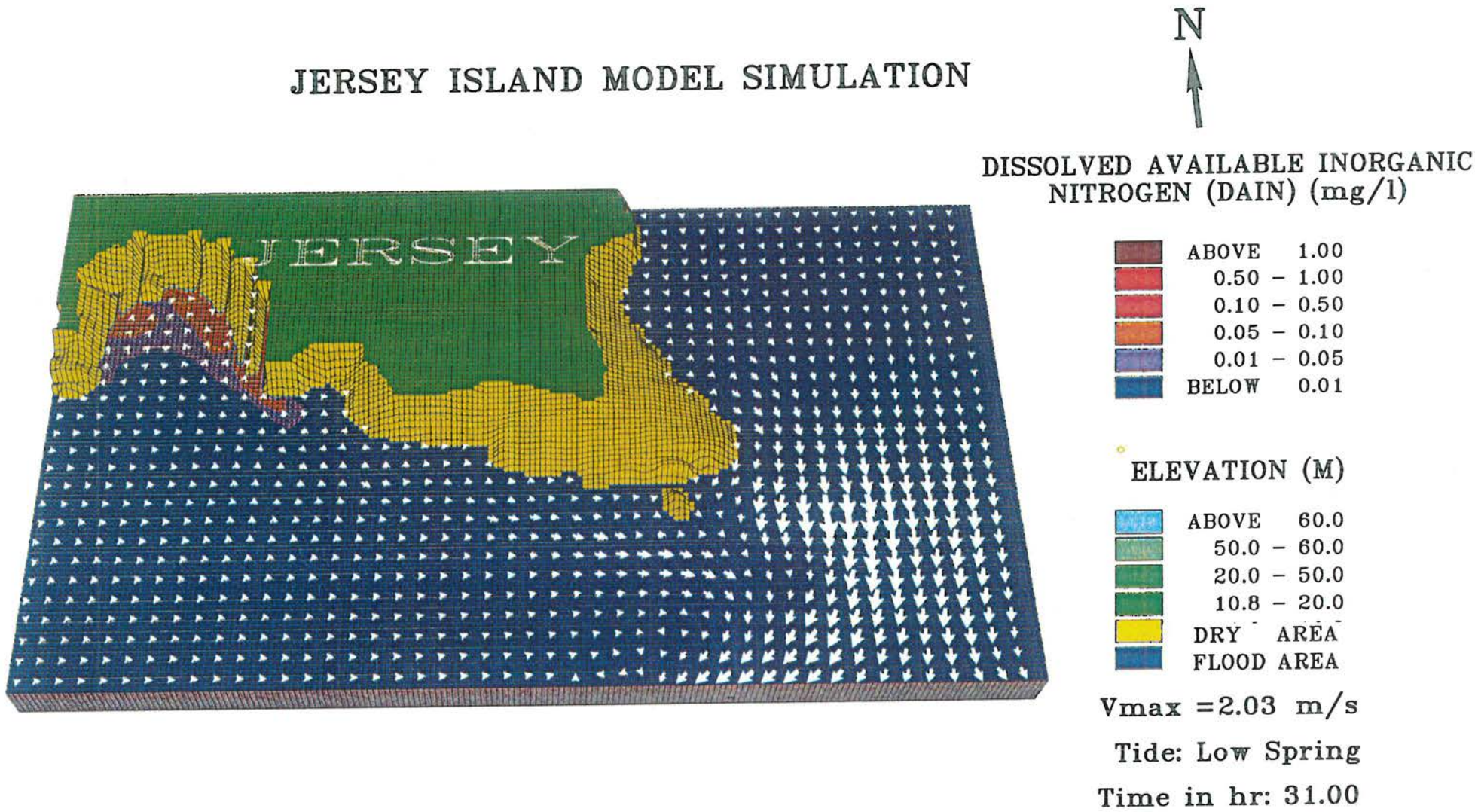

Figure 42 Predicted DAIN distribution for proposed Bellazone STW storm flow inputs at low spring tide

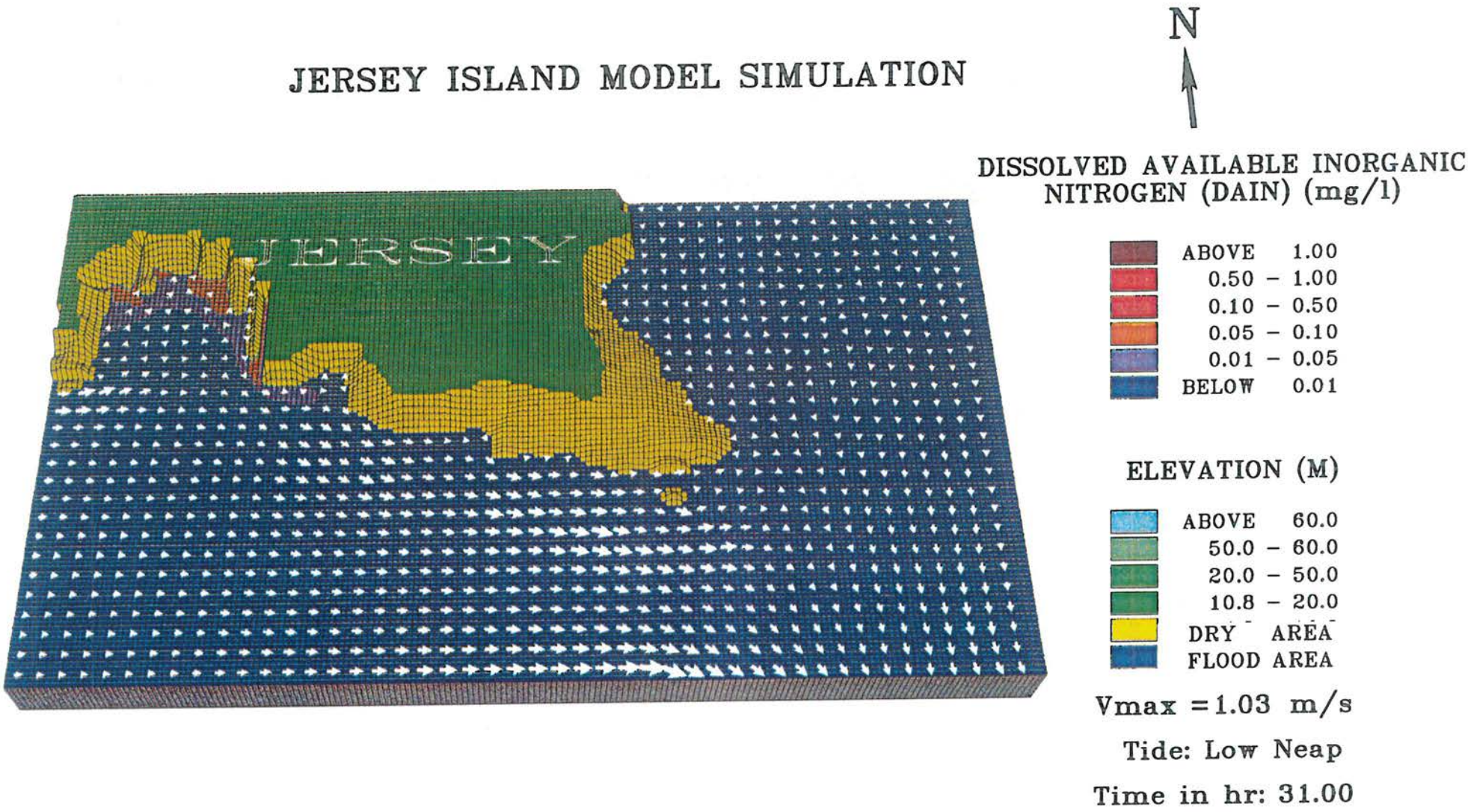

Figure 43 Predicted DAIN distribution for existing base flow inputs at low neap tide

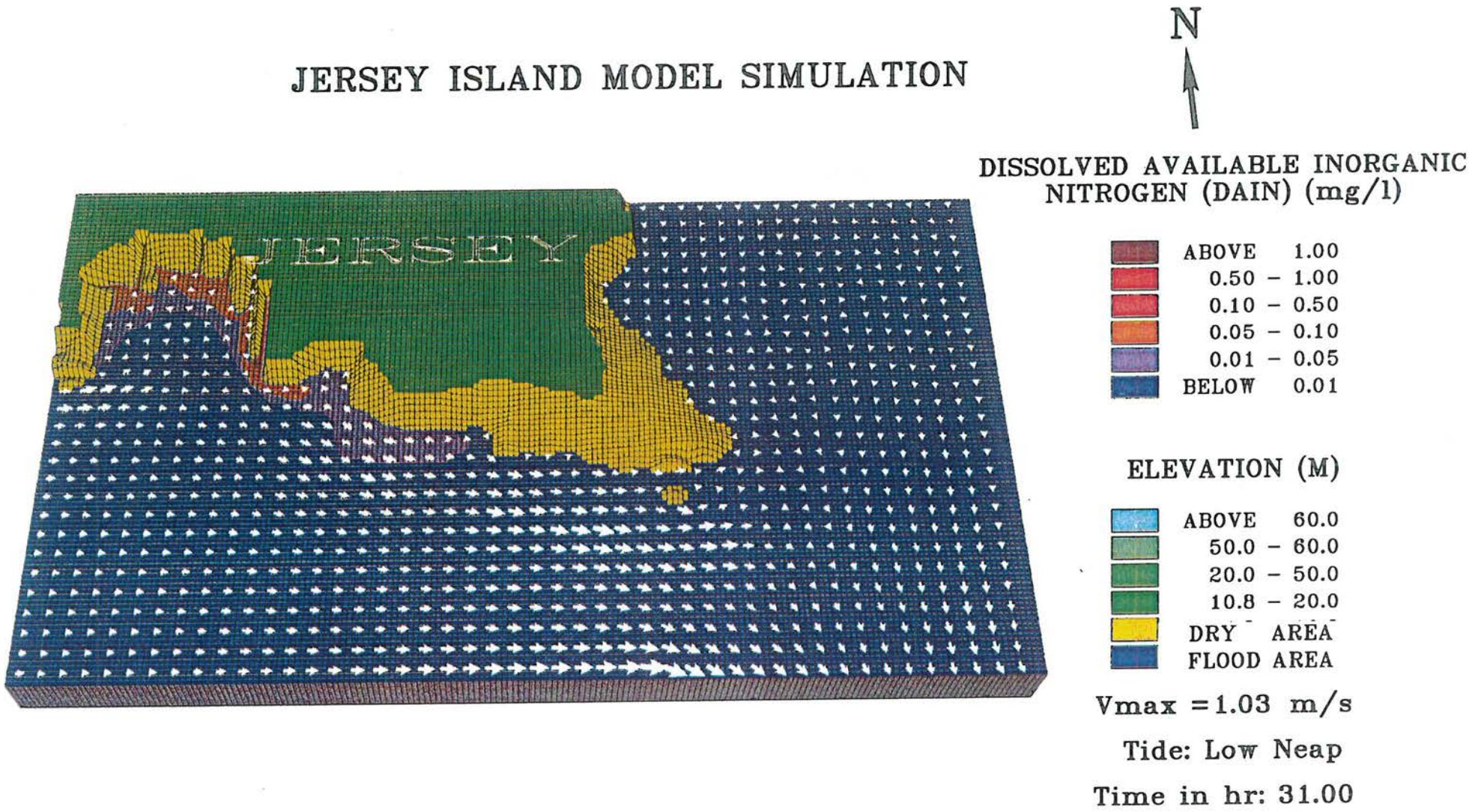

Figure 44 Predicted DAIN distribution for existing storm flow inputs at low neap tide

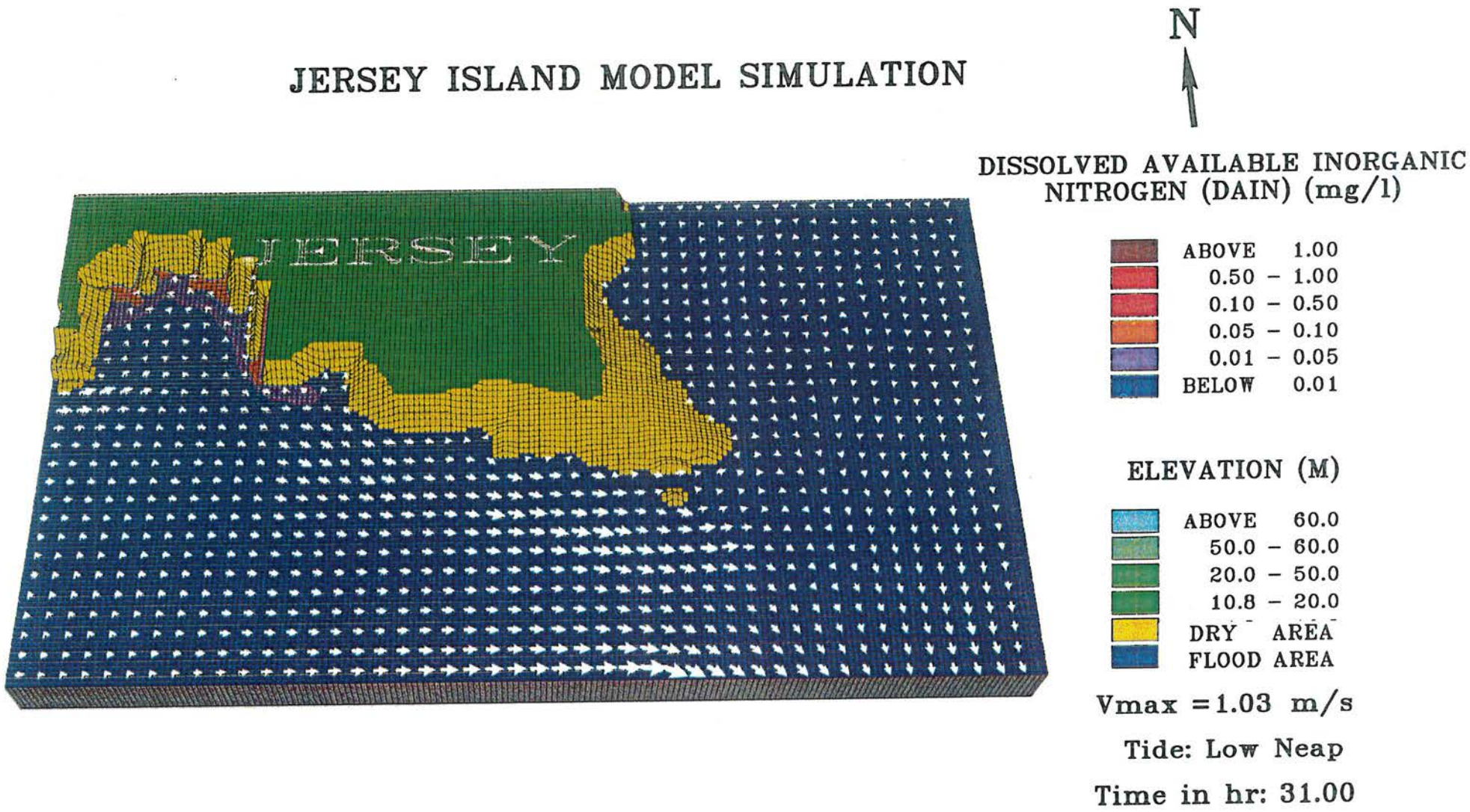

Figure 45 Predicted DAIN distribution for proposed Bellazone STW and other base flow inputs at low neap tide

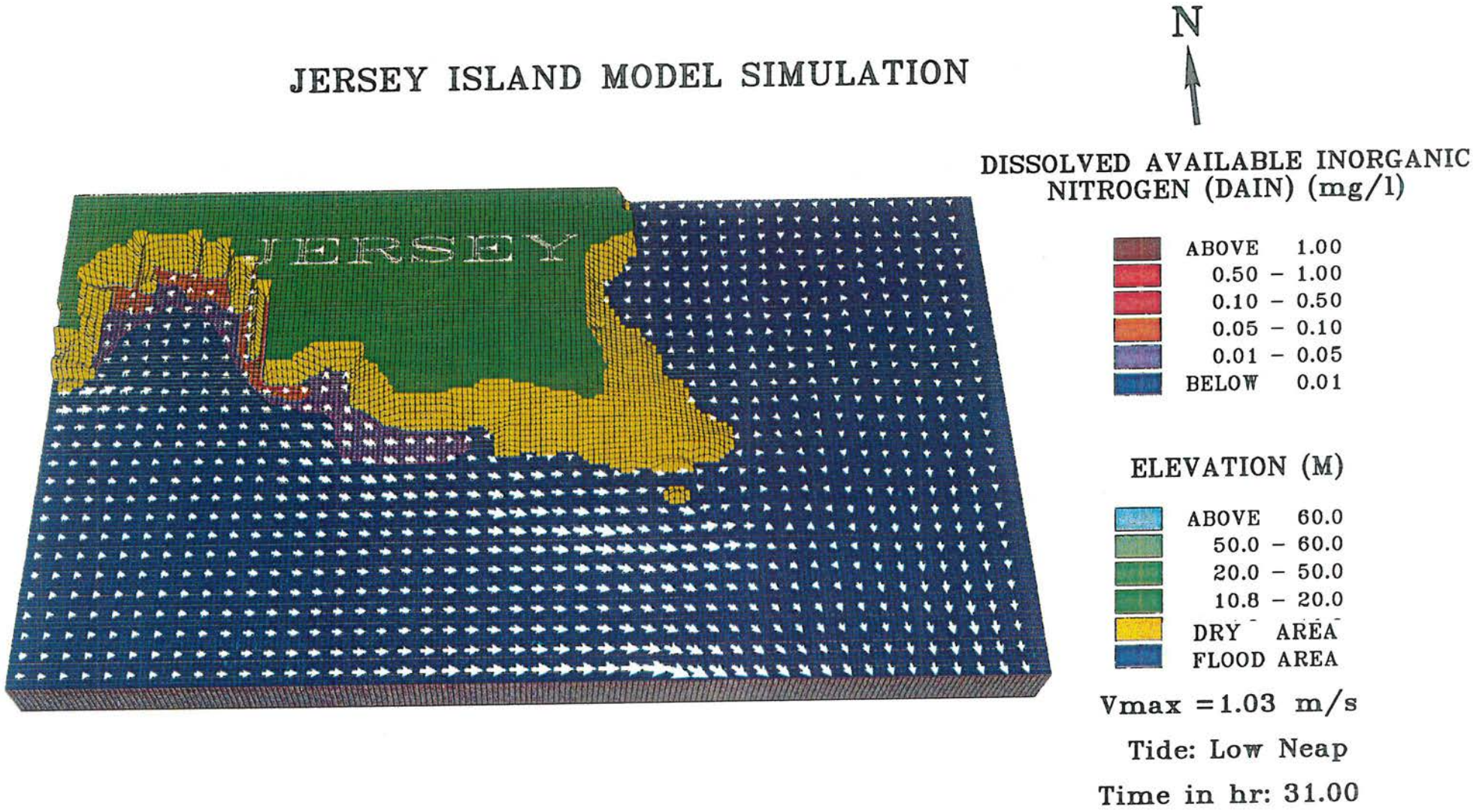

Figure 46 Predicted DAIN distribution for proposed Bellazone STW and other storm flow inputs at low neap tide

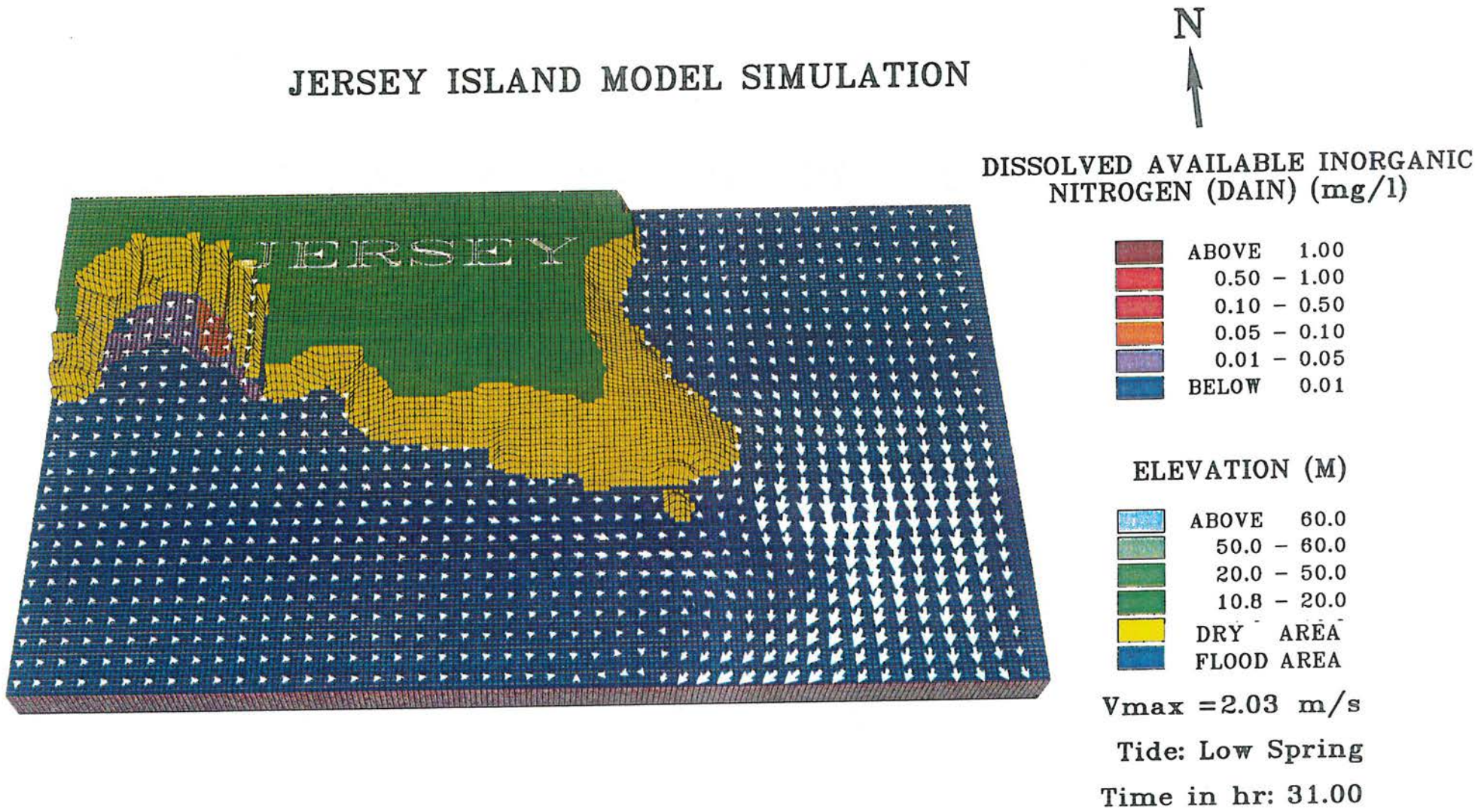

Figure 47 Predicted DAIN distribution in St. Aubin's bay for existing storm flow inputs from Bellazone STW at low spring tide

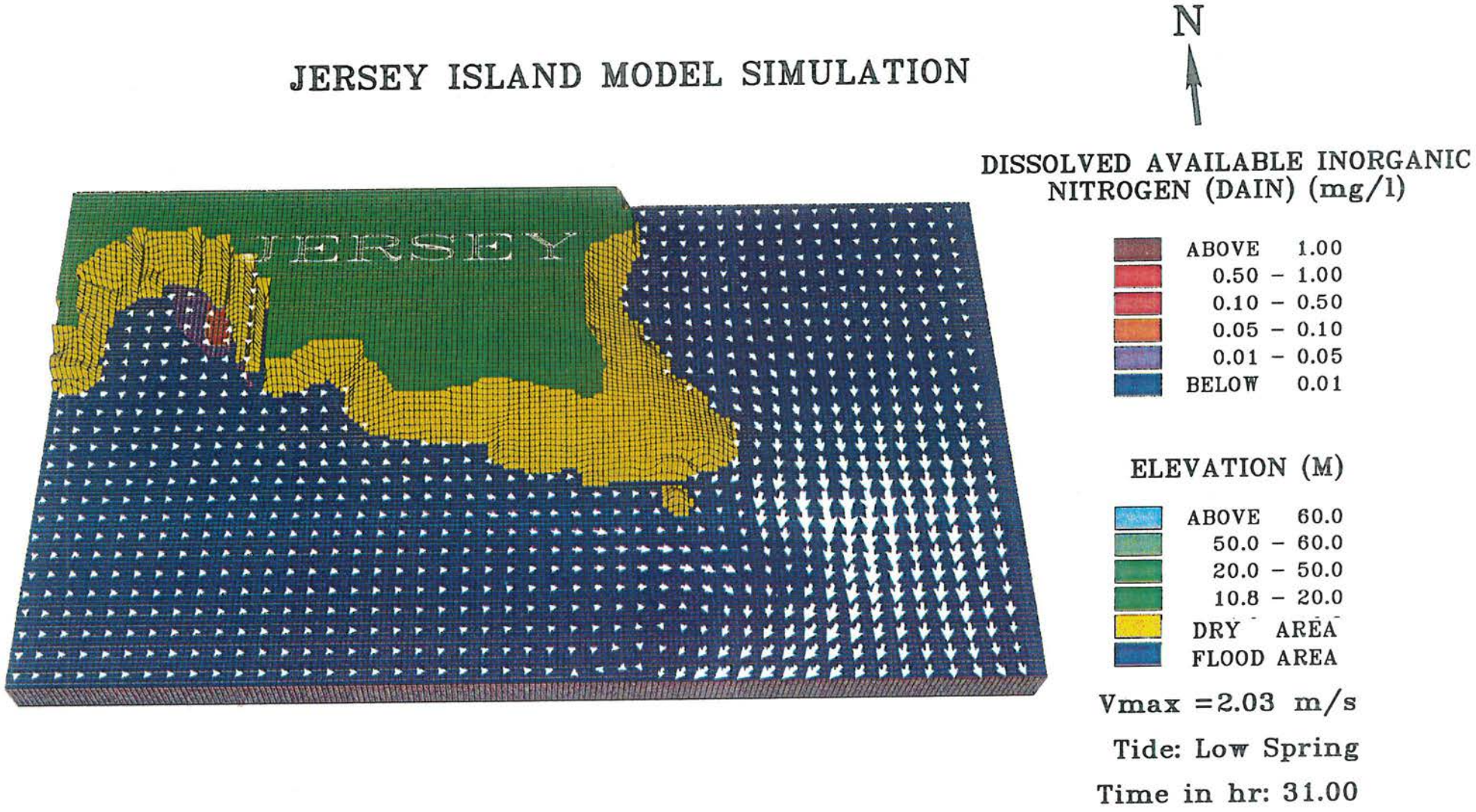

Figure 48 Predicted DAIN distribution in St. Aubin's bay for Proposed storm flow input from Bellazone STW at low spring tide

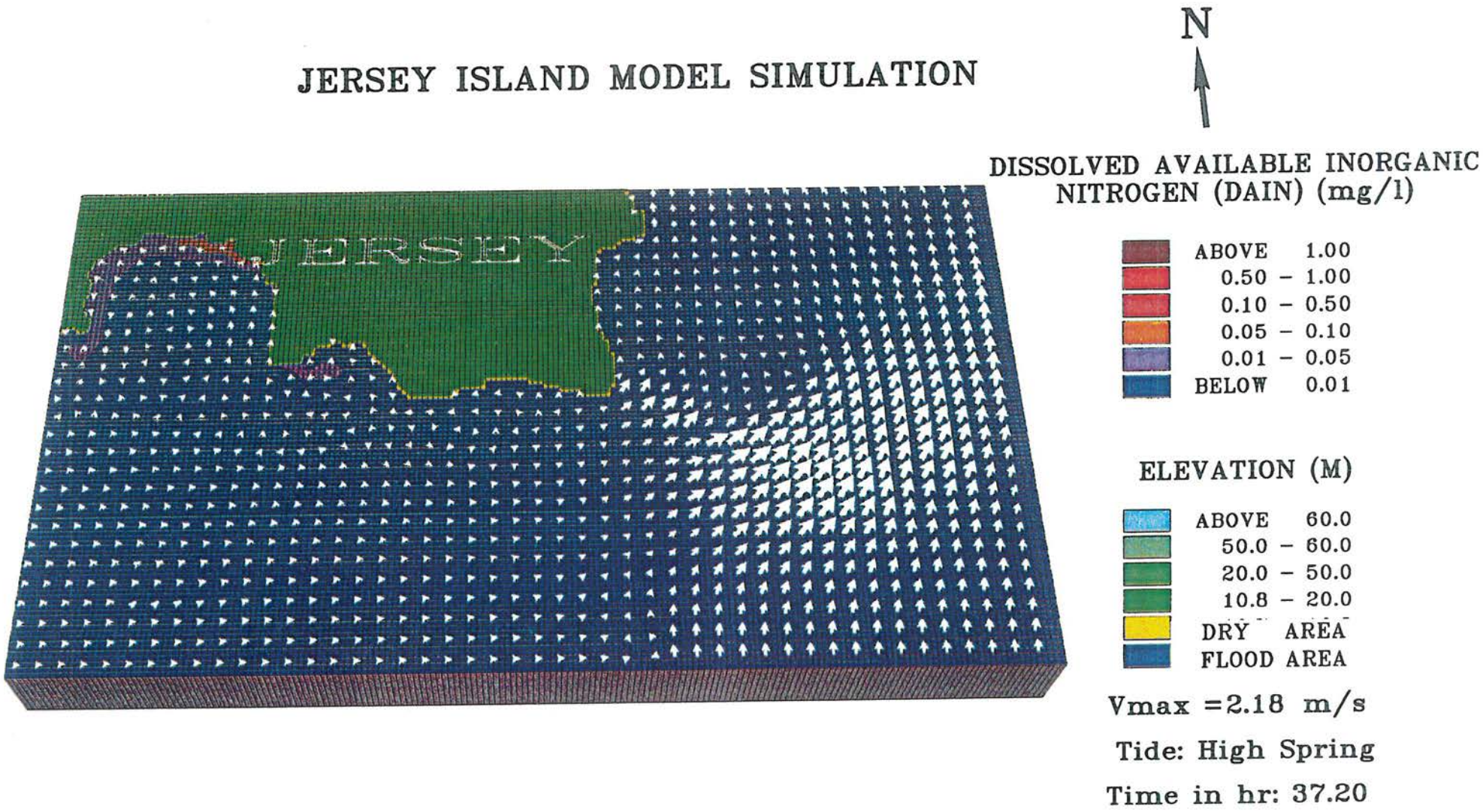

Figure 49 Predicted DAIN distribution in St. Aubin's bay for existing storm flow input from Bellazone STW at high spring tide

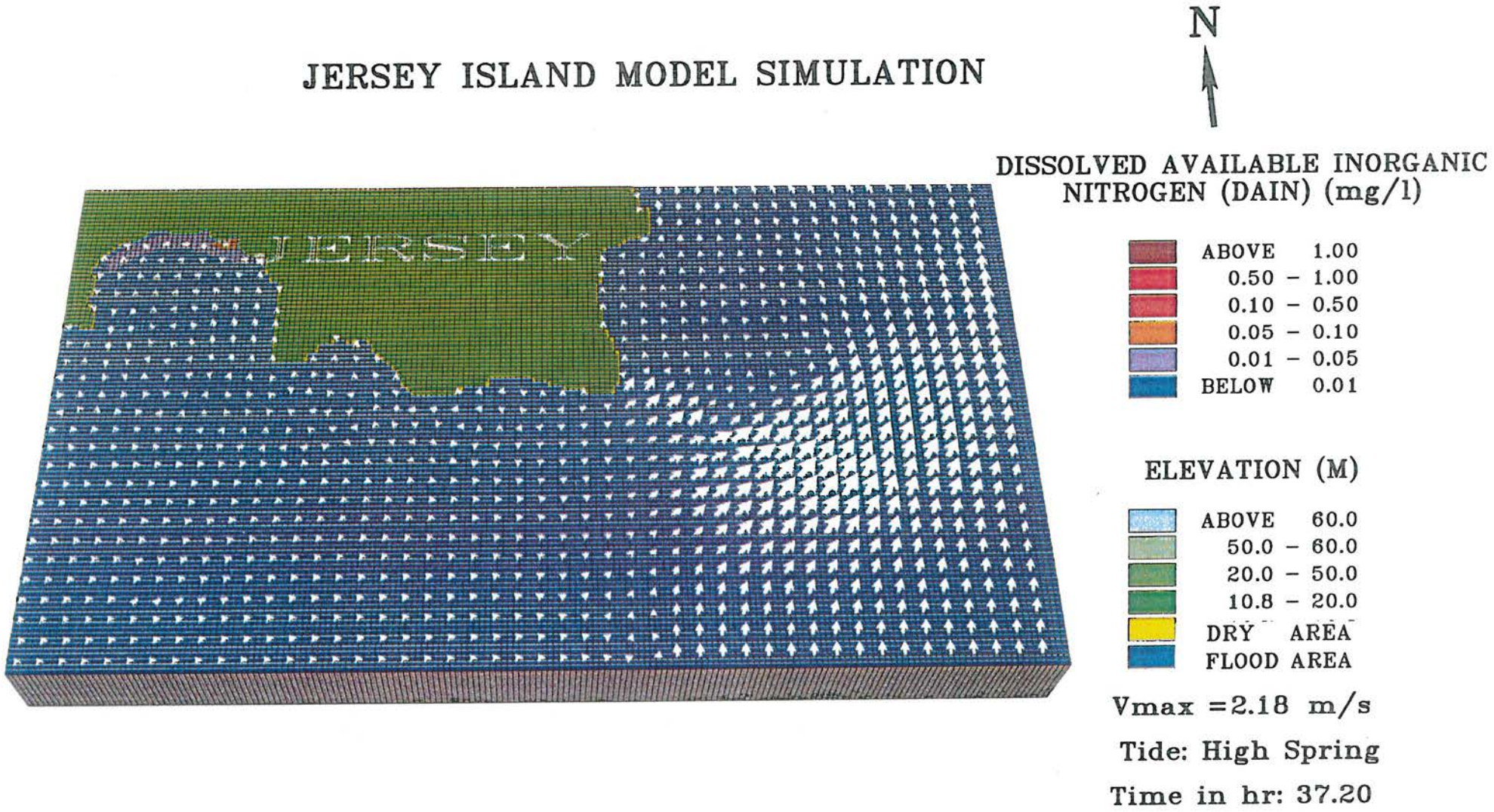

Figure 50 Predicted DAIN distribution in St. Aubin's bay for Proposed storm flow input from Bellazone STW at high spring tide

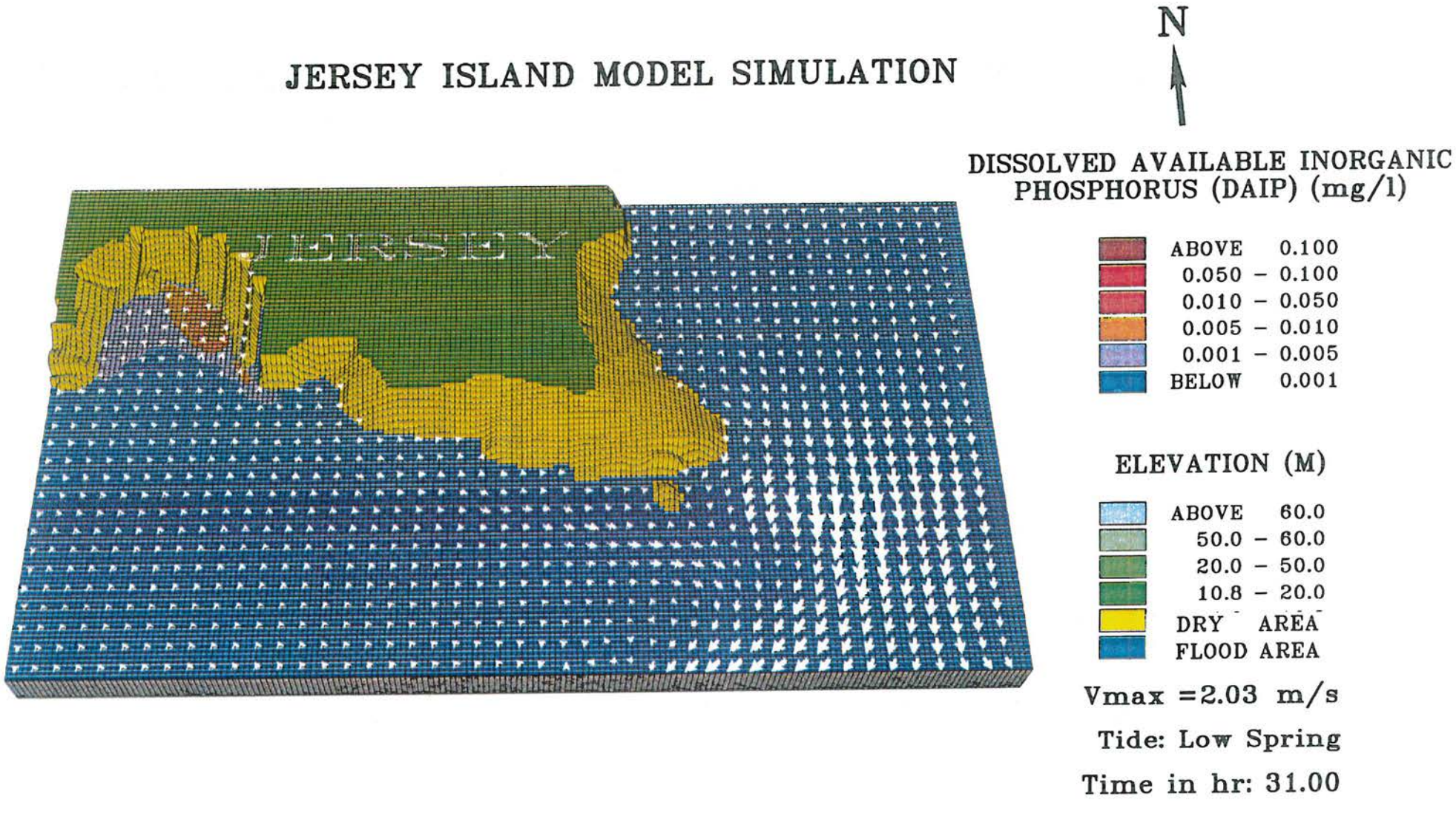

Figure 51 Predicted DAIP distribution for existing base flow inputs at low spring tide

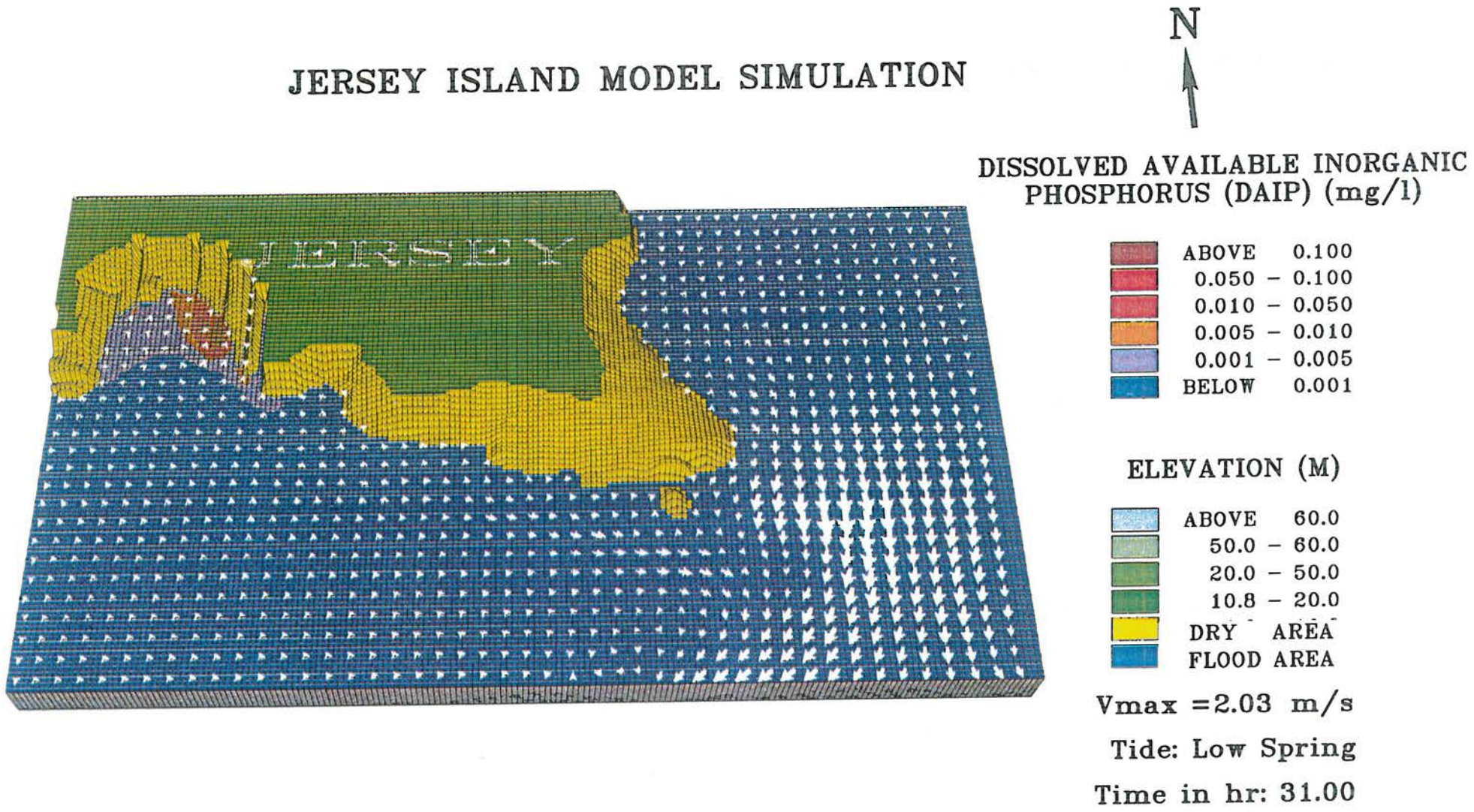

Figure 52 Predicted DAIP distribution for existing storm flow inputs at low spring tide

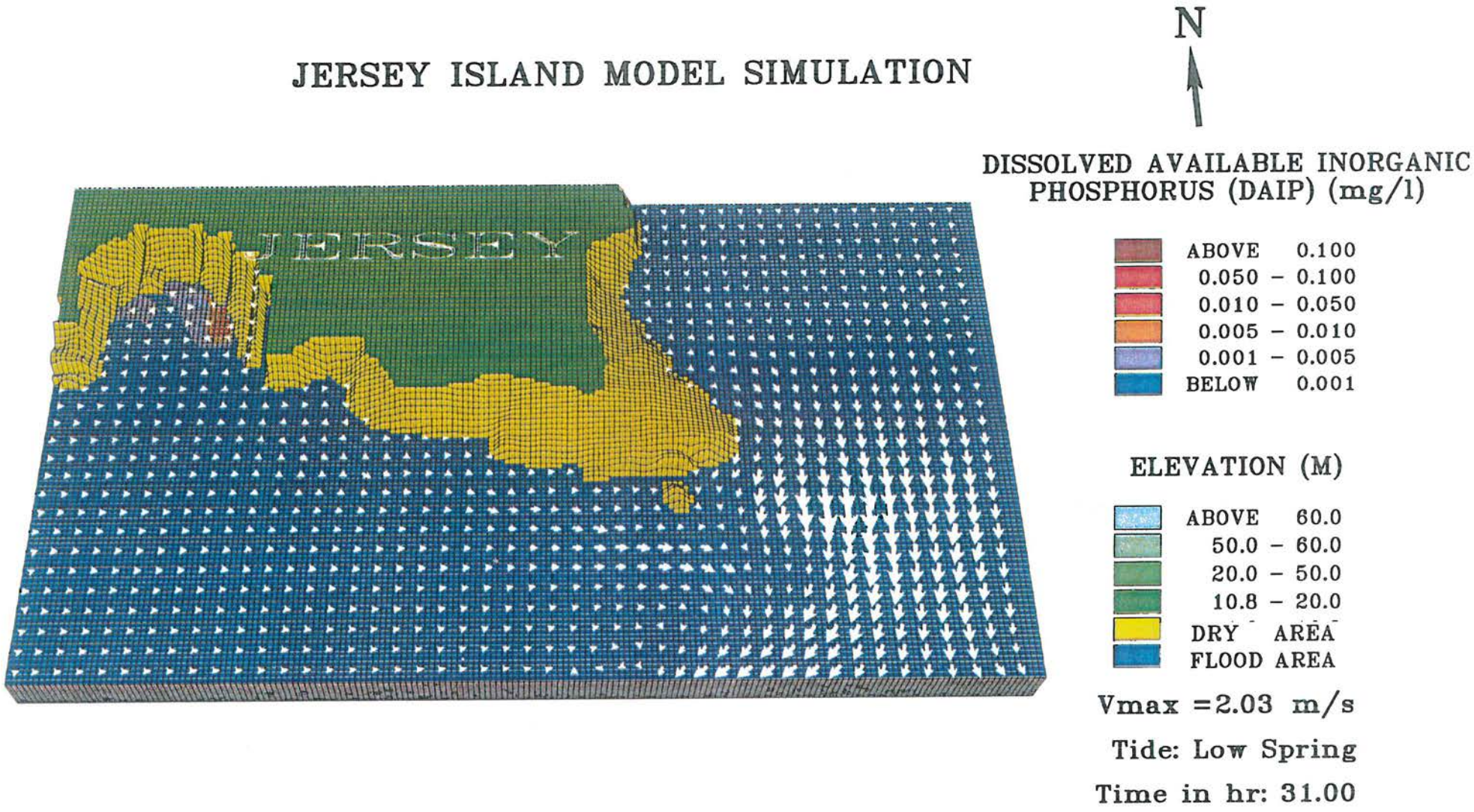

Figure 53 Predicted DAIP distribution for Bellazone STW and other base flow inputs at low spring tide

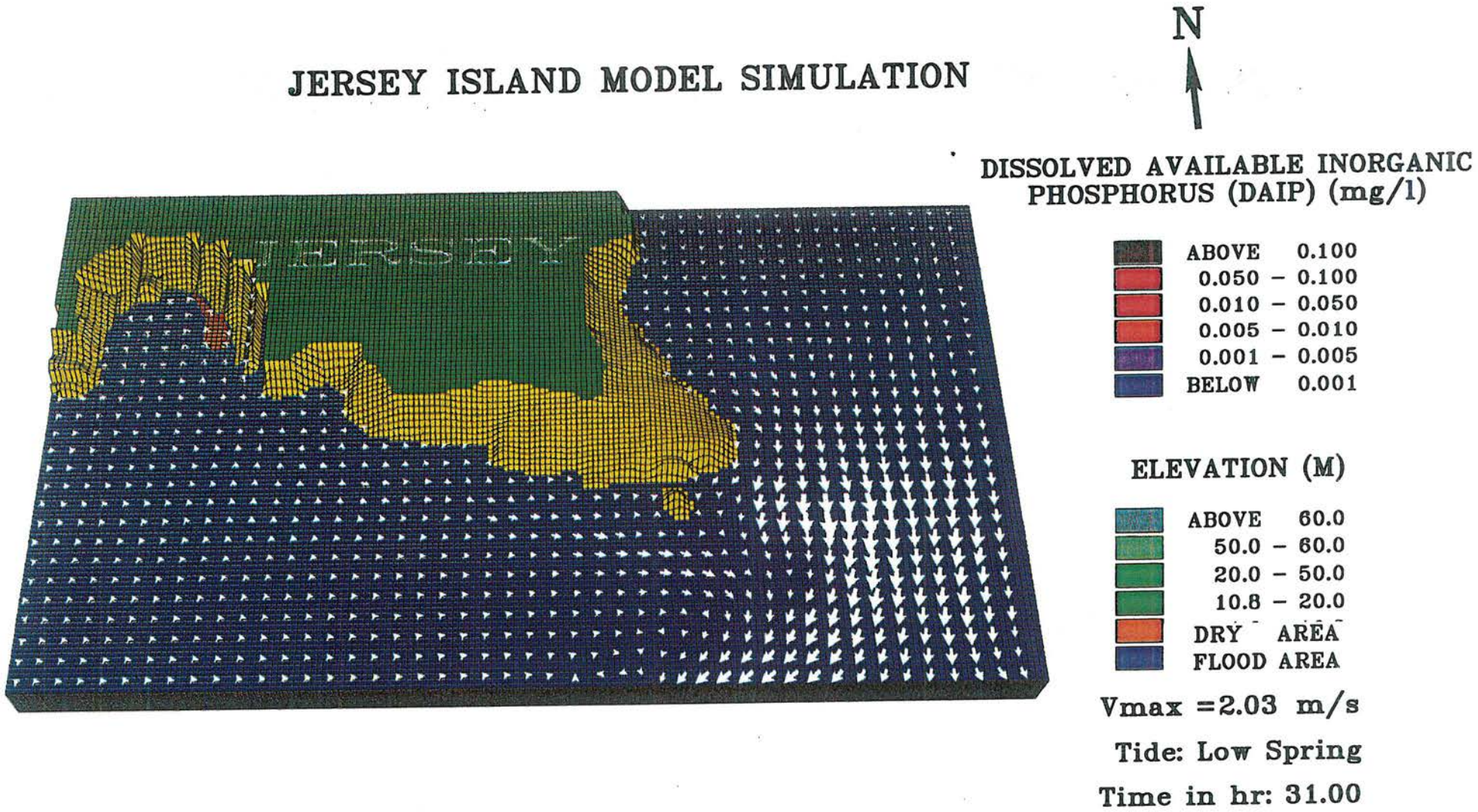

Figure 54 Predicted DAIP distribution for Bellazone STW and other storm flow inputs at low spring tide

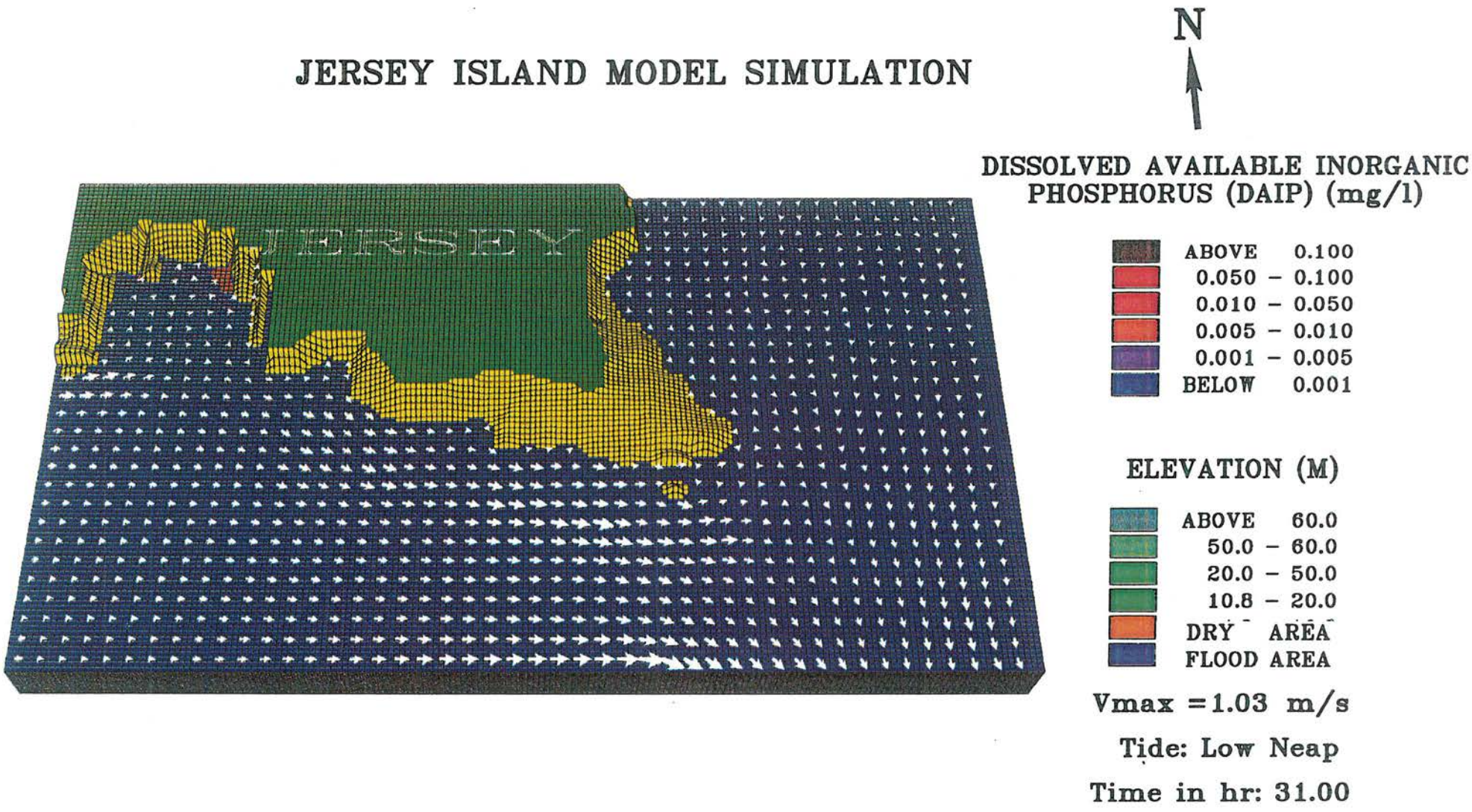

Figure 55 Predicted DAIP distribution for existing base flow inputs at low neap tide

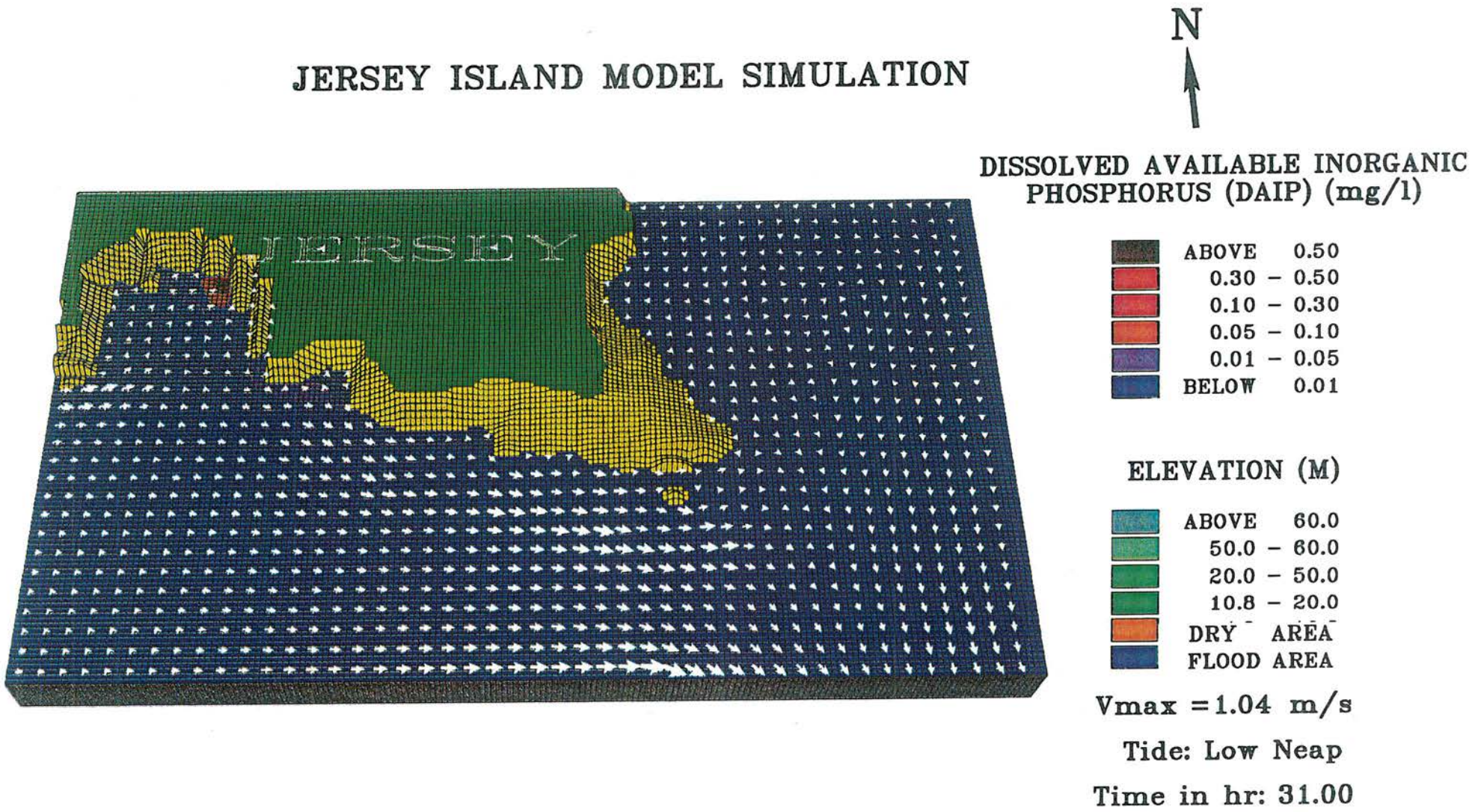

Figure 56 Predicted DAIP distribution for existing storm flow inputs at low neap tide

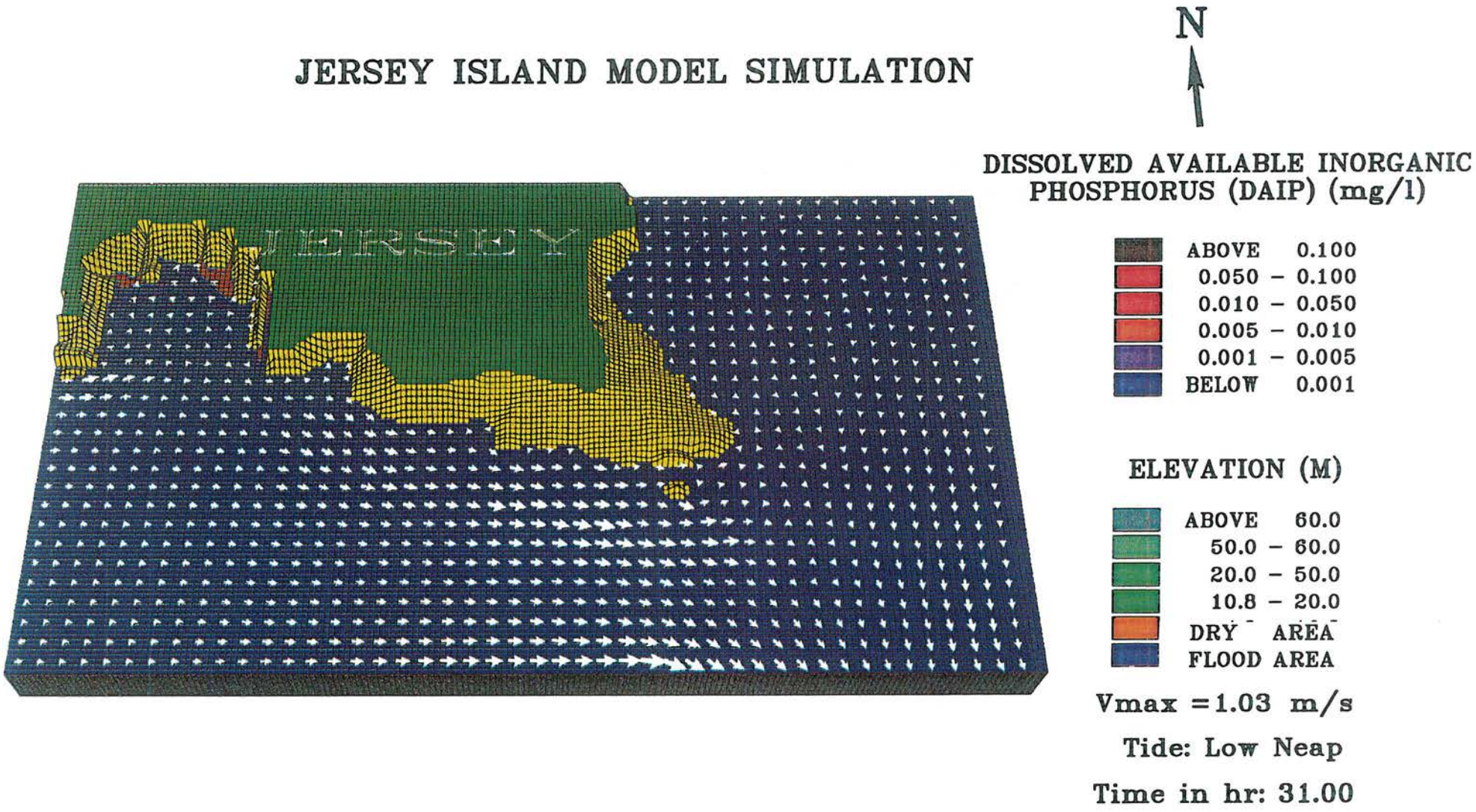

;ure 57 Predicted DAIP distribution for Bellazone STW and other base flow inputs at low neap tide

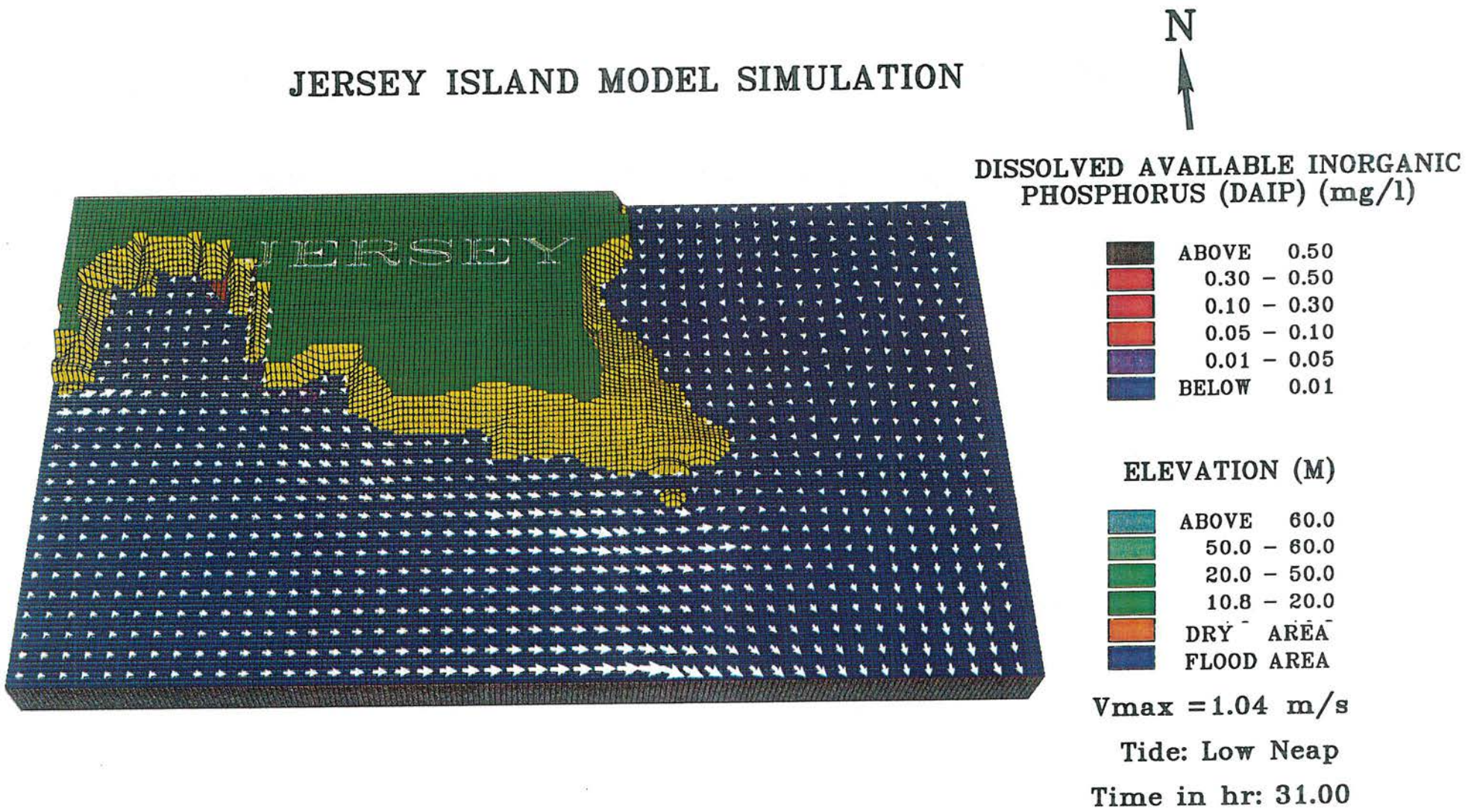

Figure 58 Predicted DAIP distribution for Bellazone STW and other storm flow inputs at low neap tide